



University of
Stavanger

Faculty of Science and Technology

MASTER'S THESIS

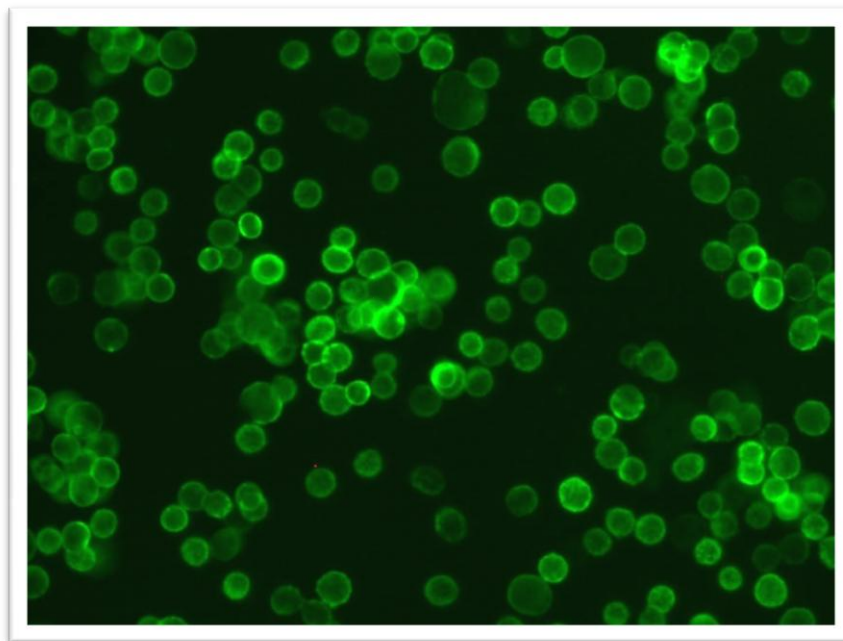
Study program/ Specialization: Master of Science in Biological Chemistry	Spring semester, 2014 Restricted access
Writer: Marija Kilibarda (Writer's signature)
Faculty supervisor: Peter Ruoff External supervisor(s): Oddmund Nordgård	
Thesis title: Molecular characterization of circulating tumor cells from pancreatic cancer patients by single-cell quantitative reverse transcription PCR	
Credits (ECTS): 60	
Key words: Pancreatic cancer Circulating tumor cells Single-cell qPCR mRNA marker RT-qPCR	Pages: 94 + enclosure: 4 Stavanger, 16.06.2014 Date/year

Molecular characterization of circulating tumor cells from pancreatic cancer patients by single-cell quantitative reverse transcription PCR

Master thesis

by

Marija Kilibarda



Master of Science in Biological Chemistry

Faculty of Science and Technology

University of Stavanger

In collaboration with Stavanger University Hospital



Abstract

Pancreatic cancer is a highly lethal disease, which kills approximately 70 000 people per year in Europe alone. The median survival after the time of diagnosis is five to six months for patients with advanced cancer, making pancreatic cancer one of the deadliest of all solid cancers. The disease has few early symptoms, therefore, most patients are diagnosed at advanced stages. The poor prognosis is related to late detection and early dissemination of the disease. The median age of diagnosis is 73 years for pancreatic cancer. The treatment options for pancreatic cancer are rather limited, and there is a great need for more effective treatment and new biomarkers for monitoring of the disease.

Circulating tumor cells (CTCs) are promising new biomarkers suggested to be of clinical relevance also in pancreatic cancer. CTCs are cells in the blood stream that are shed from the primary tumor or metastasis. These cells could offer new insight into treatment effects, monitoring of disease progression and tumor cells genotypes. Some of the CTCs contribute to the formation of distant metastasis. CTC examination is considered a minimal invasive liquid biopsy of the cancer, because the CTCs seem to represent the population of cancer cells present in solid tumors. Enrichment and detection of CTCs have been investigated for several epithelial cancers with great success. However, just a few studies have been published for pancreatic cancer.

The aim of this study was to perform molecular characterization of single CTCs. The CTCs were isolated from blood samples from pancreatic cancer patients and analyzed by quantitative reverse-transcription PCR (RT-qPCR). The pancreatic cancer patients that were recruited for this thesis were part of an ongoing trial at Stavanger University Hospital and Haukeland University Hospital, called PACT-ACT (PANcreatic Cancer Treatment And Circulating Tumor Cells). Tumor cells were enriched from the whole blood by density gradient separation, followed by immunomagnetic enrichment. The single CTCs were identified using immunofluorescent staining of EpCAM and CD45. Isolation of single cells was performed using micromanipulation. The single cells were lysed, reverse-transcribed and pre-amplified, followed by qPCR for 11 specific mRNAs.

The method for enrichment and characterization of CTCs in this study was optimized and validated through several experiments. The tumor cells were successfully separated from the

leukocytes by the molecular characterization. Blood samples from patients were analyzed and we were able to enrich, detect, isolate and perform molecular characterization of single CTCs in peripheral blood samples from patients with pancreatic cancer. However, further optimization of the method should be implemented to enhance the RNA quality of the single cells. The overall impression of the research on the field is promising, and CTC detection is expected to have future clinical utility for pancreatic cancer patients, as well as for other solid cancers.

Acknowledgement

Every year around 600 people are killed by pancreatic cancer in Norway, the prognosis and treatment options for the disease are very poor. Therefore, I consider it a great privilege to get the opportunity to perform research on pancreatic cancer.

Oddmund Nordgård gave me this privilege, and along with it came guidance, support and enthusiasm for the research. Thank you so much! You have shared your impressive knowledge within the field with me, in addition to encourage me to think independently. I would like to express my very great appreciation to Morten Lapin for always helping me and answering my questions. Satu Oltedal and Kjersti Tjensvoll, I would like to thank you so much for always being available. I would also like to thank Rune Småland for giving me the opportunity to perform this thesis at his research group. Thanks to Peter Ruoff for helping me arrange this master's thesis. To everyone at the lab, it has been a pleasure to get to know you!

The last year working on this thesis has been intense, especially the last months of writing. My special thanks are extended to Tina, Kari and Liv for supporting me through this intense period and taking me out on walks. At last, but not at least I would like to offer my most special thanks to Ole Andreas for all the support and help you have given me.

Marija Kilibarda,

Stavanger, June 2014

Table of content

ABSTRACT	I
-----------------	----------

ACKNOWLEDGEMENT	III
------------------------	------------

LIST OF ABBREVIATIONS	VII
------------------------------	------------

1. INTRODUCTION	1
------------------------	----------

1.1 Pancreatic cancer	1
------------------------------	----------

1.1.1 Epidemiology and risk factors	1
-------------------------------------	---

1.1.2 Anatomy of the pancreas	2
-------------------------------	---

1.1.3 Staging	2
---------------	---

1.1.4 Treatment	4
-----------------	---

1.1.5 Tumor biology	5
---------------------	---

1.2 Circulating tumor cells	6
------------------------------------	----------

1.2.1 CTC Characteristics	6
---------------------------	---

1.2.2 Epithelial-to-mesenchymal transition	7
--	---

1.2.3 Self-seeding	8
--------------------	---

1.2.4 CTC Enrichment	9
----------------------	---

1.2.5 CTC Detection	12
---------------------	----

1.2.6 Clinical value of CTC detection in pancreatic cancer	14
--	----

1.3 Single-cell gene expression	16
--	-----------

1.3.1 mRNA levels in single cells	16
-----------------------------------	----

1.3.2 mRNA quantification	17
---------------------------	----

2. AIM OF THE STUDY	20
----------------------------	-----------

3. MATERIALS	21
---------------------	-----------

3.1 Blood samples	21
--------------------------	-----------

3.2 Cell lines	22
-----------------------	-----------

3.3	Reagents	22
3.4	Materials and equipment	24
4.	<u>METHODS</u>	<u>25</u>
4.1	Cell culture	25
4.2	Density gradient separation	27
4.3	Dead Cell Removal	29
4.4	MACS Cell Separation	29
4.5	Immunofluorescent and nuclear staining	31
4.6	Single-cell collection	32
4.7	Single-cell cDNA synthesis and pre-amplification	33
4.8	Single-cell qPCR	36
4.9	Relative quantification	38
4.10	Criteria for evaluation of single cells	39
4.11	Statistical analysis	41
5	<u>RESULTS</u>	<u>43</u>
5.1	Overview of the experimental approach	43
5.2	Optimization of methods	44
5.2.1	Micromanipulation	44
5.2.2	Immunofluorescent staining	45
5.2.3	mRNA quality	46
5.3	Validations of methods	51
5.3.1	Validation of the method for molecular characterization of single CTCs by RT-qPCR	51

5.3.2	Validation of the method for enrichment and characterization of CTCs	55
5.4	Patient blood sample analysis	58
5.4.1	Potential CTCs	59
<u>6</u>	<u>DISCUSSION</u>	<u>65</u>
6.1	Optimization of methods	65
6.2	Validation of methods	68
6.3	Evaluation of single-cell normalization strategies	69
6.4	Analysis of patient samples	71
6.5	General methodological considerations	72
6.6	Potential clinical value of single CTC mRNA profiling	73
6.7	Future Perspectives	74
<u>7</u>	<u>CONCLUSION</u>	<u>76</u>
<u>8</u>	<u>REFERENCES</u>	<u>77</u>
<u>9</u>	<u>TABLE OF FIGURES</u>	<u>83</u>
<u>10</u>	<u>TABLE OF TABLES</u>	<u>84</u>
<u>11</u>	<u>ATTACHMENTS</u>	<u>- 85 -</u>

List of abbreviations

AJCC - American Joint Committee on Cancer

AKT2 - V-akt murine thymoma viral oncogene homolog 2

ALDH - Aldehyde dehydrogenase

ALDH1A1 - Aldehyde dehydrogenase 1 family, member A1

BRAF - V-raf murine sarcoma viral oncogene homolog B

CA19-9 - Carbohydrate antigen 19-9

CD24 - CD24 molecule

CD44 - CD44 molecule

CD45 - Leukocyte common antigen

CDKN2A - Cyclin-dependent kinase inhibitor 2A

cDNA - Complementary DNA

CEA - Carcinoembryonic antigen

CK19 - Keratin 19

CK20 - Keratin 20

CK8 - Keratin 8

CT - Computed tomography

CTC - Circulating tumor cell

DAPI - 4',6-diamidino-2-phenylindole

DNA - Deoxyribonucleic acid

DTC - Disseminated tumor cells

ECACC - European Collection of Cell Cultures

EDTA - Ethylenediaminetetraacetic acid

EGFR - Epidermal growth factor receptor

EMT - Epithelial to mesenchymal transition

EpCAM - Epithelial cell adhesion molecule

FBS - Fetal bovine serum

FcR - Fc receptor

FDA - US Food and Drug Administration

FISH - Fluorescence *in situ* hybridization

FITC - Fluorescein isothiocyanate

FOLFIRINOX - Fluorouracil, irinotecan and oxaliplatin

HPRT1 - Hypoxanthine phosphoribosyltransferase 1

INK4A - Inhibitor of cyclin-dependent kinase 4

ISET - Isolation by size of epithelial tumor cells

KRAS - V-Ki-ras2 Kirsten rat sarcoma viral oncogene

KRAS2 - V-Ki-ras2 Kirsten rat sarcoma viral oncogene homolog 2

MACS - Magnetic-activated cell sorting

MAPK - Mitogen-activated protein kinase

MET - Mesenchymal to epithelial transition

MMI - Molecular machines & industries

MQ - Milli-Q

mRNA - Messenger RNA

MYB - V-Myb Avian Myeloblastosis Viral Oncogene Homolog

PALB2 - Partner and localizer of BRCA2.

PBMC - Peripheral blood mononuclear cell

PBS - Phosphate buffered saline

PC - Pancreatic cancer

PCR - Polymerase chain reaction

qPCR - Quantitative PCR

Ras - Tat sarcoma viral oncogene

RNA - Ribonucleic acid

RT-qPCR - Reverse transcriptase qPCR

SD - Standard deviation

SMAD4 - SMAD family member 4

SSD - Sum of standard deviations

TNM - Tumor-node-metastasis classifications.

TP53 - Tumor protein P53

TRITC - Tetramethylrhodamine isothiocyanate

UV - Ultraviolet

ZEB1 - Zinc finger E-box binding homeobox

1. Introduction

1.1 Pancreatic cancer

Pancreatic cancer is a highly lethal disease, ranked fourth among cancer-related deaths in Norway [1]. Yearly 600-650 new cases are detected, corresponding to 13 per 100 000 inhabitants. The survival rate is very low, less than 5 % of the patients are still alive five years after being diagnosed [2]. Approximately 90 % of the patients diagnosed with advanced pancreatic cancer survive less than one year, with a median survival of five to six months. The high mortality rate is connected to patients being diagnosed at advanced stages, early metastasis and poor response to chemo- and radiotherapy [3]. Pancreatic cancer can be inherited, however 90 % of cases are considered sporadic [2]. The major histological type of pancreatic cancer is ductal pancreatic adenocarcinoma, which accounts for around 80 % of the cases [3]. Acinar cell carcinoma and neuroendocrine tumors are minor histological types of the cancer.

1.1.1 Epidemiology and risk factors

Pancreatic cancer is the seventh most frequent cancer in Europe and is predicted to become the fourth leading cause of cancer-related deaths in the European Union according to the World Health Organization [3]. Pancreatic cancer is one of the deadliest of all solid cancers, it kills approximately 70.000 people per year in Europe [3], and 40.000 people per year in the United States [4]. The incidence rate is approximately 12 per 100 000 inhabitants both in Europe and in the United States. In the United States it has been observed that the age-adjusted incidence is higher for African Americans than for Caucasian Americans, and that it is higher for men than for women [4]. The median age of diagnosis is as high as 73 years, and the disease is rare among people younger than 40 years of age [4, 5].

Several risk factors have been identified for pancreatic cancer. Studies have reported that cigarette smoking doubles the risk of pancreatic cancer [6]. In fact, as many as one in four cases could be related to smoking. High fat and cholesterol diets, for example high consumption of processed meat and high alcohol consumption, also increase the risk of acquiring the disease [7, 8]. People with diabetes and chronic pancreatitis are also at higher risk for pancreatic cancer [2]. A recent study has suggested that there is an increased risk of disease for people with blood type A, B and AB, compared to people with blood type O [2, 9].

Evidence suggest that some families have increased risk of pancreatic cancer, implying a genetic contribution [4]. Only 5-10 % of patients have a family history of the disease [2]. However, for families with four or more cases of pancreatic cancer the risk of disease is 57 times higher than for families with no history of the disease [2]. The genetic base of this increased risk has not been clearly identified yet. However, mutations in *BRCA2* and *PALB2*, among others, are associated with higher risk of pancreatic cancer [10].

1.1.2 Anatomy of the pancreas

The pancreas is a soft gland that extends from the spleen to the duodenum [11]. The tail of the pancreas is abutting the spleen, while the head is encircled by the C-shaped duodenum. The majorities of tumors develop in the head of the pancreas and cause obstructive cholestasis [2]. An overview of the anatomical localization of the pancreas is given in Figure 1.

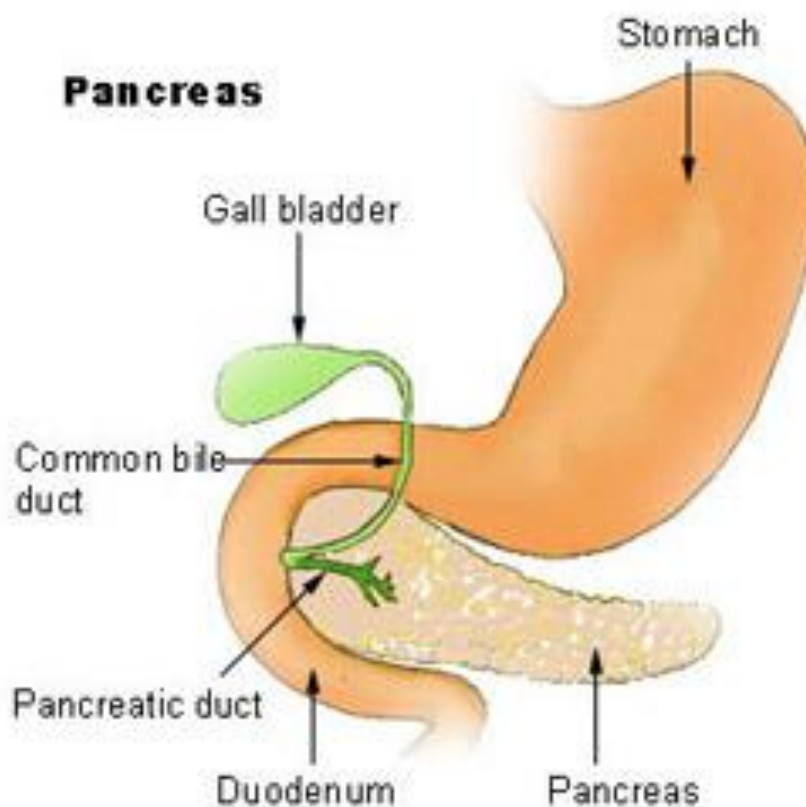


Figure 1 Illustration of the pancreas. Taken from National Cancer Institute [12].

1.1.3 Staging

Pancreatic cancer is staged according to the tumor-node-metastasis (TNM) classification of the American Joint Committee on Cancer (AJCC). This staging of tumors is based on tumor

size and localization, which is connected to resectability [2]. Further staging reflects whether lymph node metastases (N stage) or distant metastases (M stage) are present. Classification of tumor and lymph node status, and the presence of distant metastases are combined to a general clinical stage that reflects the overall disease burden, as summarized in Table 1 [2].

Table 1 Explanation of the TNM classification from the AJCC for pancreatic cancer. Taken from Hildago et al.[2] Copyright Massachusetts Medical Society.

Stage	Tumor stage	Node metastasis	Distant metastasis	Characteristics
IA	T1	N0	M0	The tumor is limited to the pancreas, with a size smaller than 2 cm.
IB	T2	N0	M0	The tumor is limited to the pancreas, with a size larger than 2 cm.
IIA	T3	N0	M0	The tumor is growing outside the pancreas, but does not involve celiac axis or superior mesenteric artery
IIB	T1-3	N1	M0	Tumor is either limited to the pancreas or has grown outside the organ, but does not involve celiac axis or superior mesenteric artery.
III	T4	N0-1	M0	Tumor involves the celiac axis or superior mesenteric artery.
IV	T1-4	N0-1	M0-1	Disease with distance metastasis.

Pancreatic cancer has few symptoms at early stages, although approximately 20 % of the patients are diagnosed with diabetes a couple of months before the diagnosis of pancreatic cancer [13]. Another 40 % have impaired glucose tolerance [10]. Vague symptoms like pain in the upper abdominal region, significant weight loss, fatigue or gallbladder enlargement can occur [14]. Pancreatic cancer is therefore often diagnosed at advanced stages of the disease, and there are few effective therapies available [15]. To diagnose pancreatic cancer histological examination of tissue biopsies, computed tomography (CT) or magnetic resonance imaging (MRI) are used [14]. Furthermore, in some cases advanced technologies such as endoscopic ultrasound (EUS) and positron emission tomography (PET) are used as additional diagnostic tools.

The potential of serum biomarkers for diagnosis, prognostic stratification and monitoring of therapy is great, although few biomarkers have revealed sufficient clinical value [2]. The only biomarker found to be functional for therapeutic monitoring and early detection of recurrent disease after treatment is carbohydrate antigen 19-9 (CA19-9). However, CA19-9 does have certain limitations [2]. It is not specific for pancreatic cancer, and the levels of the biomarker could be elevated in other conditions such as cholestasis [2]. Therefore, CA19-9 is not used as a screening tool. Clearly, new effective biomarkers are required [16].

1.1.4 Treatment

Pancreatic cancer patients should be treated by a multidisciplinary team consisting of surgeons, oncologist, radiologists, gastroenterologists, nutritionists and pain specialists [2]. The only available choice for potential curative treatment is surgery [17]. Surgery is mainly an option for patients at early stages of the disease, stage I and some at stage II, which only account for 20 % of the patients. There are no age criteria for surgery, although surgery is more dangerous for people over 75-80 years [3]. The major goal for surgery is full tumor resection, as removal of parts of the tumor has shown little to no effect in terms of survival. Even if the tumor is fully resected, the clinical outcome is disappointing in most cases [3]. In cases where the tumor is small and metastasis is not present at the time of diagnosis the 5-year survival is around 30 % [17]. In order to manage local and systemic advanced disease palliative treatment is given.

Post-operative treatment with the chemotherapeutic agents fluorouracil and leucovorin, or gemcitabine is recommended to improve progression-free and overall survival for pancreatic cancer [2]. The current standard chemotherapy for locally advanced and metastatic pancreatic cancer is single-agent gemcitabine [18]. Gemcitabine has in some studies been combined with fluorouracil or capecitabine. Some patients have had effect of a combination of gemcitabine and erlotinib, an epidermal growth factor receptor (EGFR) tyrosine kinase inhibitor [3]. The combination of chemotherapy and targeted therapies, have not shown great effect for pancreatic cancer patients. The effect of erlotinib is most likely limited due to the high frequency of *KRAS2* mutations in pancreatic cancer [2].

Patients treated with fluorouracil, irinotecan and oxaliplatin (FOLFIRINOX) were in a recent phase III study reported to have a prolonged survival compared to patients treated with single-

agent gemcitabine [19]. Only patients with a good performance status were included in the study, because FOLFIRINOX is associated with severe side effects [19].

Another recent phase III study reported prolonged survival for patients treated with nab-paclitaxel combined with gemcitabine [20]. In this study the overall median survival for patients treated with gemcitabine alone were 6.7 months, compared with 8.5 months for patients treated with nab-paclitaxel combined with gemcitabine. However, the side effects of nab-paclitaxel and gemcitabine were more severe when compared to gemcitabine alone [20].

1.1.5 Tumor biology

The presence of a dense desmoplastic reaction, surrounding the malignant epithelial cells, that consist of fibroblasts, pancreatic stellate cells and extra cellular matrix proteins is typical for tumors in the pancreas [21]. Pancreatic stellate cells are found to contribute to progression of the malignancy and to the resistance against chemotherapy [21].

Pancreatic cancer has a high frequency of *KRAS* mutations; the mutations are present in 90-95 % of the cases [4]. Mutations in *KRAS* genes at early stages of the disease suggest that *KRAS* activation is an important early event that contributes to tumorigenic transformation [22]. During the development of cancer in the pancreas there is an accumulation of mutations such as activation of *KRAS2*, inactivation of the tumor-suppressor genes *CDKN2A* and *TP53*, and deletions of *SMAD4* [2]. Nearly all patients with fully advanced disease carry one or more of these genetic defects [4]. Additionally, widespread chromosomal losses, gene amplifications and telomere shortening occur frequently [10].

CDKN2A encodes for the inhibitor of cyclin-dependent kinase 4 (*INK4A*), and is inactivated in 95 % of the tumors [2]. This results in loss of the p16 protein, which is a protein regulating the G1-S transition of the cell cycle. Mutations in the gene *TP53* is allowing cells to pass by DNA (deoxyribonucleic acid) damage control checkpoints and apoptotic signals which leave the cells' genome unstable [2]. *TP53* inactivation is seen in 50-75 % of tumors. Deletion of the *SMAD4* gene occurs in 55 % of pancreatic tumors. Several other tumor suppressor genes are also inactivated in pancreatic cancer in lower numbers [4]. Gene mutations could also occur in oncogenes such as *BRAF*, *MYB*, *AKT2* and *EGFR*, for some of the patients [10].

Another contributing factor to cancer development and progression is alterations of microRNA (miRNA, ribonucleic acid) expression [10]. miRNAs are non-coding RNA

molecules, with an average length of 20-23 nucleotides [23]. They are responsible for post-transcriptional regulation of mRNA via translational repression, mRNA cleavage and deadenylation. Over-expression of several miRNAs has been identified in pancreatic cancer [10]. miR-21, miR-34, miR-155 and miR-200 are all found in pancreatic cancer and are believed to contribute to the neoplastic progression. miRNAs have been reported to act as both oncogenes and tumor suppressor genes [24], and miRNA is both stable and detectable in human plasma. Therefore, miRNA detection in human plasma is considered to be a useful diagnostic marker in the future [10].

1.2 Circulating tumor cells

Circulating tumor cells (CTCs) are cells that detaches from the primary tumor or metastasis, intravasating into the blood stream [25]. Detection and characterization of CTCs have recently become one of the most active areas within translational cancer research [26]. The low concentration of CTC in peripheral blood, down to one per 10^6 - 10^7 cells, makes CTC enrichment and investigation a technical challenge [27, 28]. Enrichment and molecular characterization of CTCs could revolutionize the understanding of metastasis biology, and provide a tool for non-invasive assessment of tumor genotype during treatment and disease progression. CTCs are a genetic heterogeneous population [26]. Potentially, CTCs could reflect the heterogeneity within the primary tumor and the potential metastases better than a biopsy of the primary tumor. As distant metastasis is the main cause of cancer-related deaths, there is a great potential in the enrichment and characterization of CTCs [29].

1.2.1 CTC Characteristics

CTCs were first reported in 1869 by Thomas Ashworth. He characterized the CTCs as cells appearing “exactly in shape, size and appearance” as cells seen in the primary tumor [30]. A more recent study has characterized CTC as shaped oval to round with intact nucleus and cytokeratin staining throughout the cytoplasm [31]. Allard et al. 2004 also reported that CTCs could appear as doublets, clusters, irregularly shaped and with multiple nuclei, although the latter appear less frequently. Clusters of CTCs, also called circulating tumor microemboli (CTM), have also been detected by Stott et al. 2010 [32]. The study suggests that it might be possible that cancer metastasis rise predominantly from clusters of CTCs rather than single CTCs [32]. This theory is supported by work in animal models where clusters of cells are more likely to form metastasis compared to an analogous number of single tumor cells [33].

The viability of the cells will be a contributing factor to this theory, as cells in clusters are more protected against attacks from the immune system compared with single cells. Hence, CTM forms a microenvironment that is more favorable for tumor cell survival [28]. If this is correct, the presence of CTM might be more relevant as a prognostic factor for malignancy compared to single CTCs [28]. In fact, the majority of CTCs shed into the bloodstream will die, and only 0.01 % of the cells is estimated to contribute to the formation of metastasis [34].

The CTC population is heterogeneous [26]. The heterogeneity in CTCs has several sources, one is the heterogeneity within the tumor, which may lead to heterogeneity within the shed CTC population [22]. Tumor cells undergoing epithelial-to-mesenchymal transition (EMT) is one of the mechanisms that may contribute to this heterogeneity [22, 35].

1.2.2 Epithelial-to-mesenchymal transition

Epithelial-to-mesenchymal transition, EMT, occur when epithelial cells loses their differentiated epithelial characteristics in a complex molecular and cellular program [22]. The cells acquire mesenchymal features such as motility, invasiveness and resistance to apoptosis. The cells could also reverse the change by undergoing mesenchymal to epithelial transition (MET) [24]. EMT and MET are thought to have a crucial role in tumorigenic development. The transition between the two states facilitates tumor progression and intratumoral heterogeneity [24]. In distant micro-metastases epithelial properties could be more favorable for the tumor cell compared to mesenchymal properties, due to epithelial properties in the surrounding tissue in the distant organ [36]. MET could provide this needed change when the CTCs are forming metastasis.

E-Cadherin is expressed in epithelial cells, where it is involved in epithelial cell-to-cell adhesion [37]. It codes for a transmembrane glycoprotein that facilitates calcium dependent intercellular adhesion [38]. Expression of E-Cadherin is connected to epithelial cell behavior, tissue formation and suppression of cancer. An important feature of EMT is the repression of E-cadherin, which activates known oncogenic signaling pathways such as mitogen activated kinase (MAPK) and rat sarcoma viral oncogene (Ras) [39]. When E-cadherin is expressed it prevents cell motility, invasion and metastasis. During EMT, when E-cadherin is down-regulated, other cadherins like the mesenchymal N-Cadherin is expressed. Hence, the cells are more likely to intravasate to form distant metastasis [40]. Recently, specific miRNAs have been identified as EMT regulators, by regulating EMT-inducing transcription factors [24].

Cancer cells with stem cell like properties, which have been formed by cells undergoing EMT, are associated with increased cellular migration and resistance to therapy [35]. Potentially tumor-initiating cells seem to persist in an inactive non-proliferative dormant state for years, triggering recurrence of the disease [22]. Studies of EMT among CTCs are very few. However, some studies of tumor cells isolated from bone marrow biopsies (DTCs) report expression of characteristic EMT markers [35].

1.2.3 Self-seeding

Self-seeding is a relatively new theory for metastasis formation. The theory is based on CTCs' ability to migrate from the primary tumor to regional and distant sites in the body, but also back to the tumor they originate from [41]. In Figure 2 the concept is illustrated in greater details, where A, B, C, D and E are different pathways CTCs could follow in self-seeding [42]. According to the self-seeding model, the CTCs will return to the primary tumor and aid its growth from the outside [41]. The CTCs that manage to return to their place of origin will find themselves in a welcoming microenvironment, where they could easily grow [42]. Actually, some CTCs may offer a more effective growth in the primary tumor compared to the initial tumor cells.

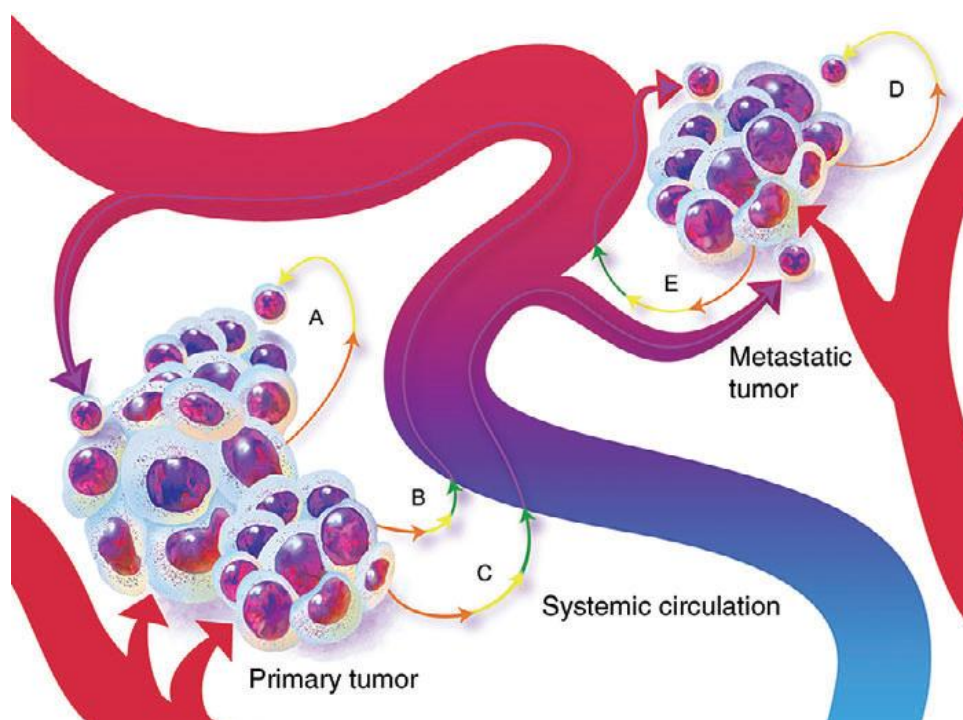


Figure 2 The self-seeding concept of cancer growth and metastasis. From Norton and Massagué 2006 [42].

1.2.4 CTC Enrichment

CTCs are very rare among the numerous blood cells. Therefore, several strategies for CTC enrichment have been investigated based on physical and biological properties of the CTCs [25], some more successful than others. Physical properties, like size, density or charge can be utilized to distinguish CTCs from leukocytes. Biological properties usually employ immunological procedures for enrichment of CTCs using antibodies against either epithelial antigens which are associated with epithelial tumors or leukocyte antigens for detection of contamination blood cells [25]. Various methods are available, of which several are presented below. Table 2 summarizes the main CTC enrichment techniques available.

Table 2 Overview over CTC enrichment methods. Information based taken from Alix-Panabieres et al. 2013 and Krebs et al. 2014. [25, 26]

Technology based on physical properties	CTC enrichment method
Density gradient separation: Lymphoprep™, Ficoll-HyPaque™, OncoquickR	Size based selection using centrifugal force
Rosette-Sep™	
Dean Flow Fractionation	
ISET	Filtration based on cell size
Technology based on biological properties	
CellSearch®	EpCAM coated ferromagnetic beads
MagSweeper	EpCAM coated magnetic beads on rod
GILUPI Nanomedizine	EpCAM coated medical wire
Adna Test Cancer Select/Detect	Immunomagnetic beads, EpCAM and MUC1
CTC Chip	EpCAM coated microfluidic device
Herringbone Chip	EPCAM coated microfluidic device with herringbone structure
IsoFlux	EpCAM coated magnetic beads, microfluidic processing
CTC iChip®	Magnetic bead capture, microfluidic inertial focusing
Ephesia CTC chip	Paramagnetic beads, microfluidic device

A common method for isolation of CTCs is a positive immunomagnetic enrichment using paramagnetic particles coated with antibodies against the surface marker epithelial cell adhesion molecule (EpCAM) [43]. Another method is immunomagnetic depletion of hematopoietic CD45 positive cells. The current “gold standard” for CTC detection is probably the CellSearch® system (further information in chapter 1.2.5). According to the CellSearch® system documentation, CTCs that are larger than 4 µm, should express EpCAM and cytokeratin (8, 18 or 19) and at the same time not express CD45 [44].

The most common method for detection is based on targeting EpCAM molecules [43]. This raises the question of whether the cells with the highest metastatic potential are enriched and detected [43]. Recent studies state that detection of epithelial phenotypes, indeed prevent the detection of other and perhaps more important phenotypes [45, 46]. If an antibody against EpCAM is used for detection, it is not likely that cells with mesenchymal characteristics will be detected. Hence, the choice of the enrichment method, will reflect the population of the identified CTCs [26]. It is believed that mesenchymal cells, that are expected to have greater metastatic potential compared to CTCs expressing EpCAM, could be detected by using a wider range of markers [43].

1.2.4.1 Density gradient separation

Density gradient separation is the traditional enrichment method. Tumor cells and mononuclear cells are separated from the erythrocytes based on different buoyant density. The separation is performed by centrifugation in an iso-osmotic medium such as Lymphoprep™ (Axix-Shield PoC AS), Ficoll-HyPaque™ (Sigma-Aldrich) or Oncoquick^R (Greiner Bio-One) [22]. Further details are found in chapter 4.2.

Rosette-Sep™ Human Circulating Epithelial Tumor Cell Cocktail (StemCell Technology) is a technique for CTC enrichment that is also based on density gradient separation, combined with biological properties [22]. This technique uses a tetrameric antibody complex to link the white and the red blood cells together, thus the density of the white blood cells rises, separating them from the CTCs by centrifugation. Dean Flow Fractionation is yet another method which uses centrifugal force for a density based collection [26].

1.2.4.2 Filtering

CTCs could be enriched based on size filters, as CTCs are often significantly larger compared to leukocytes. The enrichment procedure utilizes membrane filtration, where the cells are

separated according to size. The pores in the membrane are small enough to capture CTCs and at the same time large enough for blood cells to pass through. ISET (Isolation by Size of Epithelial Tumor cells) is the best known membrane filter device for enrichment of CTCs [25].

1.2.4.3 Immunomagnetic Enrichment

Immunomagnetic enrichment has been a successful method for capturing of CTCs, and are therefore the most widely used enrichment approach [26]. Immunomagnetic enrichment is based on antibodies against epithelial antigens associated with epithelial tumors for positive selection or leukocyte antigens for negative selection [25]. The antibodies are coupled to paramagnetic beads. The use of a magnetic field facilitates the separation of the antigen-antibody complex [25].

The CellSearch® system (Veridex) are the only method for CTC enumeration so far approved by the US Food and Drug Administration (FDA) [25]. CellSearch® employs immunomagnetic enrichment using antibodies against EpCAM to separate the CTCs from the white blood cells. After the enrichment process the CTCs are detected based on immunocytochemical identification. The identification of tumor cells are performed by labelling the captured cells with fluorescent dye conjugated antibodies specific for leukocytes (CD45) and epithelial cells (CK8, 18 and 19) [22]. CTCs are identified by positive CK staining and lack of CD45 staining, in combination with nuclear dye DAPI (4',6-diamidino-2-phenylindole).

MagSweeper (Stanford University, USA) is another immunomagnetic enrichment system, where CTCs expressing EpCAM are enriched [25]. MagSweeper is not yet commercially available. The method uses paramagnetic beads conjugated to an EpCAM antibody. The labeled cells are removed from the suspension with a rod connected to a magnetic field. MagSweeper has a high CTC purity, and by isolating viable cells, it enables investigation of individual cells by genetic and proteomic analyzes [26].

GILUPI Nanomedicine (Germany) CTC collector is a functionalized EpCAM-coated medical wire, which is positioned into the antecubital vein and left for 30 minutes collecting CTCs in a large blood volume [26]. CTCs are later identified by looking at the expression of *CK* or *EPCAM*.

AdnaTest Cancer Select/Detect (AdnaGen AG, Langenhagen, Germany) is a promising method where immunomagnetic separation is followed by a multiplex real-time PCR [47]. This method is proven to be a very sensitive approach with a detection limit of two tumor cells. A clinical validation of the method for pancreatic cancer has not yet been reported, however, a study has shown prognostic value of the method when used on colon cancer patients [47].

1.2.4.4 Microfluidics

In addition to the immunomagnetic enrichment methods, there is a growing interest for microdevices. Microdevices are based on immunomagnetic or physiological enrichment methods, or a combination of both. The CTC Chip, the first version of microdevice, was made of an array of anti-EpCAM antibody-coated micropores. Later a herringbone structure was added to the CTC Chip, it was then called a Herringbone Chip [25]. The Herringbone Chip provides passive mixing of cells through the generation of microvortices caused by the herringbone-shaped ribs within the flow cell, increasing the possibility of the CTCs to encounter the EpCAM-coated chip surface [22].

CTC iChip® (Massachusetts General Hospital Center, USA) introduced by Ozkumur *et al.* is yet another promising CTC enrichment method [48]. Most of the methods presented so far are dependent on the cells to be EpCAM positive. However, CTC iChip® could collect either EpCAM positive cells or cells collected by the depletion of CD45. This is performed using the automated CTC iChip® by series of debulking, inertial focusing and magnetic separation steps [26]. After the potential tumor cells are enriched, the cells are still viable and available for further molecular analysis, also on a single cell level [48].

Ephesia CTC chip is composed of biofunctionalized superparamagnetic beads in columns, which are assembled in a microfluidics system that uses high-throughput selection, enumeration and electrokinetic manipulation of low-abundance CTCs [25]. IsoFlux (Fluxion, USA) is another microdevice for enrichment of CTCs, it uses EpCAM-coated paramagnetic beads combined with microfluidics [26].

1.2.5 CTC Detection

Most of the enrichment methods for CTC do not provide a pure CTC suspension, rather a suspension contaminated with blood cells. This raises the need for a final verification of CTCs on a single cell level [25]. Immunocytochemistry and PCR based detection are the most

common methods employed. Another key question is whether the cells are viable or apoptotic, as only viable cells contribute to the formation of distant metastasis [25].

1.2.5.1 Immunocytological detection

For regular immunocytochemistry the enriched cells are fixated on a solid support to allow for easy handling [22]. The cells are either labeled with fluorescent dye conjugated antibodies or with antibodies connected to other detectable tags. Such as colored precipitates which is a common detection method for visible light, or gold particles which is a less common detection method. The CTCs are detected and counted using light or fluorescence microscopy [22]. The FDA approved CellSearch® systems along with many other CTC assay use immunocytochemical identification of tumor cells [22, 25].

As previously stated, detection of viable CTCs are believed to have a greater clinical impact compared to apoptotic CTCs. Epithelial immunospotting (EPISPOT) is a method which detect only viable cells [25]. This method is based on detection of proteins released from epithelial CTCs by secondary antibodies labeled with fluorochromes [49]. The cells are cultured on plates and later coated with specific antibodies [50]. Different target proteins have been used for different types of cancer. Studies in colon cancer demonstrate a clinical relevance of detection of viable CTCs using the EPISPOT assay [50].

1.2.5.2 PCR based detection

PCR based detection is the most frequently used alternative to immunological assay for CTC identification [25]. Usually detection of mRNAs that are over-expressed in tumor cells are used to detect CTCs [22]. The availability of tumor specific mRNA is limited though, and epithelial specific assays are therefore often used. Many of the transcripts measured are also expressed in normal blood cells, which could be contaminating the CTC fraction. Hence, a detection threshold of 90 % or higher of the highest normal blood level is required as a lower threshold for CTC detection [22]. Certain gene transcription could be down regulated in the CTCs undergoing EMT, thus a multi-marker assay for mRNA detection would be a favorable strategy [22, 25]. Multi-marker assays allow for simultaneous analysis of several mRNAs. Reverse transcriptase quantitative PCR (RT-qPCR) is found to be less subjective compared to immunocytochemistry, because of instrument-derived numerical output and easy automation [22]. The MUC1 expression on activated T lymphocytes appears as a limitation of the assay, and should be taken into consideration [51]. Currently the most used method is RT-qPCR on a

fraction of CTCs, however RT-qPCR on single CTCs offer much more information. This method will be further described in chapter 1.3.

1.2.6 Clinical value of CTC detection in pancreatic cancer

CTCs are likely to provide valuable information for clinical applications such as prediction of treatment response, monitoring of treatment, personalization of treatment and prediction of clinical outcome [35]. The clinical value of CTC detection has been proven in several studies of lung, colon and breast cancer [26].

The clinical utility of CTCs in pancreatic cancer management is still poorly investigated. However, there is some evidence for CTC detection in operable and inoperable pancreatic cancer patients, although the clinical relevance of CTC detection in pancreatic cancer may need further investigation [22]. An overview of the most important studies of clinical outcomes of CTC detection in pancreatic cancer, are listed in Table 3 below [22].

Table 3 Studies of the clinical relevance of CTC detection in pancreatic cancer patients. Only studies with 15 or more patients have been included. Reproduced with permission from Tjensvoll *et al.* 2013 [22].

Study	Markers	Enrichment	CTC detection method	Number of patients
Z'graggen <i>et al.</i>, 2001	AE1/AE3, CK7, CK19, CK20, and glycoproteins	Density gradient centrifugation	Immuno-cyto-chemistry	N=105
Mataki <i>et al.</i>, 2004	CEA mRNA	Density gradient centrifugation	Nested PCR	N=20
Soeth <i>et al.</i>, 2005	CK20 mRNA	Density gradient centrifugation	Nested PCR	N=154
Hoffmann <i>et al.</i>, 2007	CK19 mRNA	Density gradient centrifugation after erythrocyte lysis	Compared nested PCR and RT-qPCR	N=37
Kurihara <i>et al.</i>, 2008	CK8, CK18, and CK19	Immuno-magnetic enrichment with EpCAM	Cell Search	N=26

De Albuquerque *et al.* [52], recently reported that CTC detection was associated with shorter progression free survival. CTCs were enriched using immunomagnetic separation, followed by detection of CTCs by RT-qPCR using an mRNA panel consisting of *CK19*, *MUC1*, *EPCAM*, *CEACAM5* and *BIRC5*. CTCs were detected in 16 of 34 patients (47.1 %) with pancreatic cancer. The patients were considered to have positive CTC detection if at least one of the mRNA markers were expressed in peripheral blood samples [52].

Sergeant *et al.* [53] did not demonstrate any significant association between *EPCAM* positive samples and cancer-specific or disease-free survival in their study using RT-qPCR assay for *EPCAM* mRNA detection. 40 patients with resectable pancreatic cancer and additionally 8 patients with unresectable pancreatic cancer participated in the study. *EPCAM* positive samples were detected for 10 of 40 (25 %) patients in the pre-operative samples, compared with 27 of 40 (67 %) in the peri-operative samples. Only 8 of 34 (23.5 %) samples were *EPCAM* positive post-operative. Even though the results did not demonstrate any association between *EPCAM* positive samples and overall survival, a trend of shorter overall survival among patients with *EPCAM* positivity were observed among the pre-operative samples [53].

Soeth *et al.* [54] examined the diagnostic potential of *CK20* detection with RT-PCR of DTC and/or CTCs in a study in 2005. The study included 172 patients with pancreatic cancer, staged I-IV. Evaluations of preoperative bone marrow and peripheral blood samples were performed, from respectively 135 and 154 of the patients. Successful detection of disseminated tumor cells was reported for 81 of 172 (47.1 %) patients. The results demonstrated a significant association between detection of DTCs and CTCs and overall survival. Also, the mean overall survival was higher for patients negative for *CK20* compared with patients positive for *CK20*, respectively 26.1 and 17.9 months [54].

Mataki *et al.* [55] used nested RT-PCR to detect carcinoembryonic antigen (*CEA*) in peripheral blood. Blood samples from 53 patients with biliary pancreatic cancer were evaluated, where 20 of these patients underwent a curative-intended surgery. Positive *CEA* mRNA status was demonstrated for 6 of 20 (30 %) patients with pancreatic cancer. 5 out of 6 patients with one or more *CEA* positive samples experienced recurrence of the disease, compared to only 2 of 12 patients that had *CEA* negative sample. This discovery suggests that CTC assessments could contribute to disease monitoring. [55]

Kurihara *et al.* [56] examined the CTC level in peripheral blood from 26 pancreatic cancer patients with either operable or inoperable disease. The CellSearch® system was used for the

enumeration of the CTCs. 11 of 26 (42 %) pancreatic cancer patients were positive for CTC. These patients were found to have a significantly shorter median overall survival when compared with those without CTCs detected ($p < 0.001$) [56].

Khoja *et al.* did a comparison of the CellSearch® system and the ISET technique regarding CTC enumeration and detection. Patients with newly diagnosed progressive metastatic or inoperable adenocarcinoma of the pancreas were included in the study. Detection of CTCs did not correlate with progression-free or overall survival, however a trend towards shorter survival for patients with CTCs detected using the CellSearch® system was reported.

Z'graggen *et al.* used immunocytochemistry to detect CTCs in pancreatic cancer patients. A total of 105 patients, both operable and inoperable, were included in the study, along with a control group consisting of 66 healthy individuals. CTCs were successfully detected in peripheral blood samples from 3 of 33 (9 %) patients with resectable disease, and in 24 of 73 (33 %) patients with unresectable disease. A significant association between CTC detection and disease progression were not demonstrated.

Several of the studies failed to demonstrate a significant prognostic relevance for CTCs in pancreatic cancer. The CTC population for pancreatic cancer, as for other cancers, seems to be highly heterogeneous [22]. This implies the need to focus on methods to other than *EPCAM* enrich specific CTC populations, which could improve the clinical value of CTC detection in the future [22]. Furthermore, the clinical impact of CTC detection in pancreatic cancer should be thoroughly investigated in larger studies.

1.3 Single-cell gene expression

There are potential advantages of single CTC analysis compared to analysis of a CTC fraction with potential contaminating leukocytes [26]. This chapter will give an overview of available methods for measurement of single cell gene expression and illustrate the challenges of analyzing gene expression at a single-cell level.

1.3.1 mRNA levels in single cells

Individual CTCs differ in many ways, even if they derive from the same primary tumor. Differences between single cells from the same tissue are found in size, morphology and protein levels, and most important in the expression levels of mRNA and miRNA [57]. The CTC population is highly heterogeneous, in addition to the heterogeneity within a population of cells, the mRNA levels within a single-cell could vary over time. This heterogeneity can be

caused by transcriptional burst. Transcriptional burst was a theory proposed in 1994 by Ross et al., where transcription was found to occur in short bursts with long periods of inactivity between the bursts [58]. A more recent study describes that transcriptional burst is found to be present across the human genome [59]. The burst frequency and size within a cell is altered by transcriptional activators, such as trichostatin A, and are depending on the expression levels of the locus [59]. The transcriptional burst model should be taken into considerations in single cell analysis of CTCs.

1.3.2 mRNA quantification

A single cell contain an exceptionally small amount of mRNA, between 0.01-2.5 pg per cell, where the mRNA is unstable and easily degraded if not treated against RNases or transcribed to the more stable cDNA [60]. Several methods to measure the low concentration of mRNA from single cells are presented in the following chapters.

1.3.2.1 RT-qPCR

Reverse transcription (RT) followed by qPCR could be employed to detect low concentration of mRNA in single cells [61]. Studies show that accurate measurements of gene expression is possible at a single-cell level, but depend upon well-validated experimental procedures for low-level mRNA analysis [62].

The cells are isolated by micromanipulation or other isolation methods, followed by lysis of the cell, before measurement of mRNA levels are performed [63]. mRNA is reverse transcribed to stabilize the information, usually followed by a pre-amplification step. Pre-amplification is a procedure used to certify that the required amounts of molecules are obtainable. The number of accessible molecules is important when analysing several mRNAs in singleplex PCR reactions. The disadvantages with sub-sampling are reduced if multiplex pre-amplification is used. The RT-qPCR analysis could be affected by the low amount of nucleic acids, and high variations are expected. These variations might be caused by physiological or biological effects such as transcriptional burst, but also technical setup such as sampling, storage, pre-amplification or other aspects, which should be kept to a minimum [61]. Several mRNA markers could be measured simultaneously in RT-qPCR [64].

1.3.2.2 Next generation sequencing

Next-generation sequencing has made it possible to sequence mRNA faster and to a lower cost than previously [30]. Using RNA-Seq the number of RNA sequences reflects the RNA

level in the sample. There are several next generation sequencing approaches available, such as: 454 Genome Sequencers (Roche Applied Science), SOLiD platform (Applied Biosystems; Foster City, CA, USA) now the Ion Torrent/Proton (Life Technologies), PacBioRSTM (Pacific Biosciences) and HiSeq 2000 (Illumina) [65]. High-throughput mRNA sequencing has been used in order to quantify mRNA from single cells. mRNA is pre-amplified to generate the required amount of sample. Several attempts have been made to successfully generate high transcriptome coverage [66, 67]. A protocol for improved transcriptome coverage (Smart-Seq) was published by Ramsköld et al.[68]. The study reports a transcriptome coverage close to 40 % of mRNA sequencing from individual CTCs [68].

1.3.2.3 cDNA microarray

DNA microarray is produced by spotting and immobilizing a large set of DNA fragments on a solid support. The mRNA sample is labelled with fluorescent dyes and hybridized [23]. To obtain the necessary amount of mRNA for hybridization, the samples should first be pre-amplified. The level of fluorescence in a specific DNA spot is proportional to the level of the mRNA corresponding to the probe immobilised in that spot. The chip is scanned with a laser to detect signals [69]. An additional possibility is to use two different dyes for each spot in the array to compare gene expression between two samples [23].

Successful quantification of whole transcriptome from single human cells has been performed [70]. cDNA microarray has not yet been used for CTC detection on single CTCs, however, Welty et al. succeeded in profiling ten CTCs from bone marrow samples for patients with prostate cancer, using 10 731 known genes [70].

1.3.2.4 Digital PCR

The theory behind digital PCR was proposed as early as in 1992 [71]. However, the method was first developed in 1999 by Vogelstein and Kinzler [72]. Digital PCR transforms the exponential PCR reaction into a linear, digital signal. The method enables sensitive and precise quantification of rare events in nucleic acids [73]. Each molecule in the sample is separated into micelle compartments, and the compartments are analysed separately for the incidence of acquired DNA molecule by using a fluorescent probe. The compartment will either be negative or positive. The quantification is independent of variations in the amplification efficiency, since one, successful amplification is counted as one molecule [73].

Digital PCR has not yet been employed for single CTCs. A recent publication explores the possibility of detecting rare CTCs in a pool of Peripheral blood mononuclear cell (PBMC) in cervical cancer using digital PCR [74]. Pfitzner *et al.* hypothesises that quantification of CTCs should be possible if a high background of non-target cells are tolerated. The study has a very limited number of patients included, where CTCs were detected in two out of three patients. A low number of CTC present in patients with cervical cancer is reported. These findings are in concordance with earlier published data on the field [74].

1.3.2.5 Fluorescence *in Situ* Hybridization (FISH)

Fluorescence *in Situ* Hybridization (FISH) was originally developed to detect *in situ* localization of specific sequences on chromosomes and later adapted to detect single molecule RNA [75]. A DNA probe, corresponding to the mRNA of interest, is labelled before hybridization, either directly or indirectly [76]. The labelled probe and the target RNA are denatured, which permit annealing of complementary DNA and RNA [75] (Figure 3). The cells are fixated and fluorescence signal visualize the presence of target mRNA by microscopy. The level of fluorescence is to some extent reflecting the level of the studied mRNA.

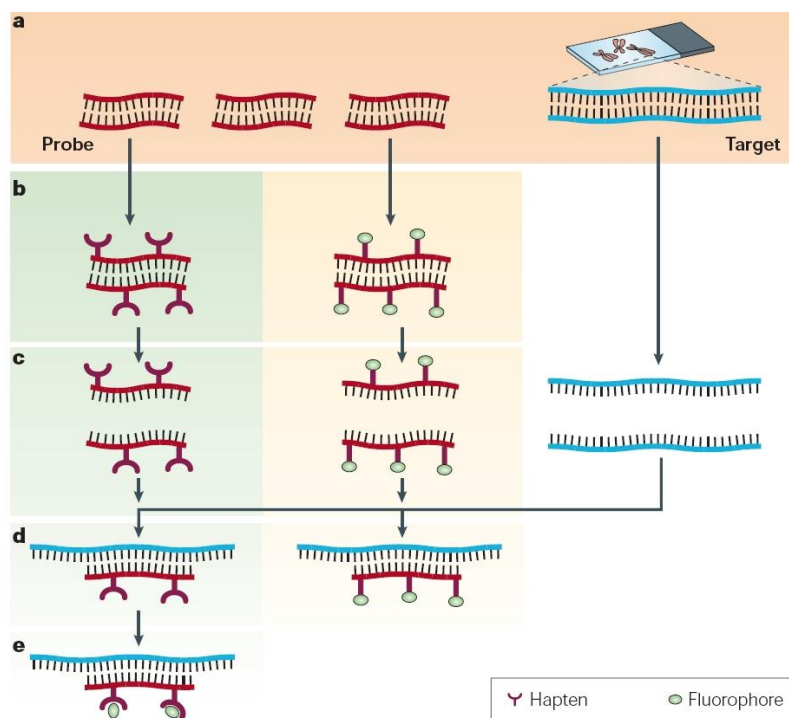


Figure 3 Principles of FISH. Reproduced from Nature Publishing Group [75]

2. Aim of the study

The aim of the work in this thesis was to optimize methods for molecular characterization of single CTCs from pancreatic cancer patients by single cell reverse transcription PCR, validate these methods and apply them to blood samples from healthy control persons and patient undergoing treatment for locally advanced and/or metastatic pancreatic cancer. The patients were recruited from an ongoing trial at Stavanger University Hospital and Haukeland University Hospital, called PACT-ACT (PANcreatic Cancer Treatment And Circulating Tumor Cells).

3. Materials

3.1 Blood samples

Blood samples from patients and healthy control individuals were collected in 9 mL Vacuette® EDTA tubes, which are designed for the examination of whole blood. The inner wall of the tube is coated with either K₂EDTA or K₃EDTA. EDTA (Ethylenediaminetetraacetic acid) binds to calcium ions and block the coagulation cascade [77]. Precautions were made to not contaminate the blood sample with epithelial cells from the puncture. This was carried out by collecting the first 1-2 mL blood in a spare tube that was thrown away, before taking the blood sample.

3.1.1 Patient samples

The patient samples used in this study were obtained from patients admitted to Stavanger University Hospital and Haukeland University Hospital with locally advanced and/or metastatic pancreatic cancer. The included patients participated in the PACT-ACT study, which is an open two-armed phase IIB trial of the new nab-paclitaxel + gemcitabine combination in comparison with standard gemcitabine monotherapy. The primary aim of the PACT-ACT study is to investigate the clinical utility of CTC detection and characterization as potential biomarkers for treatment monitoring, treatment response, disease progression and survival in the recruited pancreatic cancer patients.

Patients included in this study from Stavanger University Hospital were diagnosed with locally advanced and metastatic pancreatic cancer. Only patients with metastatic pancreatic cancer were included from Haukeland University Hospital. The first blood samples were drawn before chemotherapy, later blood samples were drawn monthly from each patient during chemotherapy. Samples for this study were taken simultaneously with routinely collected samples to minimize additional sampling burden for the patients.

All patients included in this study were informed both orally and written about the study, and consented to be a part of it. The study protocol was approved by the Regional Ethical Committee (REK 2011/475).

3.1.2 Control samples

Control samples were collected from healthy individuals aged 25 to 55 years.

3.2 Cell lines

Below is a description of the cell lines used as models in this thesis. See Table 4 for detailed information about distributor and order number. All cell lines used are adherent.

- AsPC-1: Epithelial cell line obtained from ascites fluid in a 62 years old woman with metastatic adenocarcinoma in the head of the pancreas. The cell culture is known to produce abundant mucin, carcinoembryonic antigen (CEA), human pancreas specific antigen and human pancreas associated antigen [78].
- BxPC-3: An epithelial cell line derived from a 61 year old female with a primary adenocarcinoma of the pancreas. Produces CEA, human pancreas-specific antigen, human pancreas cancer-associated antigen and traces of mucin [78].
- PANC-1: Cell line from cells derived from 56 years old male with adenocarcinoma in the head of the pancreas with invasion of the duodenal wall, metastasis to the peripancreatic lymph node were discovered [78].

Table 4 Cell Lines used in the thesis

Cell line	Distributor	Order number
AsPC-1	European Collection of Cell Cultures (ECACC)	96020930
BxPC-3	European Collection of Cell Cultures (ECACC)	93120816
PANC-1	European Collection of Cell Cultures (ECACC)	87092802

3.3 Reagents

The reagents used in this thesis are listed in Table 5. TaqMan® gene expression assay (20x) used are listed in Table 6.

Table 5 Reagents used in this thesis

Product	Manufacturer	Order number
0.25 % Trypsin/EDTA	Sigma	T4049
NaCl	Sigma Aldrich	S3014-1KG
10 % Foetal Bovine Serum (FBS)	Sigma	F7524
1mM Sodium Pyruvate (NaP)	Sigma	S8636
2mM Glutamine	Sigma	G7513
Albumin from Bovine Serum	Sigma-Aldrich	A70030-10G
Alexa Fluor® 555-anti-EpCAM	Cell Signal Technology®	5488

Product	Manufacturer	Order number
Alexa Fluor® 647 anti-human CD45 antibody	BioLegend®	304020
Anti-EpCAM antibody [B29.1 (VU-ID9)] (FITC)	Abcam	ab8666
CD326 (EpCAM) MicroBeads, human	Miltenyi Biotech	130-061-101
CD326 EpCAM FITC, human	Miltenyi Biotech	130-080-202
CD45-Dylight550	BioTrend	C162150
CD45-eFluor 605NC	Affymetrix, eBioscience	93-0459-41
CD45-FITC, human (clone: 5B1)	Miltenyi Biotec	130-080-202
CellsDirect™ One-Step qRT-PCR kit	Invitrogen by Life Technology	11753-100
DAPI (4',6-diamidino-2-phenylindole)	Sigma Aldrich	32670
DMEM medium	Gibco by Life Technologies	1196-044
FcR Blocking Reagent, human	Miltenyi Biotech	130-059-901
Lymphoprep™	Axix Shield, by Alere™	1114545
MACS® Dead Cell Removal	Miltenyi Biotec	130-090-101
MMI CapillaryClean solution	Molecular Machines & Industry (MMI)	80107
NucBlue® Live ReadyProbes® Reagent (Hoechst 33342)	Life Technologies	R37605
Penicillin Streptomycin (100x)	Sigma	P4333
Phosphate Buffered Saline (PBS)	Sigma Aldrich	D8537
RNase OUT, RNase Inhibitor	Invitrogen by Life Technology	10777-019
RPMI 1640 medium	Sigma	R0883
TaqMan Gene Expression Master Mix 2x	Invitrogen by Life Technology	4369016
Trypan Blue Solution (0.4 %)	Sigma Aldrich	T8154

Table 6 TaqMan® Gene Expression Assay

Gene Symbol	Gene Name	Ensembl Gene	Amplicon Length	Order Number
ALDH1A1	ALDH1A1	ENSG00000165092	61	Hs00946916_m1
CD24	CD24	ENSG00000272398	140	Hs02379687_s1
CDH1	E-Cadherin	ENSG00000039068	61	Hs01023894_m1
CDH2	N-Cadherin	ENSG00000170558	66	Hs00983056_m1
EPCAM	EPCAM	ENSG00000119888	64	Hs00158980_m1
HPRT1	HPRT1	ENSG00000165704	82	Hs02800695_m1
KRT 8	CK8	ENSG00000170421	164	Hs01595539_g1
PTPRC	CD45	ENSG00000081237	57	Hs04189704_m1
VIM	Vimentin	ENSG00000026025	73	Hs00185584_m1
ZEB1	ZEB1	ENSG00000148516	63	Hs00232783_m1
CD44	CD44	ENSG00000026508	70	Hs01075861_m1

3.4 Materials and equipment

All materials and equipment used in this thesis are listed in Table 7, in addition regular laboratory equipment was used.

Table 7 Materials and equipment

Product	Producer	Product number
15 µ-Slide 8 Well	Ibidi	80826
GeneAmp® PCR System 2700	Applied Biosystems	N/A
Light Cycler 480	Roche	N/A
LS Column	Miltenyi Biotech	130-042-401
Mini MACS Starting kit	Miltenyi Biotech	130-042-102
MMI Capillaries 40 µm	Molecular Machines & Industry (MMI)	80105
MMI CellEctor with Olympus IX81 and X-Cite 120PCQ	Molecular Machines & Industry (MMI)	N/A
MS Column	Miltenyi Biotech	130-042-201
SepMate™ tubes	Stem Cell Technologies	15450
T25/T75 culture flask	Sarstedt	831810/831811
Vacuett® EDTA tubes	Greiner Bio-One	455036

4. Methods

4.1 Cell culture

4.1.1 Introduction

Cancer cell cultures derived from human tissue or fluid are today cultured in laboratories around the world. Primary cultures are the first lines of cells taken from humans. If subcultures of the primary culture are made, these are called cell lines. Flasks or petridishes are used to facilitate growth, as many cell lines adhere to glass or plastic. For optimal growth the environment of the cells must be regulated. Furthermore, the cells growth medium must be adjusted to the specific cell lines cells and their requirements for optimal growth. [79]

Human cancer cell lines are widely used as models for studying the biology of cancer. The cell line cells represent a subpopulation of the tumor that they derive from, therefore, they do not give a picture of the heterogeneity of the cancer cells within the tumor. [80]

4.1.2 Protocol

All handling of cell cultures, reagents and equipment must be performed in accordance with good antiseptic techniques, in a laminar air flow cabinet.

4.1.2.1 Resuscitation of cryocultures

1. Turn on UV-light in a laminar air flow cabinet 30 minutes before use. Place the correct growth medium for the cell line in a water bath and preheat to 37°C.
2. Add 10/25 mL pre-heated culture media to a T25/T75 flask.
3. Transfer a cryoculture from the liquid nitrogen freezer to a 37°C water bath. Allow the cell suspension to thaw almost completely.
4. Transfer the cells in a drop-wise manner into the medium.
5. Incubate cells in a 5 % CO₂ humidified atmosphere at 37°C. Split the cells when they are 70-80 % confluent according to the protocol below.

4.1.2.2 Subculturing

1. Turn on the UV-light in a laminar air flow cabinet 30 minutes before use. Place the correct culture media, PBS and trypsin/EDTA for the cell line in a water bath and preheat to 37°C.
2. Remove the old culture media from the cells by pipetting.
3. Wash the cells with 10 mL PBS, preheated to 37°C.
4. Trypsinate the cells using 2 mL Trypsin/EDTA preheated to 37°C.
5. Incubate cells at 37°C for 2-7 minutes or until the cell are completely detached from the plastic surface.
6. Add an excess of culture media, preheated to 37°C, to stop the enzyme activity.
7. Add 25 mL culture media to a new culture flask. Transfer 1:3 to 1:6 (depending upon cell line) of the cell suspension to the new flask.
8. Incubate cells in a 5 % CO₂ humidified atmosphere at 37°C. Split the cells when they are 70-80 % confluent.

4.1.2.3 Cell counting of cultures

1. Transfer 50 µL cell suspension (after trypsination if the cells are adherent) to an Eppendorf tube and add 50 µL Trypan Blue, incubate for a minute.
2. Transfer 20 µL of the mix to a standard hemocytometer.
3. Count a minimum of 200 cells using a microscope at 10x magnification. Count as many counting squares as needed to reach 200 cells. One counting square is combined by 16 smaller squares within the three narrow lines (Figure 4). Only count the viable cells, which are those not stained with Trypan Blue.

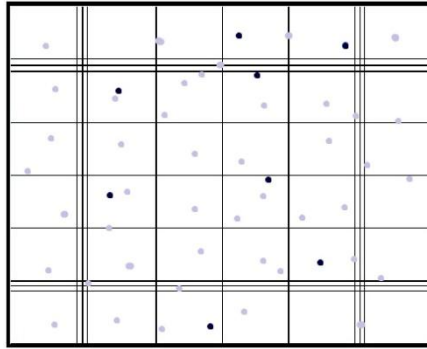


Figure 4 Illustration of counting area in a hemocytometer

4. Calculate the number of cells in the original cell suspension, according to the formula below.

$$\text{average amount of cells per square} = \frac{\text{total cells counted}}{\text{number of squares counted}}$$

$$\text{Cell concentration} = \frac{\text{cells}}{\text{ml}} = \text{average amount of cells per square} \times 2 \times 10^4$$

4.2 Density gradient separation

4.2.1 Introduction

Lymphoprep™ is a density gradient medium recommended for the isolation of mononuclear cells from peripheral blood cells [81]. Density gradient separation is a common method used to separate different cell types. Mononuclear cells with densities under 1.077 g/mL could be isolated by centrifugation in an iso-osmotic medium [82]. Therefore, granulocytes and erythrocytes with higher densities will separate under the Lymphoprep™ layer during centrifugation, and CTC will sediment above together with the other mononuclear cells [83]. This is possible because CTCs also are mononuclear cells. This method for isolation of mononuclear cells is simple and effective and has been used for over 35 years [81].

SepMate™ tubes were used together with Lymphoprep™ to facilitate the isolation. SepMate™ tubes contain an insert that provides a barrier between the density gradient medium and the blood.

4.2.2 Protocol

1. Collect the blood samples in 9 mL Vacuett® EDTA tubes. Process the blood samples within 24 hours.
2. Add 15 mL Lymphoprep™ to a SepMate™ tube. Prepare the tube carefully to avoid bubbles.
3. Transfer the collected blood (9 mL) to a 50 mL tube and add 9 mL 0.9 % NaCl. Ensure that all of the blood is transferred.
4. Transfer the diluted blood to the SepMate™ tube by carefully pouring the sample.
5. Centrifuge the tubes at 2000 rpm (800xg) for 30 minutes (20 minutes if the sample is taken within less than 2 hours) with breaks.
6. Remove as much of the plasma fraction as possible without interfering the monolayer containing PBMCs.
7. Transfer all the remaining liquid above the plastic filter in the SepMate™ tube to a new 50 mL tube by pouring. This must be performed quickly to ensure that the liquid and the cells beneath the plastic filter are not decanted.
8. Wash the PBMCs with 45 mL cold 0.9 % NaCl and centrifuge at 1100 rpm (300xg) for 10 minutes. Discard the supernatant. From this point all the reagents and the centrifuge should be kept at 4°C if not stated otherwise. Work on ice.
9. Wash with 45 mL cold PBS and resuspend the pellet carefully by inverting the tubes or by careful pipetting.
10. Centrifuge the cell suspension at 1100 rpm (300xg) for 10 minutes and discard the supernatant.
11. Add 1 mL cold PBS and resuspend cell pellet carefully by gentle pipetting.
12. Count the cells according to chapter 4.2.2.1 below.
13. Proceed to MACS cell separation (4.3).

4.2.2.1 Cell counting of PBMC

Count the mononuclear cell suspension from peripheral blood sustained with density gradient separation according to protocol below.

1. Transfer 50 μL Trypan Blue to an Eppendorf tube and add 5 μL cell suspension.
2. Transfer 20 μL of the mix to a standard hemocytometer.
3. Count a minimum of 200 cells using a microscope at 10x magnification. Count as many counting squares as needed to reach 200 cells. One counting square is combined by 16 squares within the three narrow lines, see Figure 4. Only count the viable cells, which are those not stained with Trypan Blue.
4. Calculate the number of cells in original cell suspension, according to the formula in below.

$$\text{average amount of cells per square} = \frac{\text{total cell count}}{\text{number of squares counted}}$$

$$\text{Cell concentration} = \frac{\text{cells}}{\text{ml}} = \text{average amount of cells per square} \times 20 \times 10^4$$

4.3 Dead Cell Removal

4.3.1 Introduction

The Dead Cell Removal kit from Miltenyi Biotec provides a method for elimination of cell debris and apoptotic or dead cells in a cell suspension. The unwanted cells are magnetically labeled with micro beads and buffer, and removed by magnetic separation.

4.3.2 Protocol

The Dead Cell Removal experiments were performed according to the Dead Cell Removal Kit manufacturer's protocol.

4.4 MACS Cell Separation

4.4.1 Introduction

MACS® cell separation based on micro beads coated with antibodies against epithelial cell adhesion molecule (EpCAM) was used to isolate CTCs from the PBMC fraction generated by protocol 4.2.2 above. EpCAM is expressed on the surface of cells with epithelial origin such

as epithelial derived tumor cells [84]. FcR Blocking Reagent is used to prevent FcR-mediated non-specific labeling of non-epithelial cells, before the magnetic labeling [84].

The EpCAM positive cells are labeled with CD326 EpCAM Micro Beads. The labeled cells are separated from the rest of the suspension when loaded onto a MACS® column placed in a magnetic field [84]. The labeled cells will retain in the column, while the unlabeled cells runs through. After removing the column from the magnetic field the EpCAM positive cells could be eluted and collected for further analysis [84].

4.4.2 Protocol

Proceed with the cell suspension of mononuclear cells separated with density gradient separation from chapter 4.2.2.

4.4.2.1 EpCAM microbead labeling

1. Centrifuge the cell suspension at 1100 rpm (300xg) for 10 minutes and aspirant the supernatant completely. Keep the centrifuge constantly at 4°C and work on ice throughout the procedure.
2. Resuspend the cell pellet in 300 µL cold MACS buffer per 5×10^7 total cells.
3. Add 100 µL cold FcR Blocking Reagent per 5×10^7 total cells and mix well.
4. Add 100 µL cold CD326 (EpCAM) Microbeads per 5×10^7 total cells and mix well.
5. Incubate in a refrigerator (4°C) for 30 minutes.
6. Wash the cells by adding 5-10 mL MACS buffer per 5×10^7 total cells and centrifuge at 1100 rpm (300xg) for 10 minutes.
7. Resuspend up to 10^8 cells in 500 µL cold MACS buffer.
8. Proceed to magnetic separation (4.4.2.2).

4.4.2.2 Magnetic separation

1. Place an MS column in a MiniMACS Separator in the magnetic field of a MACS magnet.

2. Prepare the column by rinsing with 500 μ L cold MACS buffer. Do not let the column run dry.
3. Apply the cell suspension onto the column.
4. Discard the unlabeled cells that pass through the column. Wash the columns with 3 x 500 μ L cold MACS buffer. Add new buffer only when the column reservoir is empty.
5. Remove the column from the separator and place it in a suitable collection tube.
6. Pipette 1 mL cold MACS buffer onto the column. Immediately flush out the magnetically labeled cells by firmly pushing the plunger into the column.
7. Proceed to immediately to chapter 4.5.

4.5 Immunofluorescent and nuclear staining

4.5.1 Introduction

Immunofluorescent staining was used to distinguish CTCs from contaminating leukocytes during micromanipulation. Immunofluorescent staining is a method used in almost all aspects of biology. The fluorescent stains should have low photo bleaching. Photo bleaching is permanent loss of fluorescence and could be caused by several factors. Antibodies are chemically conjugated to fluorescent dyes such as fluorescein isothiocyanate (FITC) and rhodamine isothiocyanate (TRITC) to create immunofluorescent stain. The antibodies of interest, in this case EpCAM and CD45, will bind directly to their respective antigens [85].

In order to determine the viability of the cells of interest the cell nucleus was stained with Hoechst DNA dye. When a DNA dye is used in live cell fluorescent microscopy, it is important that the dye has low cytotoxicity and phototoxicity, along with low photobleaching. Hoechst dyes emit blue fluorescence under ultraviolet (UV) illumination, when bound to DNA. UV light might damage cellular DNA and the exposure time should be restricted [86].

4.5.2 Protocol

1. Centrifuge the cell suspension at 1100 rpm (300xg) for 5 minutes at 4°C. Discard the supernatant and resuspend the pellet in 100 μ L cold MACS buffer.
2. Add 25 μ L FcR Blocking Reagent. Incubate for 1 minute on ice.

3. Add 2 μL 0.1 mg/mL CD45 Dylight 550 (Biotrend) (1:63)
4. Add 2 μL CD326 EpCAM, FITC (Miltenyi Biotec) (1:63)
5. Add 7.5 μL Hoechst 33342NucBlue® Live ReadyProbes® Reagent (Life Technologies) (1:16)
6. Incubate for 20 minutes in the dark at room temperature.
7. Centrifuge the cell suspension at 1100 rpm (300xg) for 10 minutes at 4°C. Discard the supernatant and resuspend the pellet in 100-300 μL cold MACS buffer.
8. Proceed to single cell collection by micromanipulation.

4.6 Single-cell collection

4.6.1 Introduction

MMI CellEctor (by Molecular Machines & Industry) was used to isolate single CTCs by micromanipulation. MMI CellEctor is a capillary which is controlled by a 3D CellRobot arm, connected to an inverted microscope (Olympus IX81). The software is developed to scan through a cell suspension marking out the cells of interest. The cells of interest could then be isolated for further analysis. The microscope has fluorescence filters making it possible to distinguish cells according to antibody specific staining.

4.6.2 Protocol

1. Turn on the computer, the microscope and the MMI software. Calibrate according to the user manual.
2. Transfer 11 μL Lysis Solution to a PCR sealing foil on the deposit slide. Ensure that the droplets will fit in the wells of a 96 well PCR plate by using a template.
3. Pump out oil in order to fill half the capillary. Fill the rest of the capillary with MQ H_2O from the service slide. Leave an air bubble between the oil and the water in the capillary.
4. Use a slide that is pre-siliconized with RepelSilan.
5. Transfer the cell suspension, from step 7 chapter 4.5.2, to the sample slide. Turn of the lights, and work in the dark for the rest of the procedure.

6. Let the cells settle on the slide. This might take up to 10 minutes.
7. Use the CellExplorer function and scan the cell suspension using the pre-chosen criteria. The criteria are described in chapter 4.10.1. Pick up to 15 potential CTC and 5 leukocytes from each patient sample.
8. Locate the cells of interest. Acquire the cells by pumping in 10-100 nL suspension.
9. Transfer the cells to a droplet of Lysis Solution on the PCR sealing foil by pumping out 500 nL from the capillary.
10. Wash the capillary between each aspiration with MQ H₂O, or MMI Washing Solution if the capillary is dirty.
11. Repeat for all cells of interest.
12. Clean the capillary and turn off the microscope according to the user manual.

4.7 Single-cell cDNA synthesis and pre-amplification

4.7.1 Introduction

When using CellsDirect™ One-Step qRT-PCR kit, the single cells are lysed and all the lysate is reverse transcribed and pre-amplified, with minimal handling time and sample loss. An additional step with DNase I are added to the lysate to eliminate genomic DNA prior to the PCR reaction [87].

The amount of mRNA in a single-cell is low. In order to gain enough material to perform a successful qPCR analysis, CellsDirect™ One-Step qRT-PCR kit has used. The CellsDirect™ kit allows multiplex pre-amplification with mRNA-specific primers.

4.7.2 Protocol

4.7.2.1 Lysis of single cells

1. Carefully transfer the PCR sealing foil containing cells, from step 9, chapter 4.6.2, to a 96 well PCR plate. Ensure the droplets on the PCR sealing foil are placed directly above a well, and that the PCR sealing foil is attached to the PCR plate.

2. Centrifuge briefly to collect the droplets containing the single cells in the wells of the PCR plate.
3. Remove the old PCR sealing foil. Seal the plate with a new PCR sealing foil, transfer the plate to a PCR machine pre-heated to 75 °C. Incubate for 15 minutes.
4. Vortex and centrifuge the plate briefly to collect the contents.

4.7.2.2 DNase I digestion

1. Add 6.6 µL DNase I Reaction Mix (Table 8) to each sample well while the plate is kept on ice.

Table 8 DNase I digestion reaction mix from the CellsDirect™ One-Step qRT-PCR kit

Reagent	Volume per reaction
DNase I, Amplification Grade (1U/µL)	5 µL
10x DNase I Buffer	1.6 µL
Total DNase I Reaction Mix	6.6 µL

2. Mix gently by pipetting. Centrifuge briefly to collect the contents.
3. Incubate the samples for 5 minutes at room temperature (more than 10 minutes could destroy samples). Centrifuge briefly to collect the contents.
4. Add 4 µL 25 mM EDTA to each well in order to stop the reaction. Work on ice. Mix gently by pipetting and centrifuge briefly to collect the contents.
5. Incubate the samples in a pre-heated PCR machine at 70 °C for 10 minutes. Centrifuge briefly and place the PCR plate on ice.

4.7.2.3 One-step reverse-transcription and pre-amplification

1. Add 30.5 µL CellsDirect Master Mix (Table 9) to each well. Work on ice.

Table 9 CellsDirect™ Master Mix from CellsDirect™ One-Step qRT-PCR kit

Reagent	Volume per reaction
SuperScript®III/Platinum Taq Mix	1 µL
2x Reaction Mix	25 µL
0.5 x pooled TaqMan® assays	4.5 µL
Lysate	20.6 µL
Total CellsDirect Master Mix	51.1 µL

2. Seal the PCR plate with a new PCR sealing foil, and centrifuge briefly to collect the contents.
3. Transfer plate to a PCR machine and run the program according to Table 10 below.

Table 10 Pre-amplification and revers-transcription

Stage	Step	Temperature	Time
Reverse transcription/ Enzyme activation of Platinum Taq		50 °C	15 minutes
		95 °C	2 minutes
Cycling (14 cycles)	Denaturate	95 °C	15 seconds
	Anneal/Extend	60 °C	4 minutes
Holding		4 °C	∞

4. Dilute the samples 1:5 in MQ H₂O, transfer samples to pre-labeled 1.5 mL Eppendorf tubes.
5. Store the samples at -20 °C.

4.8 Single-cell qPCR

4.8.1 Introduction

Polymerase chain reaction (PCR) is a biochemical technology used to amplify a small number of target DNA sequences to millions of PCR products (copies). This allows for a great sensitivity of detection [64]. The technique was developed by Kary Mullis in 1983, for which he received the Nobel Prize in chemistry in 1993 [88]. The principle of PCR is based on thermal cycles of heating and cooling [88]. A basic PCR reaction consists of three steps: Denaturation, annealing and extension.

Quantitative PCR (qPCR) is a much used method to detect and measure the relative amount of nucleic acid in a sample [89]. The principle behind the technique qPCR is very similar to traditional PCR. The main difference is in the measurement of PCR products. For the work in this thesis a TaqMan hydrolysis probe was used [89]. A hydrolysis probe is sequence specific. [89-91] The hydrolysis probe consists of a fluorescent reporter and a quencher. When the quencher is in proximity to the fluorescent reporter, the quenching molecules will absorb energy from the fluorophore and inhibit fluorescence signal [91] (Figure 5).

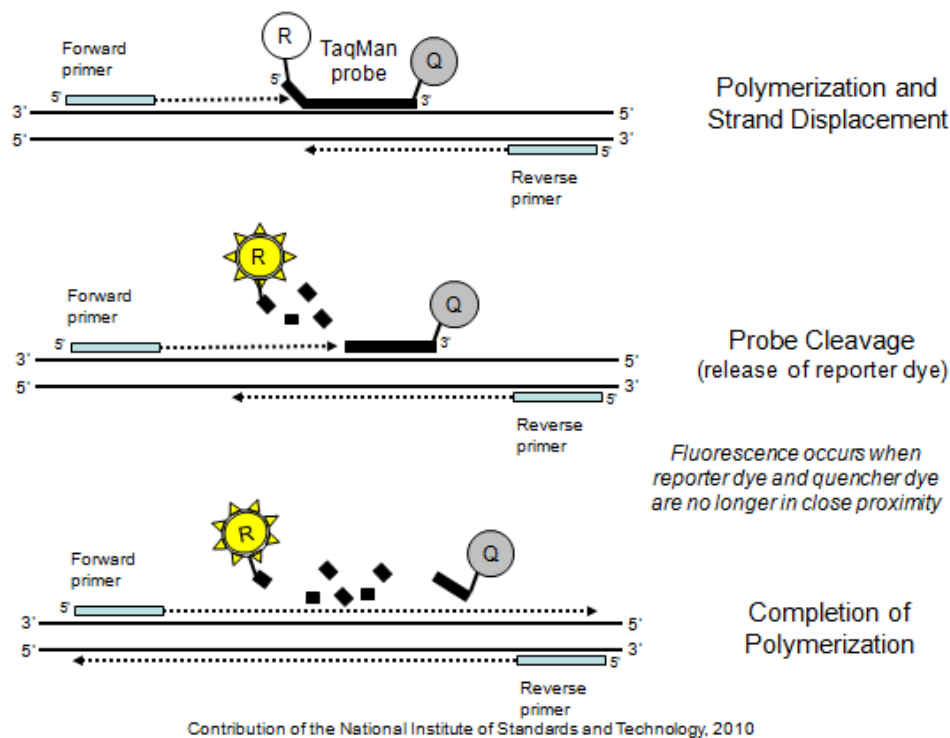


Figure 5 Hydrolysis probes, TaqMan. From Fundamentals of Forensic Science by J.Butler. [91]

Once the probe hybridizes the complementary target, the Taq polymerase cleaves the hydrolysis probe. The fluorescent reporter is then separated from the quencher. Thus, a fluorescent signal is generated and can be measured to calculate the amount of PCR product.

The amount of fluorescence signals is directly proportional to the DNA concentration in the sample [89]. Hence, there will be a linear relationship between the PCR product and the fluorescence intensity which could be used to calculate the relative amount of template in the original sample. The most important parameter for qPCR is the C_q-value [89]. The C_q-value is the point where fluorescence first is detected as significant above the baseline. If the initial amount of template is high, the faster the fluorescence will be detectable, and the C_q-value will be correspondingly low [89]. When the amount of template is low, the number of amplification cycles before the baseline is reached will be high, and the C_q-value will be correspondingly higher.

4.8.2 Protocol

1. Thaw the cDNA samples on ice.
2. Thaw the TaqMan Gene Expression Assay in room temperature. Make one master mix for each mRNA assay, according to Table 11. Vortex the master mix.

Table 11 TaqMan assay master mix

Reagents	Volume per sample
TaqMan Gene Expression Master Mix 2x	12.5 µL
TaqMan Gene Expression Assay (20x)	1.25 µL
mQ H ₂ O	9.25 L

3. Add 23 µL to each well in a LS 420 white PCR plate according to the PCR plate setup.
4. Add 2 µL calibrator cDNA to each calibrator wells. For further details regarding calibrator samples, see chapter 4.9 below.
5. Add 2 µL MQ H₂O as negative control, to each NTC well.

6. Add 2 μL cDNA samples from step 4, chapter 4.7.2.3 to each sample well.
7. Centrifuge the plate briefly and place it in a LightCycler® 420 qPCR machine.
8. Run the program according to Table 12 below.

Table 12 qPCR setup using TaqMan® probe

Stage	Step	Temperature	Time
Enzyme activation	Activation	95 °C	10 minutes
Cycling (40 cycles)	Denature	95 °C	15 seconds
	Anneal/Extend	60 °C	1 minute
Holding		4 °C	∞

4.9 Relative quantification

Several normalization strategies have been explored for single cells. The most frequently used method is normalization to a constant expressed housekeeping reference mRNA and to a calibrator sample included in every run. The aim of normalization against a reference mRNA is to correct for variations in RNA quality and reverse transcription efficiency between samples. Normalization against a calibrator sample is usually done to correct for run-to-run variations. Although normalization against a reference mRNA has been used for single cells in other studies [92], there are drawbacks with this strategy. An alternative could be to not use normalization or to only normalize against a calibrator sample. The calibrator sample will also work as a positive control. A positive control is used as an indicator of the quality of the qPCR run. The calibrator sample used was cDNA from SDM103T2 cell line, previously made by the research group to compliment the mRNA markers used in this study.

Relative gene expression was calculated for each mRNA marker using Equation 1, when normalization to a reference mRNA and a calibrator sample were conducted.

Equation 1

$$R = 2^{\Delta\Delta Cq}$$

Where:

R = relative mRNA concentration for target biomarker

2 = amplification efficiency

Equation 2

$$\Delta\Delta Cq = \Delta Cq_{sample} - \Delta Cq_{calibrator}$$

Equation 3

$$\Delta Cq_{sample} = Cq_{biomarker\ sample} - Cq_{reference\ sample}$$

Equation 4

$$\Delta Cq_{calibrator} = Cq_{biomarker\ calibrator} - Cq_{reference\ calibrator}$$

Equation 5

$$\Delta Cq_{sample} = Cq_{biomarker\ calibrator} - Cq_{biomarker\ sample}$$

When using normalization only to a calibrator sample, the relative gene expression was calculated for each mRNA marker using Equation 6. Mean Cq-values are used in the calculations, based on two replicates.

Equation 6

$$R = 2^{\Delta Cq_{sample}} = 2^{Cq_{biomarker\ calibrator} - Cq_{biomarker\ sample}}$$




4.10 Criteria for evaluation of single cells

Several CTC criteria were defined. First line of selection was made by immunofluorescent staining of potential CTCs during micromanipulation. Second line of selection was an inspection of RNA quality after the initial qPCR.

4.10.1 Immunofluorescent staining

Immunofluorescent staining was used to distinguish between contaminating leukocytes and CTCs during micromanipulation. When using Hoechst staining of the cell nucleus, it is possible to evaluate the viability of the cell. Cells were collected according to the criteria given in Table 13.

Table 13 Immunofluorescent staining criteria

Cell type	Fluorescent appearance	Picture
CTC	Strong green fluorescence (EpCAM), weak or strong blue nucleus and no red fluorescence (CD45).	
Possible CTC	Strong or weak green fluorescence (EpCAM), weak or strong blue nucleus and some fluorescence (CD45). In addition cells with strong green fluorescence (EpCAM) and weak or strong red fluorescence (CD45) are included.	
Leukocyte	No green fluorescence (EpCAM), weak or strong blue nucleus and strong red fluorescence (CD45)	

4.10.2 mRNA quality

It is a challenge to collect mRNA from single cells that have sufficient quality to perform molecular characterization. In order to confirm cells as CTCs several gene expression assays are used. If the RNA quality of the cell is poor, important information could be lost. Therefore, strict criteria for the evaluation of the mRNA quality in the single cells were made for this thesis.

All the single cells isolated by micromanipulation were first analyzed with qPCR for the mRNA markers *HPRT1* and *Vimentin*. The possible CTCs found in patient samples, from chapter 4.6, were divided into three mRNA categories as shown in Table 14 above. The categories are based on gene expression levels of the mRNA *HPRT1* and *Vimentin*. *HPRT1* is a housekeeping gene, and *Vimentin* is a mesenchymal marker, both expressed in high levels.

Only cells that meet the criteria in category III were used for further genetic analysis with the rest of the mRNA markers.

Table 14 mRNA quality criteria

Category	Description	mRNA expression
I	Poor mRNA quality	Neither <i>HPRT1</i> or <i>Vimentin</i>
II	Medium mRNA quality	Only <i>Vimentin</i> or <i>HPRT1</i>
III	Good mRNA quality	Both <i>Vimentin</i> and <i>HPRT1</i>

4.11 Statistical analysis

Hierarchical cluster analysis was used to compare the transcript profiles of the single cells obtained by RT-qPCR. The software used for the hierarchical cluster analysis was Expander 6.0. There are two strategies for hierarchical clustering which are the agglomerative and the divisive. Agglomerative is the most common strategy, used by the Expander 6.0, where each observation is placed in a separate cluster and clustering is created upwards. Distance matrix analysis was used to define the distance between the data. The method used for distance matrix calculation in this study was Pearson Correlation, which is the only available option in Expander 6.0.

Dendrograms are created by clusters, the clusters are defined by the use of either average-, single- or complete linkage [93]. Complete linkage was chosen because of the distance between the expression levels in leukocytes and cancer cell lines. In complete linkage the distance between two clusters is calculated as the distance between the two objects in each cluster that is furthest away from each other, illustrated in Figure 7. This linkage strategy tends to form compact and discrete clusters. Single-linkage will do the opposite and calculate the distance between the closest objects from two clusters. Average-linkage calculates the average of all the distances between the objects in the two clusters, illustrated in Figure 7. The raw data were log₂ transformed by Expander 6.0 before the hierarchical cluster analysis. The color coding in the heat map is weighted according to the clustering results.

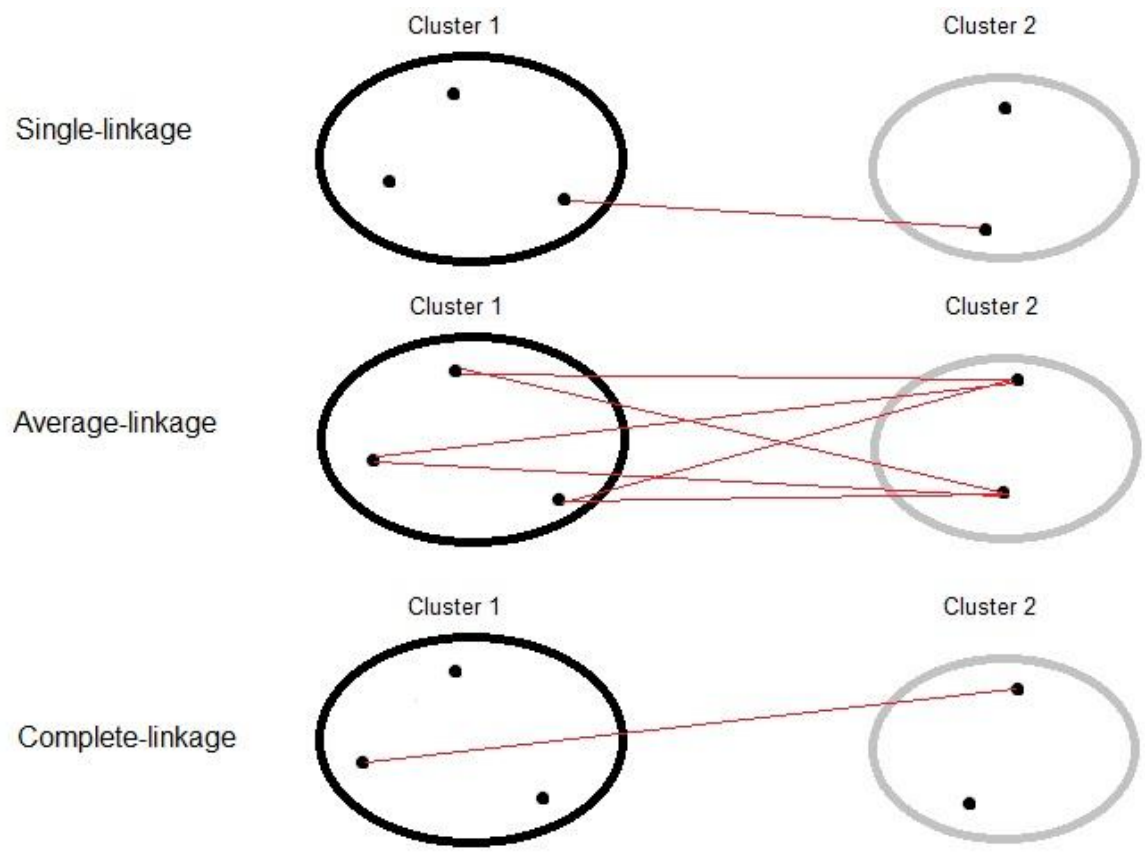


Figure 6 Illustration of the option for linkage between clusters for creation of hierarchical cluster analysis.

5 Results

5.1 Overview of the experimental approach

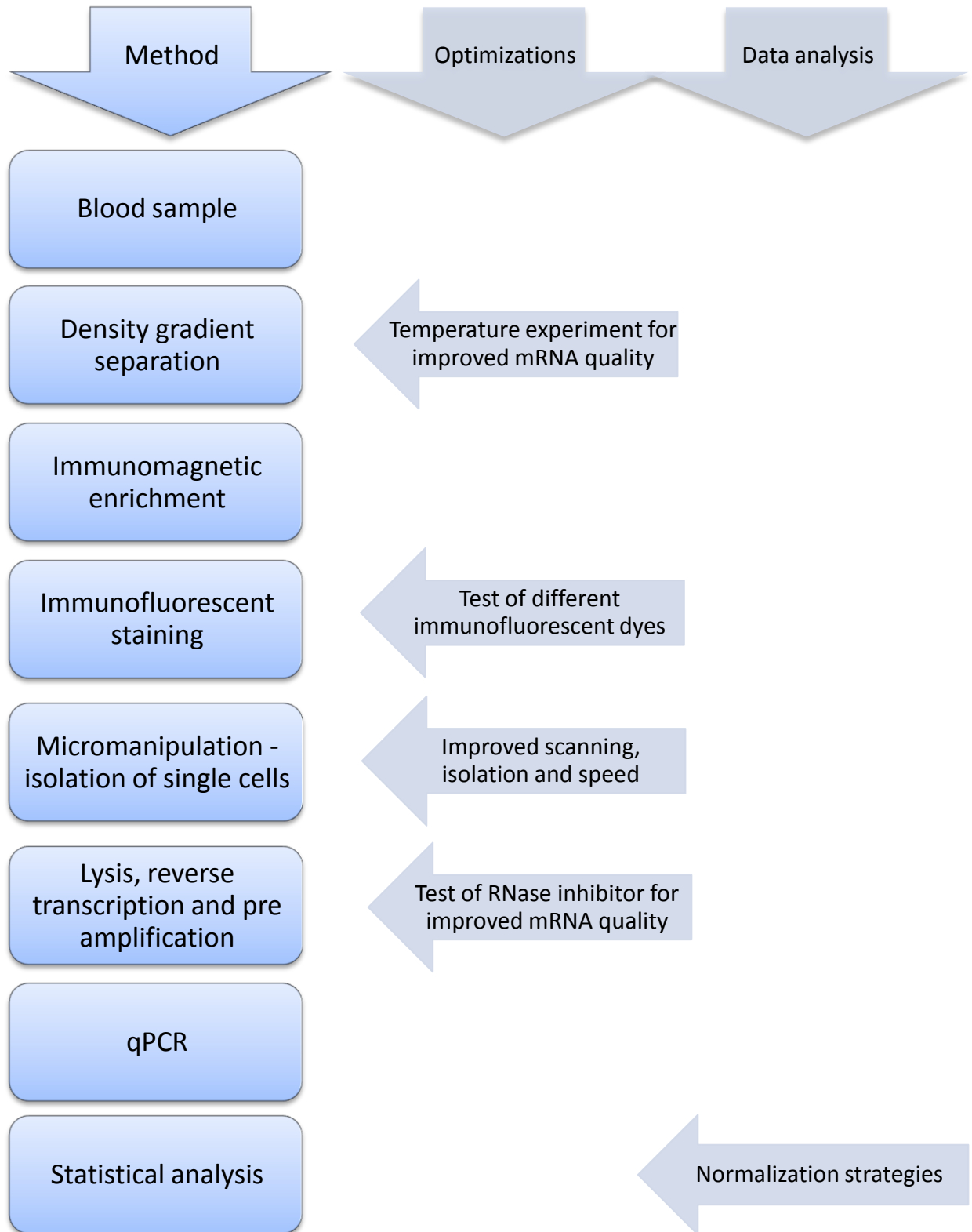


Figure 7 Overview of the experimental approach for this thesis.

The research group had previously performed initial work to establish methods for the enrichment and molecular characterization of single CTCs from peripheral blood samples. However, these methods were still immature for applications to clinical samples. Thus, the first part of the thesis deals with further optimization and validation of these methods. The second part of this thesis concerns the application of the optimized methods to clinical samples. An overview of the methodology, the optimizations and the approaches for data analysis used in this study is illustrated in Figure 7.

A comprehensive enrichment and characterization process was used for molecular characterization of CTCs by single-cell RT-qPCR. First, the mononuclear cells in the blood were separated from the rest of the blood cells using density gradient separation. Then potential CTCs among the mononuclear blood cells were enriched by an immunomagnetic approach. This was followed by immunofluorescent staining and micromanipulation for the isolation of single cells. Finally, reverse transcription and pre-amplification followed by qPCR was performed to molecularly characterize the potential CTCs. Statistical analysis was performed for interpretation of the results.

5.2 Optimization of methods

5.2.1 Micromanipulation

Micromanipulation with MMI CellEctor by Molecular Machines and Industries was used to isolate single cells. In collaboration with the manufacturer a new version of the instrument software was tested. Improvements to the software were made to complement our method. The main improvements in the software were made within the scanning function. The software facilitates scanning of the cell pool with different fluorescent filters. During scanning it detects cells according to pre-set criteria. The scanning application was enhanced to allow for easier detection and highlighting of the possible CTCs.

The acquisition process was improved to avoid contamination of the single CTC of interest from other cells or cell debris present in the cell suspension. Cells would easily adhere to the microscope slide which made it difficult to pick them. A method of siliconizing the microscope slides was developed to prevent adhesion of the cells, thus making it easier to pick cells. The improved version of the software was chosen for micromanipulation of single cells in this study.

5.2.2 Immunofluorescent staining

An antibody targeting the epithelial-specific cell-surface protein EpCAM and an antibody targeting the leukocyte-specific cell-surface protein CD45 were chosen for identification of CTCs in a great excess of leukocytes. Antibodies conjugated to fluorophores were chosen for visualization of cells in a fluorescence microscope. The chosen antibodies were required to be conjugated to fluorophores which are relatively photo-stable, have strong fluorescent signal and to not interfere with each other. The best suited type of fluorophore with the correct excitation and emission to fit the microscope was found by evaluating different kinds of fluorophores and antibodies. The optimal concentration was found through several titration experiments. Immunofluorescent staining experiments were performed on mononuclear cells from normal blood samples and AsPC-1 cells with different concentrations of the dyes to optimize the staining. In addition the optimal concentrations of the dyes were tested together and evaluated with regard to incubation time and temperature.

Table 15 Immunofluorescent staining and nuclear dyes tested for optimization of the fluorescent staining

	Anti-EpCAM Antibody	Anti-CD45 Antibody	Nuclear dye
	Alexa Fluor® 555-anti-EpCAM (TRITC) (Cell Signal Technology®)	CD45-eFluor 605NC (Affymetrix, eBioscience)	DAPI (4',6-diamidino-2-phenylindole)
	Anti-EpCAM antibody [B29.1 (VU-ID9)] (FITC) (Abcam)	CD45-FITC, human (clone: 5B1) (Miltenyi Biotec)	NucBlue® Live ReadyProbes® Reagent (Hoechst 33342)
	Anti-EpCAM antibody (Sigma)	CD45-Dylight550 (BioTrend)	
	CD326 EpCAM, FITC, human (Miltenyi Biotec)	CD45 Alexa Fluor® 647 (BioLegend®)	
Optimal:	CD326 EpCAM, FITC, human (Miltenyi Biotec)	CD45-Dylight550 (BioTrend)	NucBlue® Live ReadyProbes® Reagent (Hoechst 33342)

We considered it more important to have a sensitive EpCAM staining compared to CD45 staining. Thus, the EpCAM staining was changed from a previously used TRITC label to a FITC label, due to low camera sensitivity in the TRITC channel. Accordingly, the CD45 staining was changed from FITC to TRITC staining.

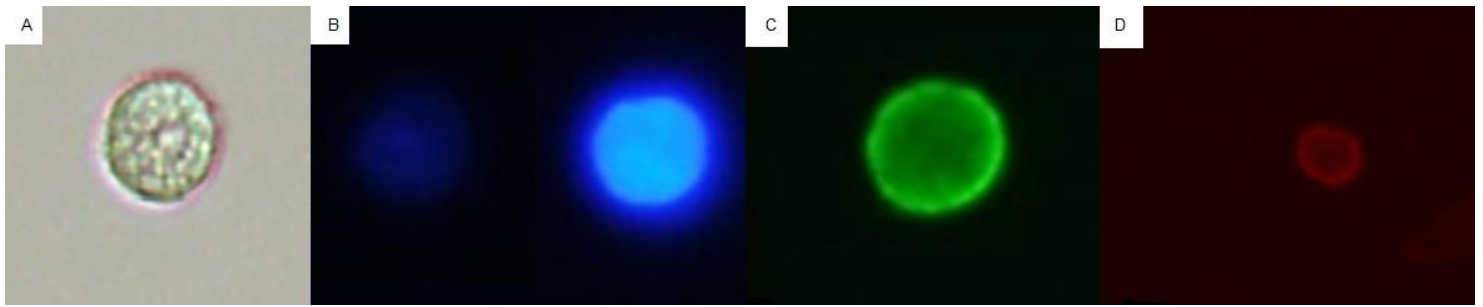


Figure 8 The final immunofluorescent staining. Figure A shows a AsPC-1 cell in bright field. Figure B shows AsPC-1 cells with Hoechst dye in the DAPI channel, with both weak and strong staining. Figure C shows AsPC-1 cell with EpCAM staining in the FITC channel. Figure D shows a leukocyte with CD45 staining in the TRITC channel.

The different kinds of staining that were tested are presented in Table 15. The Hoechst 33342 dye replaced the DAPI dye, because DAPI stained membrane compromised cells stronger compared to viable cells. Hoechst dyes were found to give a better staining of viable cells. The stains used in the final methods were chosen because the stains did not interfere with each other, they required the same incubation time and temperature, they were relatively photo-stable, and stained blood cells and AsPC-1 cells without any unspecific, cross staining. Examples pictures of the chosen stains are shown in Figure 8.

5.2.3 mRNA quality

5.2.5.1 Temperature optimization

The amount of mRNA in single cells is very low and the mRNA easily degrades if the cells die. The process to enrich and isolate single CTCs is time-consuming and involves many steps of centrifugation and resuspension followed by magnetic separation which could affect the cell viability. Living cells have intact membranes and do not absorb Trypan Blue staining. Therefore, Trypan Blue staining was used to differentiate dead and viable cells, which could be counted with a Hemocytometer (for details see chapter 4.1.2.3). Experiments were performed with the aim to discover the optimal temperature for the enrichment method.

The experiments were carried out in three replicates and all the numbers presented are the mean numbers. These experiments were performed on blood samples from healthy volunteers. The cell fraction counted was therefore mononuclear blood cells. The first set of experiments was carried out keeping the cells, the reagents and the centrifuge at room temperature unless refrigerator temperature was recommended in the manufacturers' protocol. The second set of experiments was carried out keeping the cells, the reagents and the centrifuge at refrigerator temperature unless room temperature was recommended in the manufacturers' protocol. These cells were kept on ice during the procedure, unless room temperature was

recommended in the manufacturers' protocol. The incubation of the staining was performed in room temperature for all experiments. Room temperature was chosen because the immunofluorescent staining experiments revealed that incubation in room temperature, as recommended by the manufacturer of the Hoechst 33342 staining, was favorable. A fraction of the cells were removed from the cell suspension, and counted with a Hemocytometer on four stages of the enrichment process. The first counting was performed after the density gradient separation. The second counting was performed after incubation with the immunomagnetic beads, called immunomagnetic enrichment. The third counting was performed after the immunomagnetic separation and the fourth counting was performed after incubation with the immunofluorescent staining.

The results from all the experiments are illustrated in Figure 9 and listed in Table 16. A considerable increase of cell deaths occurred after the immunomagnetic separation. The percentage dead cells in the cell suspension increased from 3 % (6/217) after density gradient separation up to 36 % (23/ 63) after immunomagnetic enrichment for the experiments performed in room temperature.

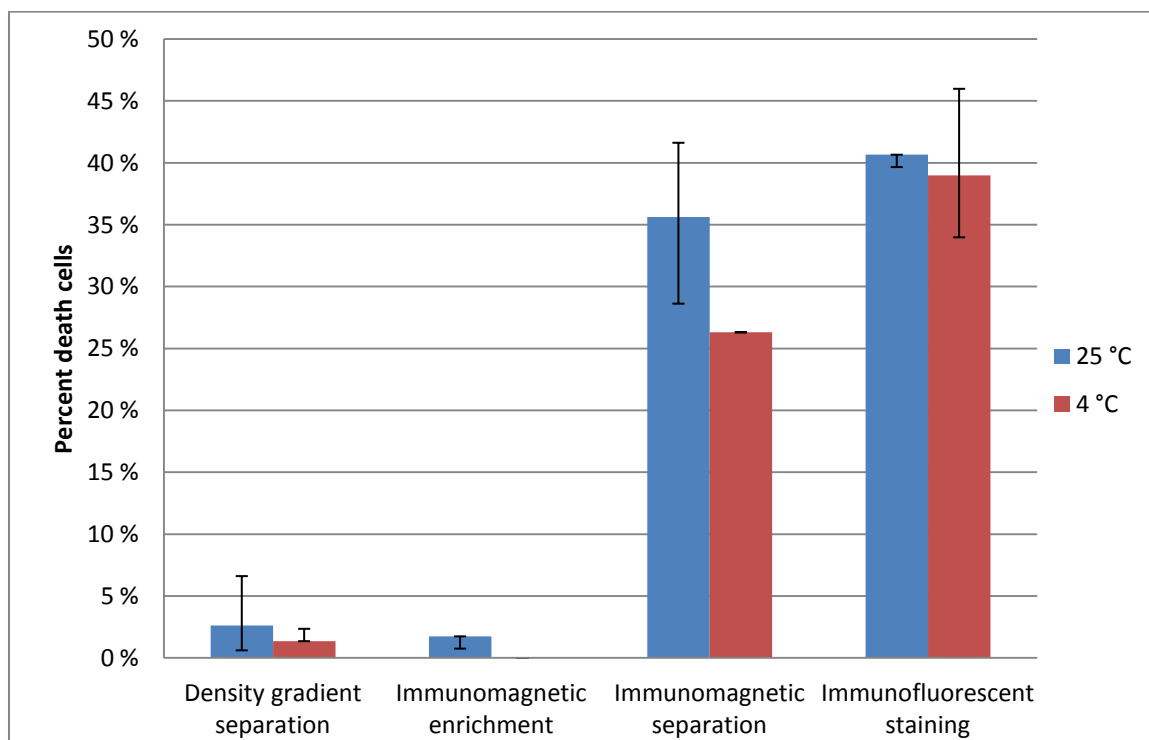


Figure 9 Percent of dead cells in the cell suspension after different steps of the enrichment process. Error bars illustrate the rate between the highest and the lowest value.

Table 16 Overview of the number of dead cells and cells in total after the different stages of the enrichment procedure performed at room temperature. The numbers given are the mean number from three replicate experiments.

25 °C	Density gradient separation	Immunomagnetic enrichment	Immunomagnetic separation	Immunofluorescent staining
Dead	6 (range 2-16)	4 (range 2-6)	23 (range 12-36)	40 (range 8-71)
Total	217 (range 199-234)	226 (range 201-248)	63 (range 33-86)	95 (range 20-169)
Percentage	3 % (range 1-7 %)	2 % (range 1-2 %)	36 % (range 29-42 %)	42 % (range 40-42 %)

Table 17 Overview of the number of dead cells and cells in total after the different stages of the enrichment procedure performed at 4 °C. The numbers given are the mean number from three replicate experiments. *only one replicate of the experiment.

4 °C	Density gradient separation	Immunomagnetic enrichment	Immunomagnetic separation	Immunofluorescent staining
Dead	3 (range 2-4)	0*	10*	23 (range 15-35)
Total	216 (range 210-229)	323*	38*	58 (range 46-80)
Percentage	1 % (range 1-2 %)	0 %*	26 %*	40 % (range 32-44 %)

The results from the second set of experiments where the cells, the reagents and the centrifuge were kept at 4 °C are listed in Table 17 and illustrated in Figure 9. For the experiments that were carried out at refrigerator temperature a trend of fewer dead cells in the cell fraction was observed. After immunomagnetic separation the average percentage of dead cells in the cell fraction was 26 % (10/38) for the cold experiments compared to 36 % (23/63) for the room temperature experiments. The difference was smaller after the immunofluorescent staining where the average percentage of dead cells in the cell fraction was 42 % (40/95) for the cold experiments compared to 40 % (23/58) for the room temperature experiments. In addition to the evaluation of the optimal temperature for the enrichment method, the experiment demonstrated that the percentage of dead cells increased substantially after immunomagnetic separation. Supposedly, the dead cells either died during the magnetic separation, and/or they were enriched during the magnetic separation.

Therefore, experiments where the dead cells in the cell fraction were removed with Dead Cell Removal kit (Miltenyi Biotec) prior to immunomagnetic separation were performed in order to evaluate which of the assumptions were correct. The percentage of dead cells after immunomagnetic separation was 27 % (9/32), when Dead Cell Removal was used before immunomagnetic separation. This was significantly lower than the 36 % (23/63) dead cells

when Dead Cell Removal was not used as in the experiments in room temperature presented in Table 16, even though the amount of cells to start with was equal. The cells were counted with a hemocytometer after the density gradient separation, after using the Dead Cell Removal kit and after immunomagnetic enrichment. The experiments were carried out at room temperature.

Table 18 Experiments using Dead Cell Removal kit. The numbers given are the number of cells counted in the hemocytometer of the dead cells and the total number of cells after counting with a hemocytometer. The experiment was carried out at room temperature. The numbers given are mean numbers from two replicate experiments, counted after each enrichment step.

25 °C	Density gradient separation	Dead Cell Removal	Immunomagnetic separation
Dead	0	0	9 (range 5-12)
Total	220 (range 215-225)	224 (range 221-227)	32 (range 21-42)
Percentage	0 %	0 %	27 % (range 24-29)

5.2.5.2 RNase inhibitor test

RNase activity could lead to poor mRNA quality in the blood cells and the CTCs in the lysis solution after isolation of single cells. RNase inhibitor (RNase OUT) was added to a lysis buffer containing control HeLa RNA to test whether the poor mRNA quality was caused by RNase activity. Control samples containing no RNase inhibitor was also added to the experiment. The lysis buffer was placed in droplets on a PCR film, similar to the method used to isolate single cells. Two droplets containing RNase inhibitor and two droplets without RNase inhibitor were evaluated. In addition three single cells were isolated separately into three droplets containing RNase inhibitor, and three droplets without RNase inhibitor. All the droplets were treated in the same way during micromanipulation of single cells, and went through reverse-transcription, pre-amplification and qPCR. The experiments were performed in two replicates.

The mRNA levels of *HPRT1* and *Vimentin* were measured to evaluate whether the RNase inhibitor had any effect on the final mRNA levels. Figure 10 shows the levels of *HPRT1* and *Vimentin* in samples containing only HeLa RNA both with and without RNase inhibitor present in the lysis. Surprisingly, the mRNA levels seemed to be higher in the samples where RNase inhibitor was not used.

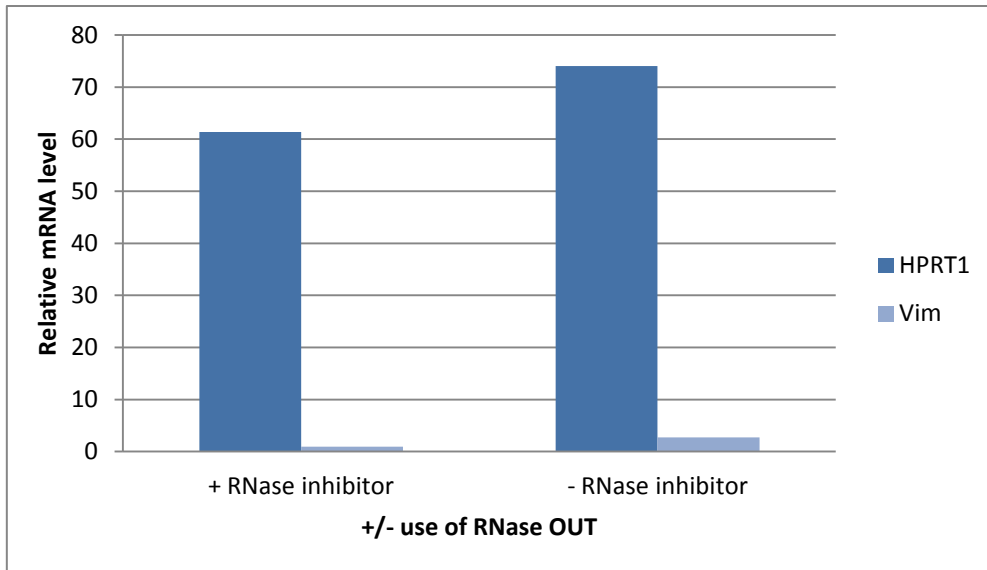


Figure 10 Relative mRNA levels in the HeLa control sample with and without RNase inhibitor. The +RNase inhibitor columns represent the mRNA levels in the HeLa control where RNase OUT was used. The - RNase inhibitor columns represent the mRNA levels in the HeLa control where RNase OUT was not used.

The droplets containing single leukocytes were also evaluated. The results were expected to reveal whether RNase from within the single cells would affect the quality of the HeLa control RNA. The mean RNA levels of *HPRT1* and *Vimentin* from the three cells placed in a droplet of lysis buffer containing RNase inhibitor are compared to the mean RNA levels of *HPRT1* and *Vimentin* from the three single cells placed in a droplet of lysis buffer not containing RNase inhibitor. The result is shown in Figure 11.

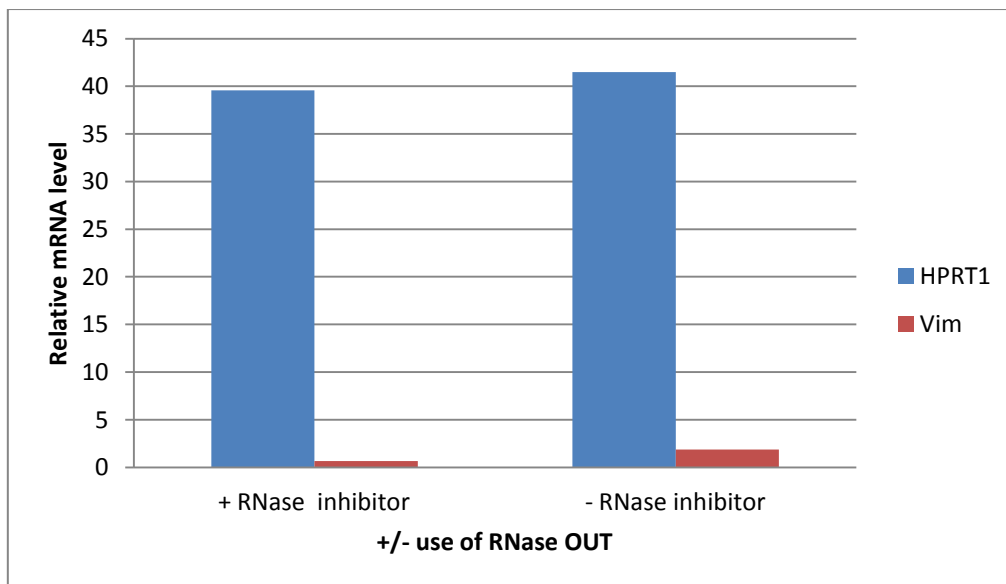


Figure 11 The mean relative mRNA levels from HeLa control containing single cells with and without RNase inhibitor. The +RNase inhibitor columns represent the mean mRNA levels from the three single cells and HeLa controls where RNase OUT was used. The - RNase inhibitor columns represent the mean mRNA levels from the three single cells and the HeLa control where RNase OUT was not used.

5.3 Validations of methods

Pancreatic cancer cell line cells along with leukocytes from blood samples from healthy controls were isolated by micromanipulation. The aim was to distinguish the different single cells based on the qPCR results, to validate the method for molecular characterization of CTCs. The whole procedure was validated by performing experiments using healthy control blood samples spiked with AsPC-1 cells. Results from all validation experiments are presented below.

5.3.1 Validation of the method for molecular characterization of single CTCs by RT-qPCR

The levels of 11 specific mRNAs in cells from three pancreatic cancer cell lines and leukocytes from normal blood samples were measured in an attempt to validate the method for molecular characterization of CTCs by RT-qPCR. The mRNA markers were previously selected by the research group to identify CTCs and included three epithelial markers, four mesenchymal markers, three cancer stem cell markers, a reference housekeeping gene and a leukocyte marker, listed below.

Epithelial mRNA markers:

- *CK8*
- *EPCAM*
- *E-Cadherin*

Mesenchymal mRNA markers:

- *Vimentin*
- *N-Cadherin*
- *ZEB1*

Cancer Stem Cell mRNA markers:

- *CD24*
- *CD44*
- *ALDH1A1*

Reference housekeeping mRNA marker:

- *HPRT1*

Leukocyte mRNA marker:

- *CD45*

The aim of the experiment was to evaluate to what extent the single cancer cell line cells could be distinguished from another and from the leukocytes based on the levels of the 11 mRNA markers in the single cells. AsPC-1, PANC-1 and BxPC-3 pancreatic cancer cell lines were used. Three single cells of each cell line in addition to four leukocytes were picked for further molecular characterization with RT-qPCR. All experiments were performed with the optimized versions of the method, given in chapter 4.4 to 4.8.

Relative mRNA levels for the cells are given in Figure 12. The data was normalized against a housekeeping reference mRNA and against a calibrator sample included in every run. The relative mRNA value of each marker should not be compared, because of the normalization of the data against the reference mRNA marker.

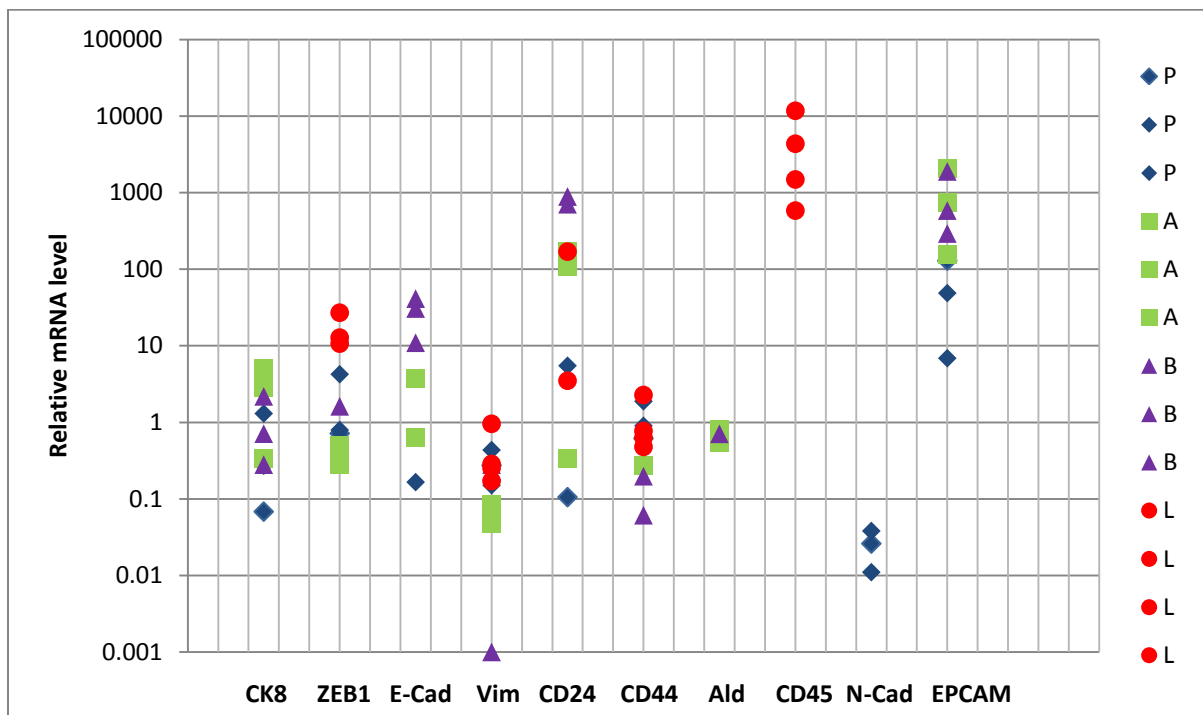


Figure 12 Relative mRNA level of CK8, ZEB1, E-Cadherin, Vimentin, CD24, CD44, ALDH1A1, CD45, N-Cadherin and EPCAM in cell line cells and leukocytes. AsPC-1 is, marked A, BxPC-3 is marked B, PANC-1 is marked P and leukocytes are marked L. Cells which did not express the marker are not plotted in the graph. Data are normalized to a reference mRNA and to a calibrator sample included in every run.

Hierarchical clustering was used to compare the results obtained from the qPCR runs in order to separate the different cell types. The data used for the hierarchical cluster analysis was normalized with two different strategies, both explained in detail in chapter 4.9. The first strategy was a normalization of the data against the *HPRT1* reference mRNA and against a calibrator sample included in every run. The second strategy was to only normalize the Cq-values against a calibrator sample included in every run.

The hierarchical cluster analysis shown in Figure 13 are performed by using data normalized against *HPRT1*, a reference mRNA and to a calibrator sample. The data was grouped using a hierarchical clustering algorithm with Pearson Correlation similarity measurements with complete linkage.

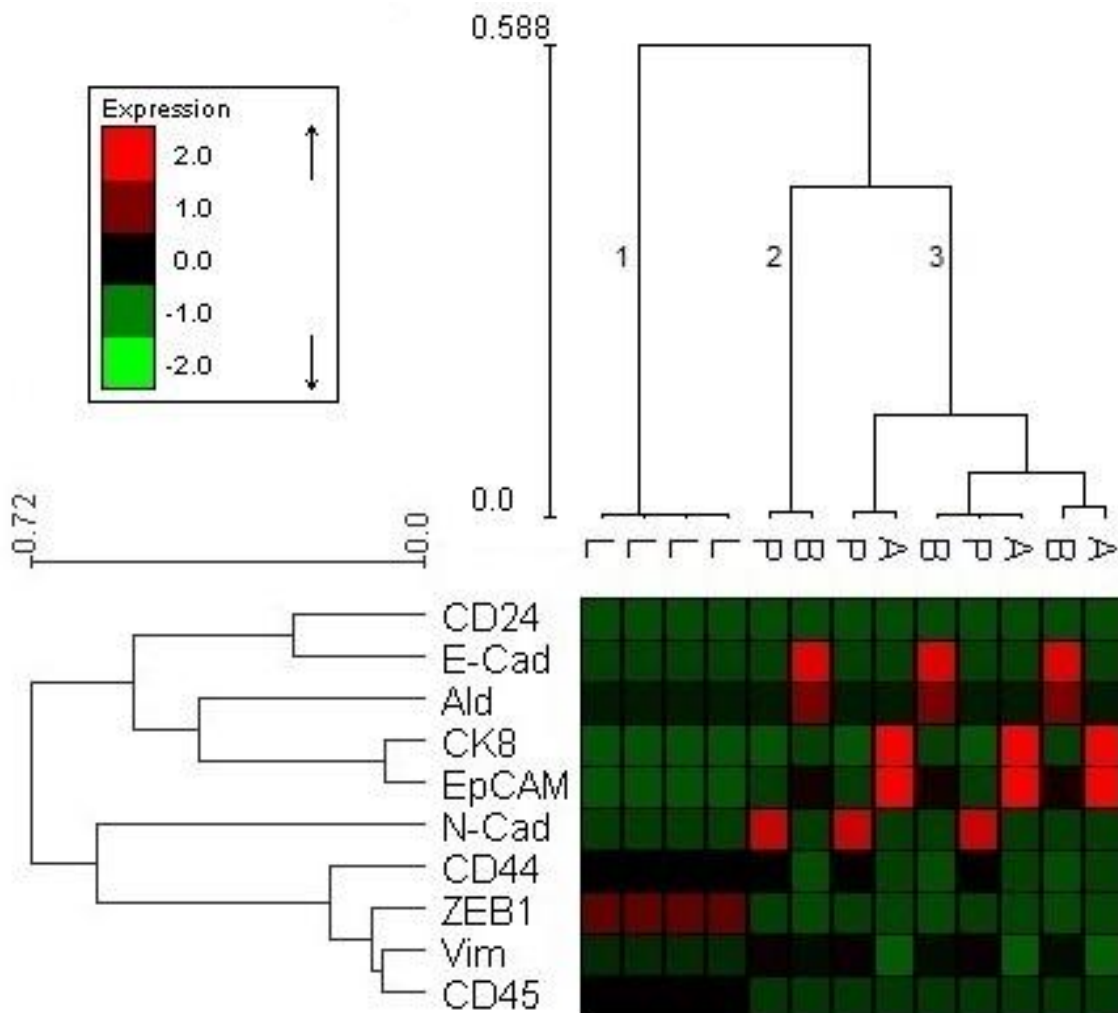


Figure 13 Hierarchical clustering analysis with heat map for the validation experiment with *HPRT1*-normalization. Single cells from pancreatic cancer cell lines and leukocytes from healthy control blood samples were analyzed by single-cell RT-qPCR. L represents the leukocytes, P the PANC-1 cells, B the BxPC-3 cells and A the AsPC-1 cells. All data used to produce this figure was normalized against the constantly expressed *HPRT1* reference mRNA and the calibrator sample included in each run. Hierarchical cluster with heat map was generated using Expander 6.0. The color coding in the heat map is weighted according to the clustering results.

Leukocytes were grouped in cluster 1 with low expression of epithelial and mesenchymal markers and higher expressions of the *CD45* leukocyte marker (Figure 13). Pancreatic cancer cell line cells were grouped in clusters 2 and 3. AsPC-1 cells had higher expression levels of epithelial markers, PANC-1 higher expression levels of mesenchymal and cancer stem cell markers and BxPC-3 high expression levels of both epithelial and mesenchymal markers. Neither of the cancer cell line cells had expression of the *CD45* leukocyte marker.

The data used to create the hierarchical cluster in Figure 14 was not normalized to the reference mRNA, but only normalized to the calibrator sample included in every run.

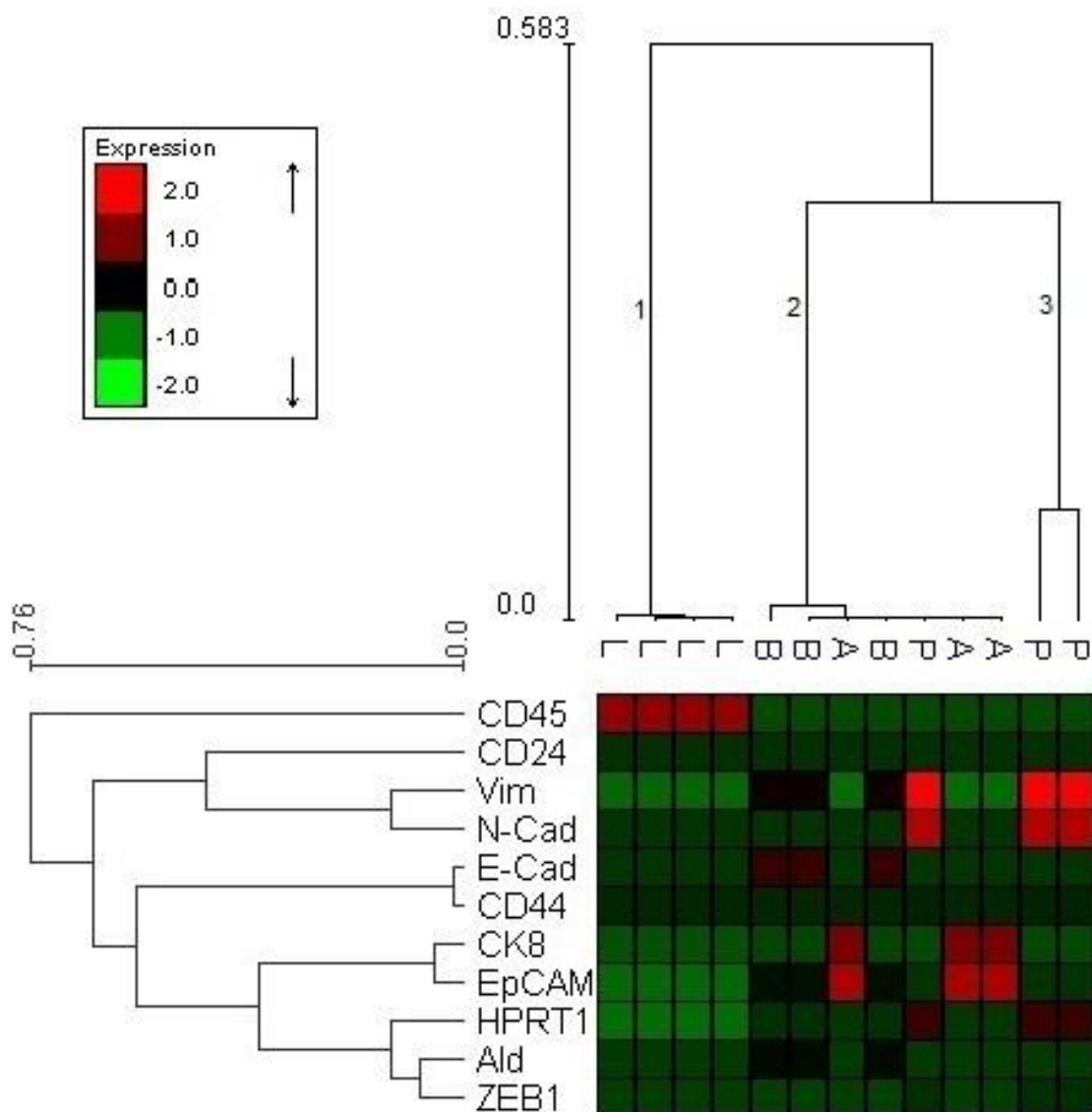


Figure 14 Hierarchical clustering analysis with heat map for the validation experiment without HPRT1-normalization. Single cells from pancreatic cancer cell lines and leukocytes from healthy vontral blood samples were analyzed by single-cell RT-qPCR. L represents the leukocytes, P the PANC-1 cells, B the BxPC-3 cells and A the AsPC-1 cells. The data used for the analysis was normalized against a calibrator sample included in each run. Hierarchical cluster with heat map was generated using Expander 6.0. The color coding in the heat map is weighted according to the clustering results.

Figure 14 shows groups of cancer cell line cells in two clusters, 2 and 3, where the cells had higher expression levels of epithelial and mesenchymal markers compared to cluster 1 consisting of only leukocytes. The leukocytes had high expression level of *CD45*, but low expression levels were observed for the rest of the markers. The expression level of the reference mRNA, *HPRT1*, was also low compared to the other cells. PANC-1 showed high expression of the mesenchymal markers *Vimentin* and *N-Cadherin*, in addition to *HPRT1*. BxPC-3 had high expression of a combination of mesenchymal, epithelial and cancer stem cell markers. Cells from the pancreatic cancer cell line AsPC-1 expressed high levels of *EPCAM* and *CK8*, both epithelial markers.

The data from this validation experiment was used as a reference for molecular characterization of possible CTCs and contaminating leukocytes, as described in the next chapter. The leukocytes expressed several mRNA markers besides *CD45*, illustrated by the relative mRNA levels given in Figure 12. All leukocytes expressed *CD45* and *CD44*, three out of four leukocytes had detectable levels of *ZEB1* and two out of four expressed *CD24*. Neither of the leukocytes expressed the markers *EPCAM*, *CK8*, *E-Cadherin*, *ALDH1A1* or *N-Cadherin*. All the pancreatic cancer cell line cells had detectable Cq-values for *CK8*, *CD44* and *EPCAM*. Neither of the cell line cells expressed the leukocyte marker *CD45*.

5.3.2 Validation of the method for enrichment and characterization of CTCs

To validate the methods for enrichment and molecular characterization of single CTCs, blood from healthy volunteers was spiked with AsPC-1 cells, simulating patient blood samples containing CTCs. Three independent experiments were performed on different days. Table 19 shows an overview of the three validation experiments with regard to the number of AsPC-1 cells that were spiked in the blood and the number of AsPC-1 cells recovered in the blood based on immunofluorescent staining.

Table 19 Overview of method validation experiments for the enrichment and characterization of CTCs

Experiment	Number of spiked AsPC-1 cells in 9 mL whole blood	Number AsPC-1 cells recovered during micromanipulation
1	1000	219 (22 %)
2	100	11 (11 %)
3	100	19 (19 %)

The recovery rates of the AsPC-1 cells from the whole blood for the three experiments were 22 %, 11 % and 19 %, which gives a mean recovery of 17.3 %. The number of AsPC-1 cells in the sample was found by scanning the FITC and TRITC channel. Cells with a strong green signal in FITC, no red signal in TRITC and a weak or strong signal in the DAPI channel (Hoechst staining) were counted as AsPC-1 cells. Experiment 1 and 2 ended after enumeration of AsPC-1 cells.

Five single suspected tumor cells were picked to validate the immunofluorescent staining procedure and the selection criteria. The suspected tumor cells were characterized as tumor cells based on their immunofluorescent staining, criteria given in chapter 4.10.1. The cells were isolated from the cell suspension using micromanipulation in Experiment 3. The suspected tumor cells were treated as suspected tumor cell, hence qPCR on the 11 mRNA markers were performed. The results from the molecular characterization are illustrated in Figure 15 and Figure 16.

The hierarchical cluster analysis presented in Figure 15 shows the suspected tumor cells along with pancreatic cancer cell line cells and leukocytes used as reference cells. The data used to create the hierarchical cluster analysis given in Figure 15 was normalized against *HPRT1*, a reference mRNA and to the calibrator sample included in every run. The suspected tumor cells were grouped in cluster 3 along with the AsPC-1 cells and some BxPC-3 cells and PANC-1 cells. Cluster 3 was divided in three branches where all the suspected tumor cells were in the same branch. Cluster 1 consisted of only leukocytes, which were positioned far away from the suspected tumor cells. All five suspected tumor cells had a very similar expression profile, with high expression levels of *Vimentin*, *E-Cadherin*, *EPCAM* and *CK8*. The suspected tumor cells had a higher average Cq-value compared to AsPC-1 cells that were not enriched from whole blood.

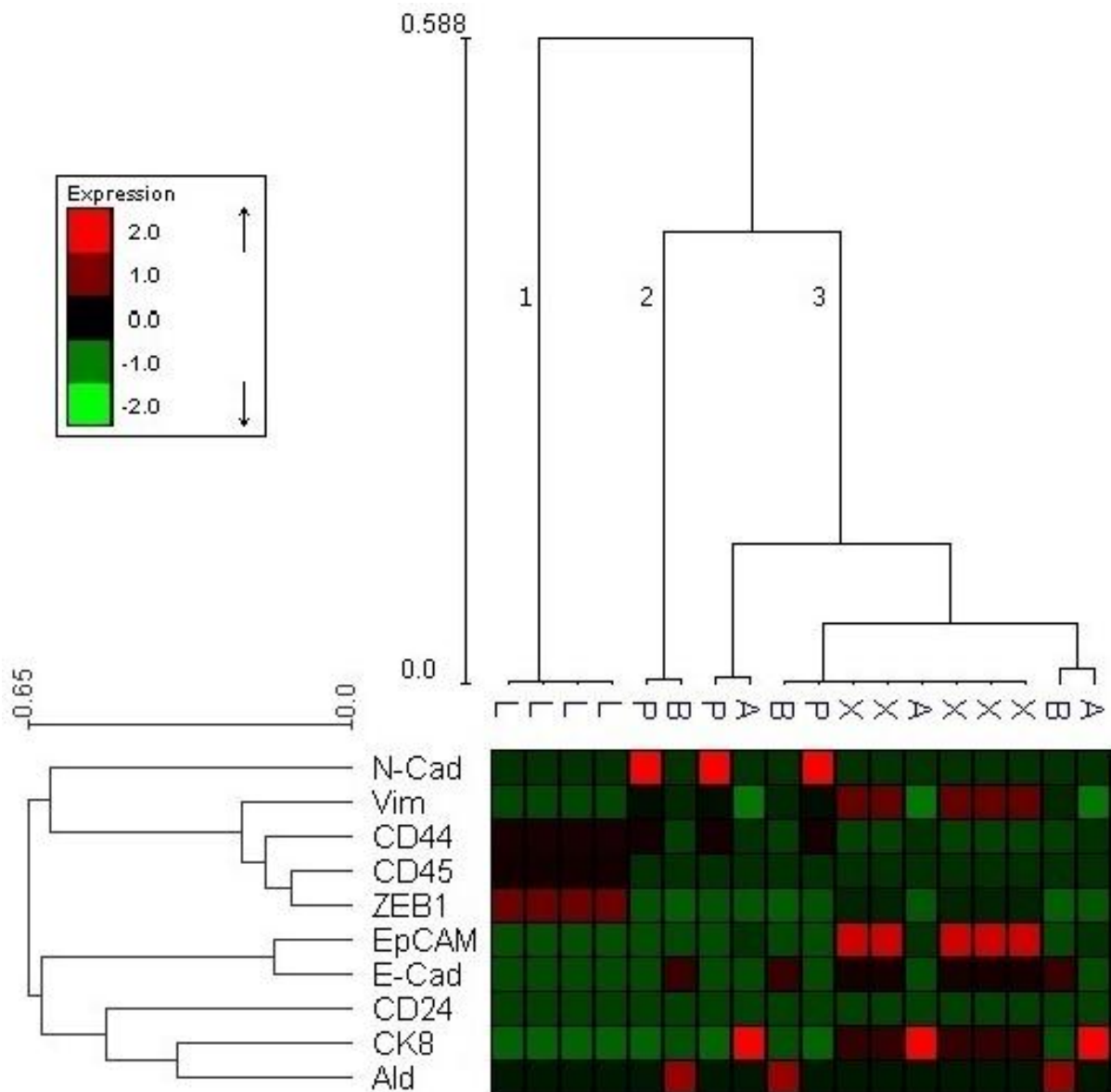


Figure 15 Hierarchical clustering analysis with heat map for the validation experiment with normalization to the housekeeping reference gene. Single suspected tumor cells, picked as AsPC-1 cells, from spiking experiments are analyzed along with single cells from pancreatic cancer cell lines and leukocytes from healthy control blood samples. X represents the suspected tumor cells, L the leukocytes, P the PANC-1 cells, B the BxPC-3 cells and A the AsPC-1 cells. All data used to produce this figure was normalized against the housekeeping reference mRNA *HPRT1* and to the calibrator sample included in each run. Hierarchical cluster with heat map was generated using Expander 6.0. The color coding in the heat map is weighted according to the clustering results.

The data used to create the hierarchical cluster in Figure 16 was not normalized against a housekeeping reference gene, only normalized to a calibrator sample included in every run. Cluster 1 was formed by the leukocytes and was clustered far away from the suspected tumor cells. All of the five suspected tumor cells were found in cluster 2, together with all the BxPC-3 and AsPC-1 cells. Cluster 3 consisted of two PANC-1 cells. All the suspected cells expressed high levels of the mRNA markers *EPCAM*, *E-Cadherin* and *Vimentin*. The AsPC-1 cells in cluster 2 had high expression levels of *E-Cadherin* and *EPCAM*.

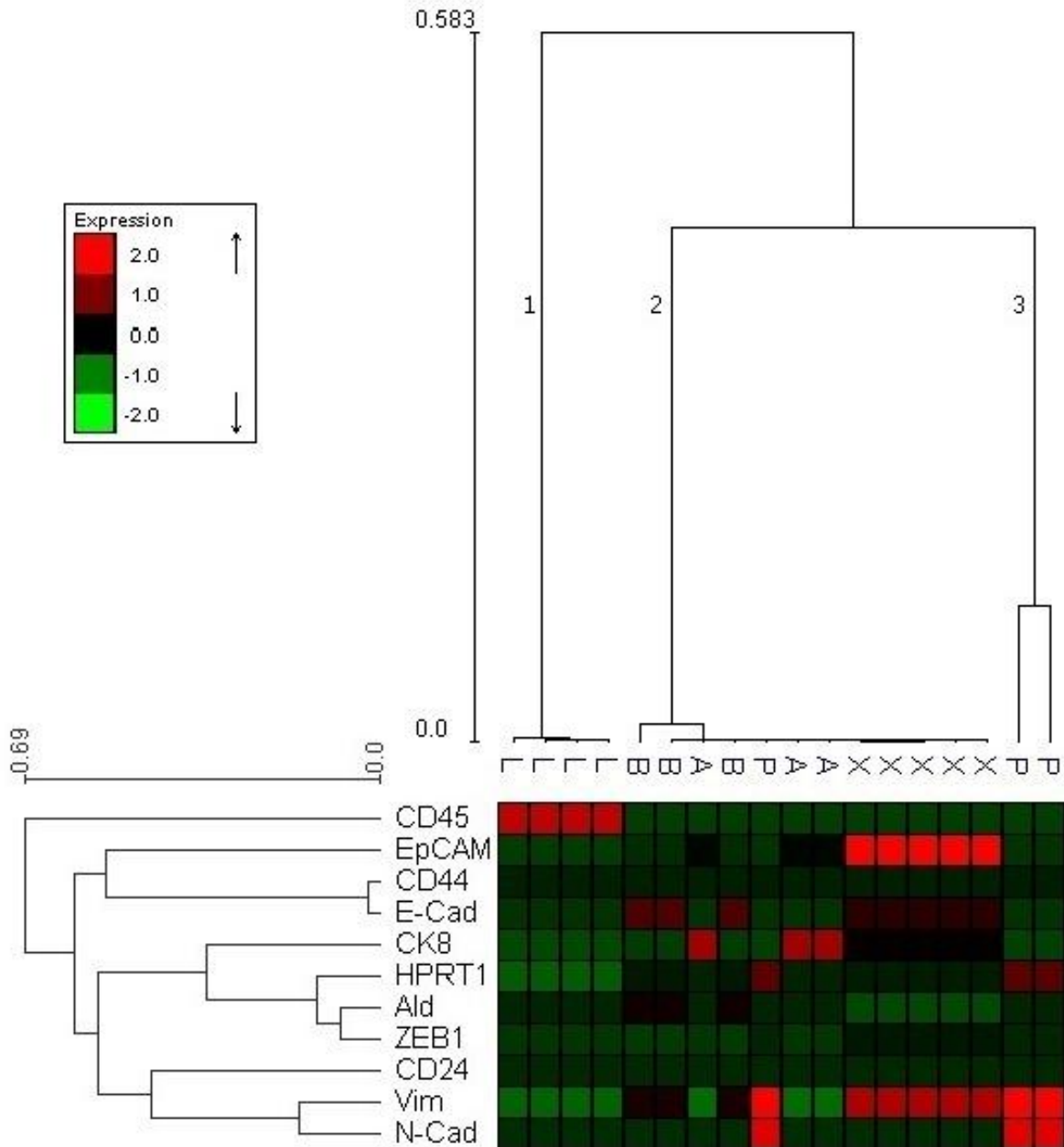


Figure 16 Hierarchical clustering analysis with heat map for the validation experiment without normalization to a housekeeping reference gene. Single suspected tumor cells, picked as AsPC-1 cells, from spiking experiments are analyzed along with single cells from pancreatic cancer cell lines and leukocytes from healthy control blood samples. X represents the suspected tumor cells, L the leukocytes, P the PANC-1 cells, B the BxPC-3 cells and A the AsPC-1 cells. All data used to produce this figure was normalized to the calibrator sample included in each run. Hierarchical cluster with heat map was generated using Expander 6.0. The color coding in the heat map is weighted according to the clustering results.

5.4 Patient blood sample analysis

Seven patients contributed to this study over a period of four months, with one to four blood samples each. Enrichment, isolation and molecular characterization of potential CTCs were performed on 18 blood samples in total. The optimization of working temperature was not

completed at the time of the first 12 patient' blood samples analyses. Therefore, the first 12 blood sample were analyzed with reagents and centrifugation steps at room temperature if no other specific temperatures were given in the manufacturers' protocols. The remaining six blood samples were processed at a temperature of 4°C.

5.4.1 Potential CTCs

Potential CTCs from blood samples that were recognized based on the immunofluorescent staining during scanning were isolated by micromanipulation. Up to 15 potential CTCs and five leukocytes as control samples were acquired from each blood sample. Based on the immunofluorescent staining the cells were categorized as CTCs, possible CTCs or leukocytes. A total of 82 single cells were isolated, 60 of these were picked as CTCs, 9 as possible CTCs and 13 as possible leukocytes. An overview of the mRNA quality and category of the single cells is given in Table 20. Details on all single cells acquired from patient blood samples in this study are enclosed in attachment 11.1.

Table 20 Overview of single cells isolated from patient blood samples. Detailed information is found in attachment 11.1. Information about the different categories is found in chapter 4.10.

mRNA quality	Color code	Total cells number	Number of CTC/possible CTCs	Number of leukocytes
Good		11	8	3
Medium		30	27	3
Poor		41	34	7
Cell categories:		Total number of cells	Number of cells with good mRNA quality	Percent of total cell number:
CTC		60	5	8 %
Possible CTC		9	3	32 %
Leukocyte		13	3	23 %
Total		82	69	13

Only 11 of 82 single cells had good mRNA quality, based on the quality criteria from chapter 4.10.2, and were chosen for further molecular analysis for the rest of the mRNA markers. 8 of these 11 cells were picked as CTCs and possible CTCs, and three as leukocytes. Only 12 % of the CTCs and the possible CTCs that were picked met the mRNA quality criteria for further testing. An overview of RNA quality in the single CTCs are given in Figure 17.

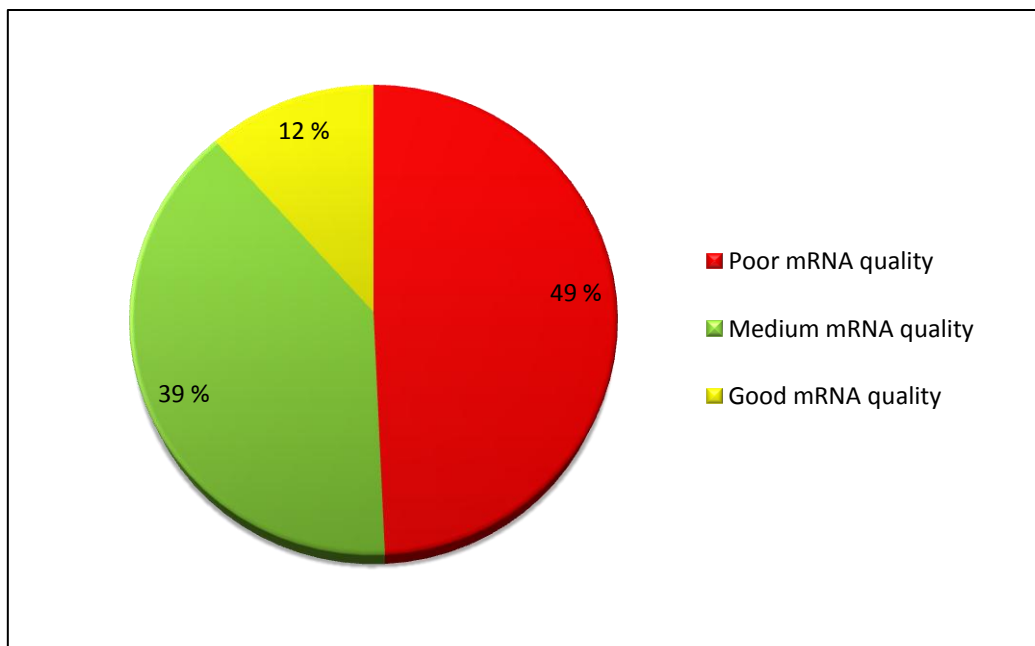


Figure 17 mRNA quality of single CTCs isolated from pancreatic cancer patients samples.

The immunofluorescent staining results for the CTCs or possible CTCs are shown in

Table 21. Example pictures of the single CTCs in the different fluorescent channels are shown in Figure 18. One cell, PC4_1 was not stained with either EpCAM or CD45, but it was stained with Hoechst and looked intact and viable in bright field. All the contaminating leukocytes in the suspension are expected to be stained with CD45, however, some CTCs might have low *EPCAM* expression levels due to EMT. Therefore, the cell was isolated as a CTC.

Table 21 Results from immunofluorescent staining of CTCs/possible CTCs with good mRNA quality acquired from patient blood samples.

Patient no./cell no.	Immunofluorescent Staining:			Celle type:
	EpCAM	CD45	Nuclear dye	
PC3_1	Strong	Strong	Weak	Possible CTC
PC3_2	Weak	Strong	Weak	Possible CTC
PC2_1	Weak	Non	Strong	CTC
PC2_2	Weak	Strong	Strong	Possible CTC
PC1_2	Strong	Weak	Weak	CTC
PC1_3	Strong	Weak	Weak	CTC
PC3_3	Strong	Non	Weak	CTC
PC4_1	Non	Non	weak	CTC

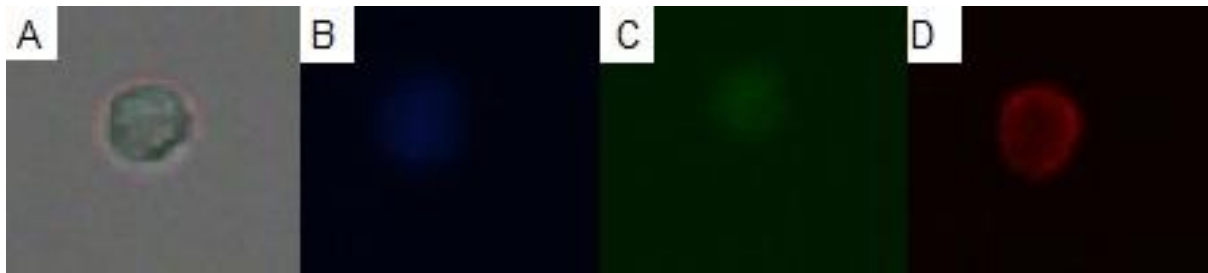


Figure 18 Example pictures of CTCs from PC2. A, B, and C shows a potential CTC. A shows the cell in bright light, B shows the cell with Hoechst dye in the DAPI channel, C shows the cell with anti-EpCAM antibody staining in the FITC channel. D shows a contaminating leukocyte with anti-CD45 antibody staining in the TRITC channel.

The RNA quality assessment was based on *HPRT1* and Vimentin mRNA levels, thus, these mRNAs were first measured in all isolated single cells. All the single cells that were characterized with good mRNA quality also had their levels of the remaining 9 mRNAs determined. The 11 patient cells were analyzed by hierarchical clustering together with the data from the validation experiments above (pancreatic cancer cell line cells and leukocytes from normal blood). The results are shown in Figure 19 and Figure 20.

The data used to create the hierarchical cluster analysis given in Figure 13 and Figure 19 was normalized against *HPRT1*, a reference mRNA and to the calibrator sample included in every run. Cq-values for all the single cells from pancreatic cancer patient blood samples are found in attachment 11.1. The hierarchical clustering analysis in Figure 19 shows two potential CTCs and two patient sample leukocytes clustered along with the reference leukocytes. The remaining six potential CTCs and one patient sample leukocyte are clustered along with the reference cancer cell line cells from the validation experiment in the previous chapter.

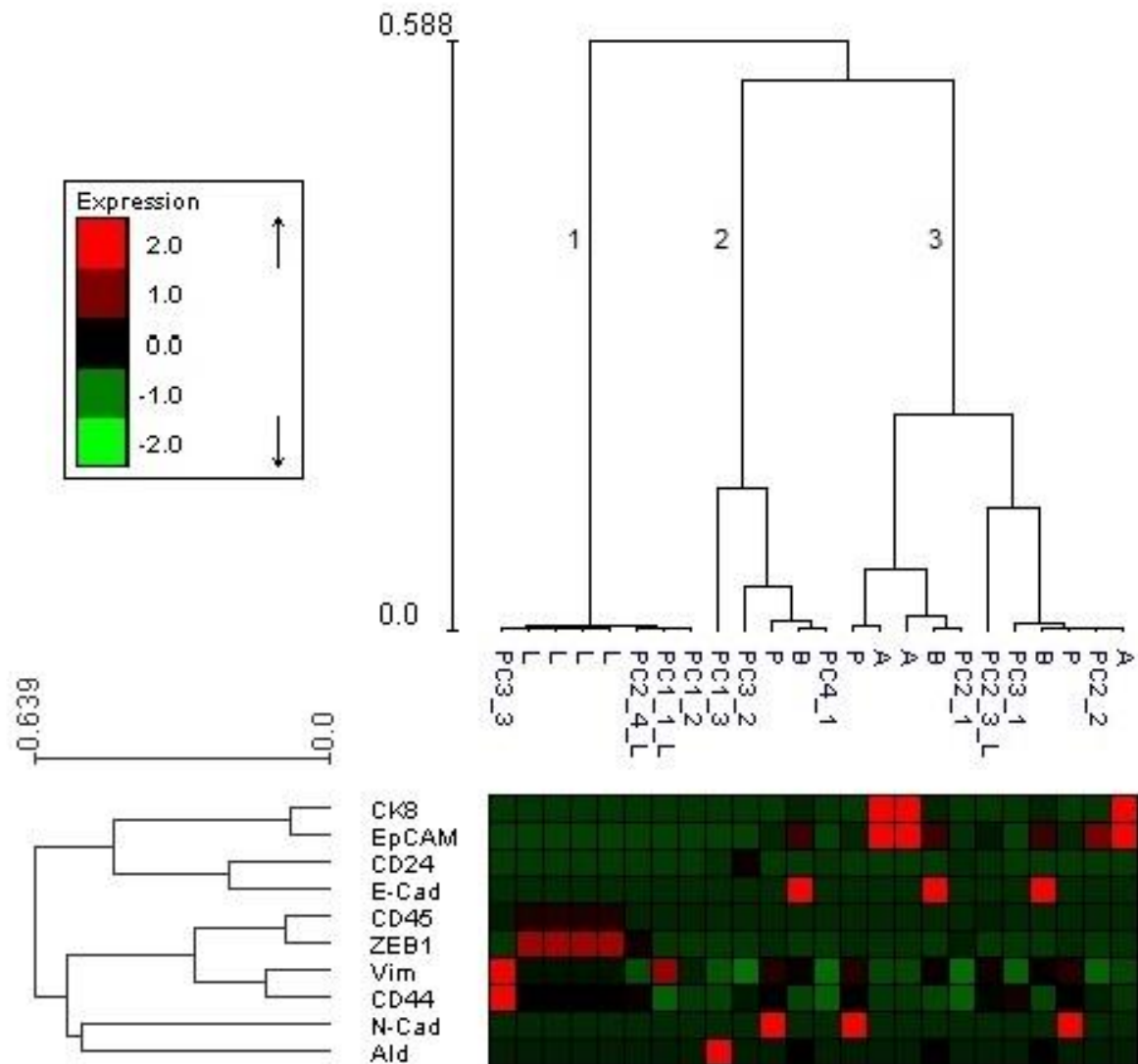


Figure 19 Hierarchical clustering analysis with heat map of single cells from patient samples with normalization to the housekeeping reference gene. Single cells from patient samples were analyzed along with single cells from pancreatic cancer cell lines and leukocytes from normal blood samples. Cells named PC are the cells from the patient samples, if the cells are additionally marked L, the cell were picked as a possible leukocyte from the patient sample. L represents the leukocytes, P to PANC-1 cells, B to BxPC-3 cells and A to AsPC-1 cells. All data used to produce this figure was normalized against the constantly expressed HPRT1 reference mRNA and to the calibrator sample included in each run. Hierarchical cluster with heat map was generated using Expander 6.0. The color coding in the heat map is weighted according to the clustering results.

The data used to create the hierarchical cluster in Figure 20 was not normalized to a housekeeping reference gene, only normalized to a calibrator sample included in every run. Neither of the single cells isolated from patient samples now showed high expression levels of any of the mRNA markers in the heat map. All the leukocytes from the healthy control samples are cluster together in cluster 1, but not with the leukocytes from the patient samples. All the single cells acquired from the patient samples are gathered in cluster 2, 3 and 4, along with the pancreatic cancer cell line cells.

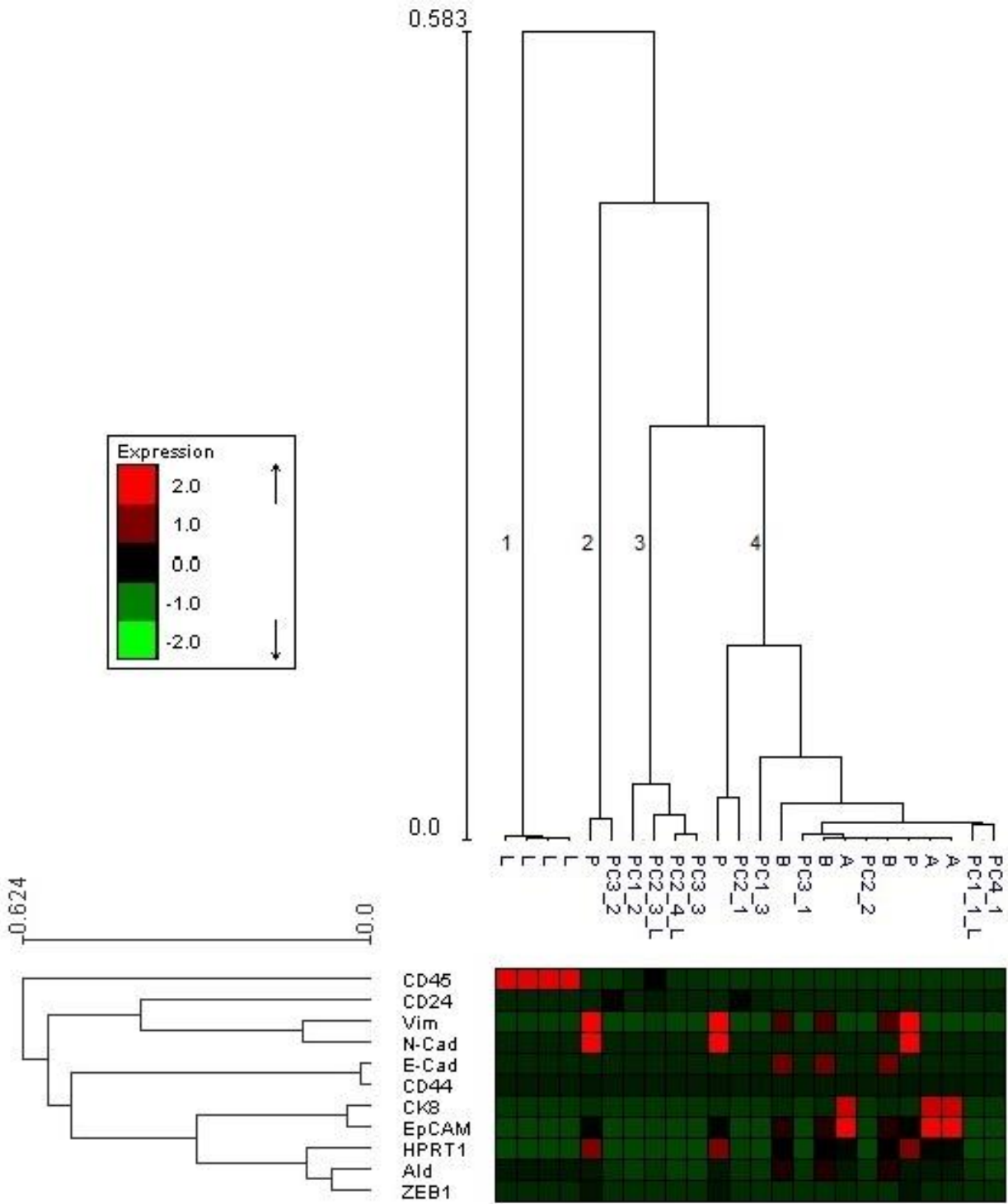


Figure 20 Hierarchical clustering analysis with heat map of single cells from patient samples with normalization only to the calibrator sample. Single cells from patient samples were analyzed along with single cells from pancreatic cancer cell lines and leukocytes from normal blood samples. Cells named PC are the cells from the patient samples, if the cells are additionally marked L, the cell were picked as a possible leukocyte from the patient sample. L represents the leukocytes, P to PANC-1 cells, B to BxPC-3 cells and A to AsPC-1 cells. Hierarchical cluster with heat map was generated using Expander 6.0. The color coding in the heat map is weighted according to the clustering results.

The immunocytological characterization of the potential CTCs was compared with the molecular characterizing of the same cells (Table 22). The molecular characterization of the

cells is based on the levels of the mRNA markers and the hierarchical clustering analysis with evaluation of both normalization strategies. The cells were characterized as CTCs, uncertain CTCs or leukocyte. Single cells with measurable expression of less than four of the 11 mRNA markers, and no expression of *CD45* were characterized as uncertain CTCs. Single cells were characterized as leukocytes when expression of *CD45* is measurable in addition to expression of *HPRT1* and *Vimentin*. The mRNA in the uncertain CTCs could be degraded, which would only lead to expression of a limited number of mRNA markers for molecular characterization.

Table 22 Evaluation of the potential CTCs from the patient blood samples based on the immunofluorescent staining, the hierarchical clustering analysis and the levels of the mRNA markers combined to a molecular characterization of the CTCs.

Patient /cell	Cell type based on immunofluorescent staining:	Cell type based on hierarchical cluster analysis:	Levels of mRNA markers:	Cell type based on molecular characterization:
PC3_1	Possible CTC	CTC	<i>HPRT1, Vimentin, CD44</i>	Uncertain CTC
PC3_2	Possible CTC	CTC	<i>HPRT1, Vimentin, CD44, CD24</i>	Uncertain CTC
PC2_1	CTC	CTC	<i>HPRT1, Vimentin, ZEB1, EPCAM, CD24</i>	CTC
PC2_2	Possible CTC	CTC	<i>HPRT1, Vimentin, CD44, EPCAM</i>	CTC
PC1_2	CTC	Leukocyte	<i>HPRT1, Vimentin, CD44, CD45</i>	Leukocyte
PC1_3	CTC	CTC	<i>HPRT1, Vimentin, CD24, ALDH1A1, CD44, CD45</i>	Leukocyte
PC3_3	CTC	Leukocyte	<i>HPRT1, Vimentin, CD44, CD24</i>	Uncertain CTC
PC4_1	CTC	CTC	<i>HPRT1, Vimentin, CD24</i>	Uncertain CTC

6 Discussion

6.1 Optimization of methods

Several steps in a previously established method for isolation of single CTCs were subjected to optimization in the current study.

The immunofluorescent staining should be optimal to distinguish CTCs from contaminating leukocytes in a mixture of both cell types. First, the dye must be relatively photo-stable in order for the staining to remain detectable even when exposed to UV light over a longer time period, for example during micromanipulation of single cells. Second, the fluorescent stain should have a strong excitation signal in order to minimize the required exposure time. A shorter exposure time would make scanning faster, which would be favorable in order to keep the cells viable during selection and micromanipulation. The required exposure time in the TRITC channel is longer than the required exposure time in the FITC channel due to a filter in the camera which removes parts of the red fluorescent light. Therefore, the EpCAM antibody was changed from conjugation to a red fluorophore with excitation in the TRITC channel to conjugation to a green fluorophore with excitation in the FITC channel. This resulted in a more efficient scanning process, as the CTCs are expected to be EpCAM stained.

Hoechst dyes stains viable cells as the dye is cell membrane permeable, whereas the DAPI dye enters the nucleus of apoptotic cells more easily than viable cells. Thus, the cells with strong DAPI fluorescence are the less viable cells. Cann *et al.* excluded DAPI positive cells as a selection criteria during single CTC isolation, by stating that DAPI dyes would not enter viable cells as easy as dead cells [94]. After evaluation of the DAPI dye it was replaced by the Hoechst dye 33342 in this study, mainly because of the strong staining of the apoptotic cells and cell debris in the cell pool. Several Hoechst dyes exist, however, the 33342 dye are recommended by the manufacturer for staining viable cells. Hoechst dyes are easy to combine with other fluorescent dyes or proteins from the green to the far red spectral, which was an advantage as the dye was used in combination with other dyes [86]. Single cells isolated in this study had both strong and weak Hoechst dye staining intensity. However, no connections were observed between staining intensity, cell viability or mRNA quality.

One method to aid identification of viable cells could be to change back again to DAPI staining of the nucleus, but change the use of the dye and only DAPI negative cells should be

isolated for further molecular characterization. This is the strategy Cann et al. used in their study [94]. However, there are several implications not to conduct this method. One reason is that DAPI staining is reported to affect gene expressions [95]. Most CTC detection methods use positive DAPI staining as a criterion to include cells for further analysis [27, 47]. However, in most of these studies the cells are permabilized or fixated.

Isolation of single cells by micromanipulation is a race against time because the cells are exposed to a far from optimal environment. Small volumes of cell suspension on microscopy slides during prolonged incubations at room temperature can lead to substantial cell death. After a period of time the whole liquid cell suspension would dry out when using such small volumes. The alterations made on the CellEctor software improved the speed of the scanning, facilitated the selection of possible CTCs and gave a more efficient isolation of single cells. However, the scanning of the cell pool is still a time-consuming procedure.

Despite the software enhancements, the RNA quality of the single cells after the enrichment process was poor. The changes in temperature for the enrichment method decreased the percentage of dead cells in the cell fraction after immunomagnetic separation from 36 % to 26 %, see Figure 9. The differences were smaller after the immunofluorescent staining (42 % against 40 %), however, the same trend was observed also here. As a result of the decreased number of cell death the temperature were permanently changed to 4 °C for the procedure. A particularly high cell death occurred after immunomagnetic separation for both temperatures in all experiments, as shown in Figure 9, which raised the question of why the cells were killed. One possibility is that the cells were not killed by the immunomagnetic enrichment, rather that already dead cells were enriched in the process. Therefore, experiments with the Dead Cell Removal kit were performed.

Dead and apoptotic cells in the cell suspension were removed prior to the immunomagnetic enrichment and separation. When counting the cells after using the Dead Cell Removal kit there were not detected any dead cells. The fraction of dead cells in the suspension after the immunomagnetic separation when Dead Cell Removal was used was 26 % as compared to 36 % when the dead cells were not removed. However, 26% is still a significant number of dead cells, and we believe that most of these cells died during the immunomagnetic enrichment. The immunomagnetic separation consists of a step in which the cells are flushed out of the column with physical force. The high cell death during this procedure may be related to this physical strain. The paramagnetic nanoparticles themselves may also have a toxic effect on

the cells [96]. The number of cells in the suspension appeared to be dramatically decreased after using Dead Cell Removal was used. This suggests that the kit also removes viable cells in the suspension. Therefore, Dead Cell Removal was not considered for the final work process for enrichment of CTCs.

Identification and isolation of single cells with micromanipulation is a time-consuming process. After isolation of a single cell by micromanipulation the cell is placed in lysis buffer while other single cells are acquired. The cell could possibly burst in the lysis buffer and be exposed to RNase enzymes in the cell. Since RNase enzymes would degrade RNA they were considered as a possible cause for the poor RNA quality of the single cells. Other studies included RNase inhibitor during isolation process of single cells [94]. An evaluation of the use of RNase inhibitor was therefore performed. The results given in Figure 10 shows that the expression levels of *Vimentin* and *HPRT1* are higher in HeLa control samples where RNase Inhibitor was not used. These results were surprising, as RNase inhibitors should not affect the RNA in the sample or the qPCR efficiency. The same trend was observed for the single cells isolated in lysis buffer containing HeLa RNA (Figure 11). Based on these results RNase inhibitor was not used in the final work process for enrichment of CTCs.

The use of micromanipulation for single cell isolation was successful, and CellEctor from MMI seems to be a good choice for isolation of single CTCs. During the micromanipulation process the cell suspension is constantly kept in room temperature, which might induce apoptosis in CTCs. Cooling of the early enrichment steps gave favorable results in terms of lower cell death. Therefore, cooling of the cells during scanning and isolation could help to further increase the mRNA quality of the cells.

Faster scanning and isolation of the cells helped by a more accurate immunofluorescent staining and made distinguishing CTCs from contaminating leukocytes easier. These optimizations combined with the change of temperature did improve the viability of the single cells. However, the mRNA quality is still poor for most of the isolated single cells and further improvements are recommended. For example, further cooling of the cells during scanning or the use of DAPI for exclusion of apoptotic cells, could possible improve the mRNA quality. Also adding reagents that would protect and stabilize RNA, such as *RNAlater*®, in the cell suspension during micromanipulation should be considered.

6.2 Validation of methods

The aim of the first set of validation experiments was to separate the leukocytes from the cancer cell line cells based on the mRNA expression profiles. In addition, background levels for the mRNA markers in leukocytes were established. The results from the validation experiment are presented in chapter 5.3.1. Cells from the same cell line were expected to have a similar mRNA expression profiles and therefore be clustered together. However, the different pancreatic cancer cell lines were not clearly separated by the hierarchical cluster analysis. The heat map in Figure 13 shows a similarity between the gene expressions of the single cells from the same cell line. For example when looking at the expression of BxPC-3 cells, Figure 13, all the cells show similar expression levels with high expression of *E-Cadherin*, *ALDH1A1* and *CK8*. A similar pattern is observed for the AsPC-1 and PAN-1 cells. Leukocytes were clustered alone and at a great distance from the cancer cells using both normalization strategies. This result validates that the multimarker mRNA assay has the capability to distinguish cancer cells from contaminating leukocytes.

Figure 12 shows the relative mRNA levels of the different markers. If the Cq-value of the sample is high compared to the Cq-value of the calibrator sample, the relative mRNA level will have a high value. This is visualised in Figure 12 for *EPCAM* and *CD45*. For most markers the mRNA level in leukocytes is not overlapping with the mRNA level in cancer cell line cells. However, relative mRNA levels of leukocytes and cancer cell line cells are not clearly separated for the mRNA markers *CD24*, *CD44* and *Vimentin*. *Vimentin* is highly expressed in all cells types. Hence, seven mRNA markers are left to clearly separate the two cell groups. The levels of the mRNA markers for the different cell types are later used as reference cells for molecular characterization of CTCs and contaminating leukocytes.

Several spiking experiments were performed to validate the entire method for the characterization of CTCs from pancreatic cancer patients. The results from these experiments are given in chapter 5.3.2. The strategy chosen for these experiments was spiking of AsPC-1 cells into blood samples from healthy volunteers to simulate a patient blood sample with CTCs. This strategy for evaluation and validation of methods for detection of CTCs has also been used in other studies [48, 97, 98]. AsPC-1 cells were chosen for these experiments, as the cell line express high levels of *EpCAM* and could easily be separated from the leukocytes. The mean recovery rate of AsPC-1 cells from the blood samples was 17.3 %. This is consistent with previous recovery experiments by the research group. However, it is low

compared to other studies who report recovery rates up to 75 % for the same immunomagnetic beads [99]. These differences could be caused by a less specific characterization of CTCs, thus characterization of more false-positive CTCs, in addition to using other cancer cell line cells from other cancers that might have higher EpCAM expression.

The immunofluorescent staining process and selection criteria were validated by acquiring five cells which were assumed to be AsPC-1 cells based on the immunofluorescent staining. The assumption was validated by qPCR using the multimarker mRNA panel. The results presented in both Figure 15 and Figure 16 show that the suspected tumor cells clusters together with the cancer cell line cells, at a great distance from the leukocytes. All the suspected tumor cells had expression of *CK8*, *ZEB1* and *EPCAM*, and all except one cell had expression of *E-Cadherin* and *CD44*. In comparison, neither of the leukocytes had expression of *EPCAM*, *CK8* and *E-Cadherin*. This confirms that the suspected tumor cells are indeed the spiked AsPC-1 cells, and not leukocytes. Hence, the experiment confirms that the established method could be used to identify single tumor cells from whole blood samples.

6.3 Evaluation of single-cell normalization strategies

Several strategies to normalize the single-cell qPCR results were studied. For single cells mean centering or auto-scaling, normalization against one or more reference gene or cell-to-cell normalization has been reported in other studies [46, 63, 92, 100]. The research group had previously compared these three normalization strategies and found the normalization against one or more reference genes seems to be the favorable option [101]. This method, explained in chapter 4.9, has been used in several other single cell studies [46, 48, 100]. In this study normalization against one reference mRNA and a calibrator sample was compared to normalization against the calibrator sample alone (Chapter 5). The sum of the standard deviations was used to evaluate the variation in the data material with regard to the two normalization strategies. Part of the variation may be due to general differences in RNA quality and transcription levels between cells. If the overall variation is reduced when normalizing against a reference mRNA, that may remove this less interesting variation and more biological relevant information may be revealed. The sum of the standard deviation for all mRNAs, excluding *HPRT1*, was $SSD = 14.2$ after performing the normalization against the reference mRNA. In comparison the data without normalization against a housekeeping reference gene, only normalized to the calibrator sample, had a sum of standard deviation of

SSD = 21.2. This shows that the variation in the data is reduced with normalization against a reference gene, which is favorable.

The leukocytes and the cells acquired from the patient blood samples showed a trend of lower overall expression for the mRNA markers in general, compared to the cancer cell line cells. These differences in expression levels could explain why the variation in the data was reduced by normalization against a reference gene. The reference gene would have a lower expression if the cell had degraded mRNA. The variation in data could without normalization, therefore, be partly caused by variation in mRNA quality rather than actual variation in gene expression.

For hierarchical cluster analysis it is common to use a distance matrix to define the distance between data. The most common metrics for distant matrix are Euclidean distances and Pearson correlation [93]. The method used for distance measures in this study was Pearson Correlation. Since, the Pearson Correlation was the only available option in the Expander 6.0 software, this metrics was used for the creation of the hierarchical clusters. It is possible to use average-, single- or complete linkage to define clusters for creation of a dendrogram [93]. For the results presented in this study complete linkage was used. Complete linkage was chosen because of the distance between the expression levels in leukocytes and cancer cell lines. In complete linkage the most distant elements in two groups are calculated, explained in details in chapter 4.11, which tend to form compact and discrete clusters, like the one shown in Figure 13.

The hierarchical clustering with normalized data gave a statistical evaluation of the cells, which was consistent with the observations made by the immunofluorescent staining and mRNA profiles. The strategy to use normalization against a reference mRNA marker seems favorable. However, a clear conclusion could not be made out of the results in this study. Reiter et al. [61] reports similar challenges for single cell normalization strategies, where they conclude that normalization against a reference gene could not be validated for single-cell analysis, due to a high variance between cells in terms of both expression magnitude and pattern, and the cellular timing of mRNA expression bursts [61].

Not all the cells included in the hierarchical cluster analysis expressed all the mRNA markers. For example none of the cancer cells expressed *CD45*. The hierarchical cluster software would not implement *CD45* as an important parameter in the cluster when there were empty values. Therefore, low values were calculated, details in chapter 4.11, by adding these values

to the hierarchical clustering analysis the software would analyse all the mRNA markers, and not exclude markers because of missing values.

6.4 Analysis of patient samples

The optimized method for enrichment and molecular characterization was used to detect CTCs in blood samples from pancreatic cancer patients. 69 potential CTCs were isolated along with 13 leukocytes from the blood samples. Poor mRNA quality of the single cells affected the number of CTCs for molecular characterization. Only 12 % of the 69 potential CTCs isolated had good mRNA quality. The number of single CTCs with poor mRNA quality is visualized in Figure 9. Cann *et al.* [94] found that 21 % of the single CTCs isolated from prostate cancer patients had good RNA quality, which is similar to our results. The study also discusses the observed tendency of RNA quality variations between patients. They observed that the patients with the highest number of CTCs also had the most viable CTCs. A similar observation was made in this study, as the eight CTCs with good mRNA quality all derived from four of the seven patients included in the study. The differences in RNA quality could be related to treatment effects [94]. One of the first events when cells are apoptotic is degradation of mRNA. Even if all the acquired cells appeared to be visually intact mRNA could still be degraded. Mehes *et al.* [102] concluded that most of the circulating tumor cells that were found in breast cancer patients were apoptotic. This could also be the case for the CTCs acquired from the pancreatic cancer patients in this study, as membrane compromised and damaged cells were not acquired, as illustrated in Figure 18.

In the hierarchical cluster analysis of potential CTCs from patient samples, illustrated in

Figure 19, eight potential CTCs and three leukocytes acquired from patient samples were included. Two of the leukocytes and two of the potential CTCs were clustered together with the leukocytes from healthy control blood samples. These two cells were isolated as potential CTCs, but were characterized as leukocytes by the clustering analysis. Both cells express the leukocyte marker *CD45*, and neither expresses the epithelial marker *EPCAM*, therefore the cells were confirmed as contaminating leukocytes. The remaining potential CTCs and the leukocytes from the patient samples were clustered together with the pancreatic cancer cell lines in cluster 2 and 3. All of these cells would be considered as CTCs, if only evaluating the hierarchical cluster in

Figure 19. However, all of the cells from the patient samples, the leukocytes included, would be considered as CTCs if only evaluating the hierarchical cluster with data without normalization in Figure 20. The hierarchical cluster with data without normalization appears to be inferior to the normalized version, as expression of the mRNA markers confirms the leukocytes from patient samples to be leukocytes through expression of the *CD45* marker.

To report potential CTCs as correct as possible within our experimental context, the results from the whole method should be evaluated. The three results that should be taken into consideration are the immunofluorescent staining, the expression rates of the mRNA markers and the statistical analysis. The results reported in Table 22 are based on all of these elements. These results confirms that two of the CTCs are indeed CTCs, as they expresses the mRNA markers *EPCAM*, *ZEB1* and *CD24*, and *EPCAM* and *CD44* respectively. Two cells that were picked as CTCs were molecularly characterized as leukocytes due to *CD45* expression. The remaining four CTCs only had expression of *CD44* and/or *CD24* in addition to *HPRT1* and *Vimentin*. The leukocytes also expressed a background level of these assays, therefore, CTCs expressing less than four mRNA markers were uncertain CTCs in Table 22. However, all the leukocytes expressed the leukocyte mRNA marker *CD45*, which neither of the CTCs expressed. Hence, there are reasons to suggest that these cells also could be CTCs, but due to poor mRNA quality a final confirmation could not be made. These cells were considered to have good mRNA quality based on the initial mRNA quality criteria, implicating a reconsideration of the mRNA quality criteria.

6.5 General methodological considerations

The immunomagnetic separation technique seems to affect the mRNA quality, even at the temperature of 4°C. There are, however, other possibilities for CTC enrichment (chapter 1.2.4). Other studies have not used MACS® separation for the enrichment of CTCs for single cell isolation, but rather worked with the whole cell suspension. In these studies the challenge of poor mRNA quality would not be as critical, because the cell suspension would be lysed or frozen immediately after separation [103]. The MACS® separation used in this study seemed to affect the viability of the cells. Another concern with the enrichment procedure is the use of EpCAM dependent enrichment when searching for the CTCs with the highest metastatic potential. Several studies report identification of CTCs that lack expression of epithelial markers, because of EMT [46]. These potentially important cells, would not be captured when using EpCAM dependent enrichment methods [99]. The methods used for immunomagnetic

enrichment and immunofluorescent staining of CTCs in our study were EpCAM-dependent. Therefore, the magnetic beads could prevent the immunofluorescent staining from attaching to the EpCAM proteins on the cell surface. The use of different antibodies for the immunomagnetic separation and the immunofluorescent staining should, therefore, be considered.

MagSweeper[®] and CTC-iChip are two of the most promising, new enrichment methods of CTCs [48, 94]. Whole blood samples are processed directly in both techniques, eliminating the need for time-consuming enrichment steps like density gradient separation. Neither of these techniques are, however, commercially available at the moment. The commercially available CellSearch[®] system has been used for enrichment of CTCs followed by isolation of single cells, the cells are fixated. Swennenhuis *et al.* [104] found a significant decrease in the DNA quality in single cells fixated using in the CellSearch[®] system enrichment, compared to non-fixated cells. mRNAs degrades even faster compared to DNA. The CellSearch[®] system is therefore not a good option for single CTC mRNA profiling. Thus, density gradient separation followed by immunomagnetic enrichment may still be the best available option for single CTC enrichment and characterization. However, a number of manufactures offers alternative immunomagnetic enrichment solutions that could be evaluated.

In this study 11 mRNA markers were used for the molecular characterization of single CTCs. The mRNA markers included epithelial, mesenchymal, cancer stem cell and leukocyte markers, in addition to a reference housekeeping gene marker. These markers provided profiles of the single CTCs acquired from patient samples, however, the amount of information is rather limited compared to other mRNA profiling strategies like RNA Seq. RNA Seq is a new technique for deep-sequencing that provides transcriptome profiling [94]. The method has been applied to single CTCs [27, 94], and holds great promise of advancing the understanding of the gene expression in CTCs.

6.6 Potential clinical value of single CTC mRNA profiling

A limited number of studies have performed mRNA profiling on single CTCs [27, 68, 94]. At this point it is too early to conclude regarding the future clinical value of the method described in this thesis. RNA profiling could not only provide an insight of the gene expression of CTCs, but potentially also of the primary tumor and metastasis. Methods for mRNA sequencing could revolutionize our use of CTCs as a liquid biopsy of tumors.

Cann et al.[94] demonstrates mRNA sequencing of single CTCs. The study detected 181 genes that were over-expressed in CTCs from prostate cancer patients compared to normal prostate tissue. These genes were involved in cell cycle control, apoptosis, cell communication and cell adhesion [94]. Ramsköld et al. [68] have developed a single-cell mRNA sequencing protocol called Smart Seq. This method removes previous concerns of poor transcriptome coverage, and demonstrates high reproducibility. When using this method in the study, new candidate biomarkers for melanoma CTCs were detected [68]. Yu et al. [27] used mRNA sequencing to identify signalling pathways in CTCs from pancreatic cancer patients. This might lead to identification of therapeutic targets, which could be used to prevent metastasis.

6.7 Future Perspectives

Patients diagnosed with metastatic pancreatic cancer have a median survival of 5-6 months, which makes pancreatic cancer a highly lethal disease [2]. The early and frequent dissemination of the disease to the liver, lung and skeletal system is one of the reasons for these numbers. The cells which are responsible for development of distant metastasis are most likely the CTCs [22]. Detection and characterization of CTCs could in the future unravel the biology behind cancer metastasis, provide information for the development of targeted therapy and help monitoring the disease. In the current study the blood samples were taken before treatment start and monthly during treatment. These samples could provide information on treatment response via detection and molecular characterization of CTCs. Also mRNA profiles of CTCs before treatment with the new chemotherapeutic agent nab-paclitaxel and after development of treatment resistance could provide information of events that leads to treatment resistance. For applications like these, the development of technology for molecular characterization of CTCs is important.

CTCs are highly heterogeneous population and the CTC isolation and characterization should be able to detect all phenotypes. CTCs are believed to represent a “liquid biopsy” of cancer. The heterogeneous CTC population could reflect the cancer cells in the primary tumor and the metastasis even better than a simple biopsy of the primary tumor. Especially, the most aggressive tumor cells could be detected from blood. A wide range of new promising technologies for CTC detection are developed, but further validation and qualification is required for CTC detection to have clinical utility [26].

Successful molecular characterization of CTCs opens up for a number of applications such as identification of novel therapeutic targets, analysis of cancer stem cells and monitoring disease progression and drug response. Hopefully, CTC detection and characterization will provide biomarkers for sensitive patient monitoring and optimal treatment management.

7 Conclusion

Existing methods for molecular characterization of single CTCs with RT-qPCR were optimized. The optimizations improved the method both in terms of easier identification of single CTCs and improved mRNA quality of the cells. The methods were validated by spiking AsPC-1 cells in peripheral blood samples. The cancer cells were successfully separated from the contaminating leukocytes by molecular characterization with RT-qPCR. Blood samples from pancreatic cancer patients were successfully analyzed and CTCs were detected and distinguished from leukocytes. There is future potential for clinical utility of this method for pancreatic cancer.

8 References

1. Norway, C.R.o., *Cancer in Norway 2010 - Cancer incidence, mortality, survival and prevalence in Norway*. 2012, Cancer Registry of Norway.
2. Hidalgo, M., *Pancreatic cancer*. N Engl J Med, 2010. **362**(17): p. 1605-17.
3. Seufferlein, T., et al., *Pancreatic adenocarcinoma: ESMO-ESDO Clinical Practice Guidelines for diagnosis, treatment and follow-up*. Ann Oncol, 2012. **23 Suppl 7**: p. vii33-40.
4. Maitra, A. and R.H. Hruban, *Pancreatic cancer*. Annu Rev Pathol, 2008. **3**: p. 157-88.
5. Bogoevski, D., et al., *Pancreatic cancer: a generalized disease--prognostic impact of cancer cell dissemination*. Langenbecks Arch Surg, 2008. **393**(6): p. 911-7.
6. Lowenfels, A.B. and P. Maisonneuve, *Epidemiology and risk factors for pancreatic cancer*. Best Pract Res Clin Gastroenterol, 2006. **20**(2): p. 197-209.
7. Larsson, S.C. and A. Wolk, *Red and processed meat consumption and risk of pancreatic cancer: meta-analysis of prospective studies*. Br J Cancer, 2012. **106**(3): p. 603-7.
8. Hassan, M.M., et al., *Risk factors for pancreatic cancer: case-control study*. Am J Gastroenterol, 2007. **102**(12): p. 2696-707.
9. Amundadottir, L., et al., *Genome-wide association study identifies variants in the ABO locus associated with susceptibility to pancreatic cancer*. Nat Genet, 2009. **41**(9): p. 986-90.
10. Vincent, A., et al., *Pancreatic cancer*. Lancet, 2011. **378**(9791): p. 607-20.
11. Marieb, E.N. and K. Hoehn, *Human Anatomy and Physiology*. 2010: Benjamin Cummings.
12. Institute, N.C. *Pancreas—Islets of Langerhans*. [cited 2014 07.06]; Available from: <http://training.seer.cancer.gov/anatomy/endocrine/glands/pancreas.html>.
13. Rolf Kåresen, E.W., *Kreftsykdommer -en basis bok for helsepersonell*. 3th ed. 2009: Gyldendal Norsk Forlag.
14. Bhat, K., et al., *Advances in biomarker research for pancreatic cancer*. Curr Pharm Des, 2012. **18**(17): p. 2439-51.
15. Klein, A.P., *Identifying people at a high risk of developing pancreatic cancer*. Nat Rev Cancer, 2013. **13**(1): p. 66-74.
16. Cen, P., et al., *Circulating tumor cells in the diagnosis and management of pancreatic cancer*. Biochim Biophys Acta, 2012. **1826**(2): p. 350-6.
17. Horn, T., Clausen, P.P., Baandrup, U., Fenger, C., Græm, N., Jacobsen, G.K., *Klinisk patologi*. 4th ed. 2002: FADL's Forlag Aktieselskab.
18. Herrmann, R., et al., *Gemcitabine plus capecitabine compared with gemcitabine alone in advanced pancreatic cancer: a randomized, multicenter, phase III trial of the Swiss Group for Clinical Cancer Research and the Central European Cooperative Oncology Group*. J Clin Oncol, 2007. **25**(16): p. 2212-7.
19. Conroy, T., et al., *FOLFIRINOX versus gemcitabine for metastatic pancreatic cancer*. N Engl J Med, 2011. **364**(19): p. 1817-25.
20. Von Hoff, D.D., et al., *Increased survival in pancreatic cancer with nab-paclitaxel plus gemcitabine*. N Engl J Med, 2013. **369**(18): p. 1691-703.

21. Rasheed, Z.A., W. Matsui, and A. Maitra, *Pathology of pancreatic stroma in PDAC*, in *Pancreatic Cancer and Tumor Microenvironment*, P.J. Grippo and H.G. Munshi, Editors. 2012: Trivandrum (India).
22. Tjensvoll, K., O. Nordgard, and R. Smaaland, *Circulating tumor cells in pancreatic cancer patients: methods of detection and clinical implications*. *Int J Cancer*, 2014. **134**(1): p. 1-8.
23. Hartwell, L., et al., *Genetics: From Genes to Genomes*. 2010: McGraw-Hill Education.
24. Kornelia Polyak, R.A.W., *Transitions between epithelial and mesenchymal states: acquisition of malignant and stem cell traits*. *Nature Reviews Cancer*, 2009. **9**: p. 265-273.
25. Alix-Panabieres, C. and K. Pantel, *Circulating tumor cells: liquid biopsy of cancer*. *Clin Chem*, 2013. **59**(1): p. 110-8.
26. Matthew G. Krebs, R.L.M., Louise Carter, Ged Brady, Fiona H. Blackhall and Caroline Dive, *Molecular analysis of circulating tumor cells - biology and biomarkers*. *Nature Review Clinical Oncology*, 2014. **11**: p. 129-144.
27. Yu, M., et al., *RNA sequencing of pancreatic circulating tumour cells implicates WNT signalling in metastasis*. *Nature*, 2012. **487**(7408): p. 510-3.
28. Hong, B. and Y. Zu, *Detecting circulating tumor cells: current challenges and new trends*. *Theranostics*, 2013. **3**(6): p. 377-94.
29. Pantel, K., C. Alix-Panabieres, and S. Riethdorf, *Cancer micrometastases*. *Nat Rev Clin Oncol*, 2009. **6**(6): p. 339-51.
30. Lowes, L.E. and A.L. Allan, *Recent advances in the molecular characterization of circulating tumor cells*. *Cancers (Basel)*, 2014. **6**(1): p. 595-624.
31. Allard, W.J., et al., *Tumor cells circulate in the peripheral blood of all major carcinomas but not in healthy subjects or patients with nonmalignant diseases*. *Clin Cancer Res*, 2004. **10**(20): p. 6897-904.
32. Stott, S.L., et al., *Isolation of circulating tumor cells using a microvortex-generating herringbone-chip*. *Proc Natl Acad Sci U S A*, 2010. **107**(43): p. 18392-7.
33. Fidler, I.J., *The relationship of embolic homogeneity, number, size and viability to the incidence of experimental metastasis*. *Eur J Cancer*, 1973. **9**(3): p. 223-7.
34. Gupta, P.B., Mani, S., Yang, J., Hartwell, K., Weinberg, R.A. , *The evolving portrait of cancer metastasis*. *Cold Spring Harb Symp Quant Biol*, 2005. **70**: p. 291-297.
35. Yu, M., et al., *Circulating tumor cells: approaches to isolation and characterization*. *J Cell Biol*, 2011. **192**(3): p. 373-82.
36. Yang, J. and R.A. Weinberg, *Epithelial-mesenchymal transition: at the crossroads of development and tumor metastasis*. *Dev Cell*, 2008. **14**(6): p. 818-29.
37. van Roy, F. and G. Berx, *The cell-cell adhesion molecule E-cadherin*. *Cell Mol Life Sci*, 2008. **65**(23): p. 3756-88.
38. Kowalski, P.J., M.A. Rubin, and C.G. Kleer, *E-cadherin expression in primary carcinomas of the breast and its distant metastases*. *Breast Cancer Res*, 2003. **5**(6): p. R217-22.
39. Rodriguez, F.J., Lewis-Tuffin, L.J., and Anastasiadis, P.Z., *E-cadherin's dark side: possible role in tumor progression*. *Biochimica et biophysica acta*, 2012. **1826**: p. 23-31.
40. Wheelock, M.J., Shintani, Y., Maeda, M., Fukumoto, Y., and Johnson, K.R., *Cadherin switching*. *Journal of Cell Science* 2008. **121**: p. 727-735.

41. L.Norton, E.C.a., *Self seeding in cancer*. Recent Results Cancer Research, 2012(195:): p. 13-23.
42. Massagué, L.N.J., *Is cancer a disease of self-seeding?* Nature Medicine, 2006. **12**(8).
43. Joosse, S.A. and K. Pantel, *Biologic Challenges in the Detection of Circulating Tumor Cells*. Cancer Research, 2012. **73**(1): p. 8-11.
44. van de Stolpe, A., Pantel, K., Sleijfer, S., Terstappen, L.W., den Toonder, J.M., *Circulating tumor cell isolation and diagnostics: toward routine clinical use*. The Journal of Cancer Research, 2011(71 (18)): p. 55-60.
45. Pecot, C.V., et al., *A novel platform for detection of CK+ and CK- CTCs*. Cancer Discov, 2011. **1**(7): p. 580-6.
46. Gorges, T.M., et al., *Circulating tumour cells escape from EpCAM-based detection due to epithelial-to-mesenchymal transition*. BMC Cancer, 2012. **12**: p. 178.
47. I Van der Auwera, D.P., IH Benoy², HJ Elst, SJ Van Laere, A Prove´, H Maes, P Huget, and P.V.a.L.D. P van Dam, *Circulating tumour cell detection: a direct comparison between the CellSearch System, the AdnaTest and CK-19/mamaglobin RT-PCR in patients with metastatic breast cancer*. British Journal of Cancer, 2010. **102**: p. 276 - 284.
48. Ozkumur, E., et al., *Inertial focusing for tumor antigen-dependent and -independent sorting of rare circulating tumor cells*. Sci Transl Med, 2013. **5**(179): p. 179ra47.
49. Alix-Panabieres, C., *EPISPOT assay: detection of viable DTCs/CTCs in solid tumor patients*. Recent Results Cancer Res, 2012. **195**: p. 69-76.
50. Alix-Panabieres, C., et al., *Detection and characterization of putative metastatic precursor cells in cancer patients*. Clin Chem, 2007. **53**(3): p. 537-9.
51. Agrawal, B., et al., *Expression of MUC1 mucin on activated human T cells: implications for a role of MUC1 in normal immune regulation*. Cancer Res, 1998. **58**(18): p. 4079-81.
52. de Albuquerque, A., et al., *Multimarker gene analysis of circulating tumor cells in pancreatic cancer patients: a feasibility study*. Oncology, 2012. **82**(1): p. 3-10.
53. Sergeant, G., et al., *Perioperative cancer cell dissemination detected with a real-time RT-PCR assay for EpCAM is not associated with worse prognosis in pancreatic ductal adenocarcinoma*. BMC Cancer, 2011. **11**: p. 47.
54. Soeth, E., et al., *Detection of tumor cell dissemination in pancreatic ductal carcinoma patients by CK 20 RT-PCR indicates poor survival*. J Cancer Res Clin Oncol, 2005. **131**(10): p. 669-76.
55. Mataka, Y., et al., *Carcinoembryonic antigen messenger RNA expression using nested reverse transcription-PCR in the peripheral blood during follow-up period of patients who underwent curative surgery for biliary-pancreatic cancer: longitudinal analyses*. Clin Cancer Res, 2004. **10**(11): p. 3807-14.
56. Kurihara, T., et al., *Detection of circulating tumor cells in patients with pancreatic cancer: a preliminary result*. J Hepatobiliary Pancreat Surg, 2008. **15**(2): p. 189-95.
57. Raj, A., et al., *Stochastic mRNA synthesis in mammalian cells*. PLoS Biol, 2006. **4**(10): p. e309.
58. Ross, I.L., C.M. Browne, and D.A. Hume, *Transcription of individual genes in eukaryotic cells occurs randomly and infrequently*. Immunol Cell Biol, 1994. **72**(2): p. 177-85.
59. Dar, R.D., et al., *Transcriptional burst frequency and burst size are equally modulated across the human genome*. Proc Natl Acad Sci U S A, 2012. **109**(43): p. 17454-9.
60. Boon, W.C., et al., *Increasing cDNA yields from single-cell quantities of mRNA in standard laboratory reverse transcriptase reactions using acoustic microstreaming*. J Vis Exp, 2011(53): p. e3144.

61. Reiter, M., et al., *Quantification noise in single cell experiments*. Nucleic Acids Research, 2011. **39**(18): p. e124-e124.
62. Fox, B.C., et al., *Comparison of reverse transcription-quantitative polymerase chain reaction methods and platforms for single cell gene expression analysis*. Anal Biochem, 2012. **427**(2): p. 178-86.
63. Stahlberg, A. and M. Bengtsson, *Single-cell gene expression profiling using reverse transcription quantitative real-time PCR*. Methods, 2010. **50**(4): p. 282-8.
64. Technologies, A., *Introduction to Quantitative PCR*. 2012, www.agilent.com/genomics.
65. Shendure, J. and H. Ji, *Next-generation DNA sequencing*. Nat Biotechnol, 2008. **26**(10): p. 1135-45.
66. Mortazavi, A., et al., *Mapping and quantifying mammalian transcriptomes by RNA-Seq*. Nat Methods, 2008. **5**(7): p. 621-8.
67. Islam, S., et al., *Characterization of the single-cell transcriptional landscape by highly multiplex RNA-seq*. Genome Res, 2011. **21**(7): p. 1160-7.
68. Ramskold, D., et al., *Full-length mRNA-Seq from single-cell levels of RNA and individual circulating tumor cells*. Nat Biotechnol, 2012. **30**(8): p. 777-82.
69. Xiang, C.C. and Y. Chen, *cDNA microarray technology and its applications*. Biotechnol Adv, 2000. **18**(1): p. 35-46.
70. Welty, C.J., et al., *Single cell transcriptomic analysis of prostate cancer cells*. BMC Mol Biol, 2013. **14**: p. 6.
71. Sykes, P.J., et al., *Quantitation of targets for PCR by use of limiting dilution*. Biotechniques, 1992. **13**(3): p. 444-9.
72. Vogelstein, B. and K.W. Kinzler, *Digital PCR*. Proc Natl Acad Sci U S A, 1999. **96**(16): p. 9236-41.
73. Hindson, B.J., et al., *High-throughput droplet digital PCR system for absolute quantitation of DNA copy number*. Anal Chem, 2011. **83**(22): p. 8604-10.
74. Pfitzner, C., et al., *Digital-Direct-RT-PCR: a sensitive and specific method for quantification of CTC in patients with cervical carcinoma*. Sci Rep, 2014. **4**: p. 3970.
75. Femino, A.M., et al., *Visualization of single RNA transcripts in situ*. Science, 1998. **280**(5363): p. 585-90.
76. O'Connor, C., *Fluorescence In Situ Hybridization (FISH)*. Nature Education, 2008. **1**(1): p. 171.
77. VWR. *Vacurette® EDTA tubes, Greiner Bio-One*. 2014 [cited 2014 21.March].
78. Deer, E.L., et al., *Phenotype and genotype of pancreatic cancer cell lines*. Pancreas, 2010. **39**(4): p. 425-35.
79. Freshney, I., *Culture of animal cells: A Manual of Basic Technique*. 5th ed. 2005: Wiley.
80. Gillet, J.P., S. Varma, and M.M. Gottesman, *The clinical relevance of cancer cell lines*. J Natl Cancer Inst, 2013. **105**(7): p. 452-8.
81. Boyum, A., *Separation of leukocytes from blood and bone marrow. Introduction*. Scand J Clin Lab Invest Suppl, 1968. **97**: p. 7.
82. Axix-Shield, *Lymphoprep™ Isolation of human mononuclear cells*, in *Axis-Shield*. Leflet with product.

83. Lara, O., et al., *Enrichment of rare cancer cells through depletion of normal cells using density and flow-through, immunomagnetic cell separation*. *Exp Hematol*, 2004. **32**(10): p. 891-904.
84. Biotec, M., *CD326 (EpCAM) MicroBeads human*, in *Enclosed with product*. 2007, Miltenyi Biotec.
85. Robinson, J.P., Sturgis, J., Kumar, G.L. , *The Educational Guidebook: IHC Staining Methods*. 5th ed. 2009: Dako, Agilent Technologies.
86. Martin, R.M., H. Leonhardt, and M.C. Cardoso, *DNA labeling in living cells*. *Cytometry A*, 2005. **67**(1): p. 45-52.
87. Invitrogen, *CellsDirect™ One-Step qRT-PCR kit*, in *Catalog Nos. 11753-100, 11753-500, 11754-100, 11754-500*. 2011, Invitrogen by Life Technology.
88. Nelson, D.L., A.L. Lehninger, and M.M. Cox, *Lehninger Principles of Biochemistry*. 2008: W. H. Freeman.
89. Aldrich, S., *qPCR Technical Guid*. 2014, Sigma Aldrich.
90. Bustin, S.A., et al., *The MIQE guidelines: minimum information for publication of quantitative real-time PCR experiments*. *Clin Chem*, 2009. **55**(4): p. 611-22.
91. Butler, J., *Fundamentals of Forensic DNA Typing*. 2009: Elsevier Academic Press.
92. Livak, K.J. and T.D. Schmittgen, *Analysis of relative gene expression data using real-time quantitative PCR and the 2(-Delta Delta C(T)) Method*. *Methods*, 2001. **25**(4): p. 402-8.
93. Pevsner, J., *Bioinformatics and Functional Genomics*. 2009: Wiley.
94. Cann, G.M., et al., *mRNA-Seq of single prostate cancer circulating tumor cells reveals recapitulation of gene expression and pathways found in prostate cancer*. *PLoS One*, 2012. **7**(11): p. e49144.
95. Leiker, M., et al., *Assessment of a nuclear affinity labeling method for tracking implanted mesenchymal stem cells*. *Cell Transplant*, 2008. **17**(8): p. 911-22.
96. Zborowski, M., Chalmers, J.J., *Magnetic cell separation*. 1st ed. The biocompatibility and toxicity of magnetic particles., ed. U.O. Häfeli, Aue, J., Damani, J. 2007: Elsevier, Amsterdam.
97. Magbanua, M.J., et al., *Genomic profiling of isolated circulating tumor cells from metastatic breast cancer patients*. *Cancer Res*, 2013. **73**(1): p. 30-40.
98. Coumans, F.A., et al., *Filter characteristics influencing circulating tumor cell enrichment from whole blood*. *PLoS One*, 2013. **8**(4): p. e61770.
99. Konigsberg, R., et al., *Detection of EpCAM positive and negative circulating tumor cells in metastatic breast cancer patients*. *Acta Oncol*, 2011. **50**(5): p. 700-10.
100. Powell, A.A., et al., *Single cell profiling of circulating tumor cells: transcriptional heterogeneity and diversity from breast cancer cell lines*. *PLoS One*, 2012. **7**(5): p. e33788.
101. Lapin, M., *Molecular characterization of circulating tumor cells from pancreatic cancer patients by single-cell quantitative reverse transcription PCR*, in *BIOCHEMISTRY AND MOLECULAR BIOLOGY*. 2013, University of Southern Denmark.
102. Mehes, G., et al., *Circulating breast cancer cells are frequently apoptotic*. *Am J Pathol*, 2001. **159**(1): p. 17-20.
103. Molloy, T.J., et al., *A multimarker QPCR-based platform for the detection of circulating tumour cells in patients with early-stage breast cancer*. *Br J Cancer*, 2011. **104**(12): p. 1913-9.

104. Swennenhuis, J.F., et al., *Efficiency of whole genome amplification of single circulating tumor cells enriched by CellSearch and sorted by FACS*. *Genome Med*, 2013. **5**(11): p. 106.

9 Table of figures

Figure 1.....	2
Figure 2.....	8
Figure 3.....	19
Figure 4.....	27
Figure 5.....	36
Figure 7.....	43
Figure 8.....	46
Figure 9.....	47
Figure 10.....	50
Figure 12.....	52
Figure 13.....	53
Figure 14.....	54
Figure 15.....	57
Figure 16.....	58
Figure 17.....	60
Figure 18.....	61
Figure 19.....	62
Figure 20.....	63

10 Table of tables

Table 1..... 3

Table 2..... 9

Table 3..... 14

Table 4..... 22

Table 5..... 22

Table 6..... 24

Table 7..... 24

Table 8..... 34

Table 9..... 35

Table 10..... 35

Table 11..... 37

Table 12..... 38

Table 13..... 40

Table 14..... 41

Table 15..... 45

Table 16..... 48

Table 17..... 48

Table 18..... 55

Table 20..... 59

Table 21..... 60

Table 22..... 64

Table 23..... - 85 -

11 Attachments

11.1 Overview of all acquired single cells

Table 23 Overview of all patient cells, both CTCs and leukocytes, acquired with immunocytochemistry characterizations and mRNA levels. Cells marked red have poor mRNA quality, green marking indicates medium mRNA quality and yellow cells have good mRNA quality.

Patient and cell number	Cq-values											Immunofluorescent Staining:			Picked as:
	<i>HPRT1</i>	<i>Vim</i>	<i>CK8</i>	<i>ZEB1</i>	<i>CD44</i>	<i>CD45</i>	<i>EPCAM</i>	<i>E-Cad</i>	<i>N-Cad</i>	<i>Ald</i>	<i>CD24</i>	EpCAM	CD45	Nuclear dye	
PC5_1	n/a	n/a	n/a	34.0		n/a	n/a					Weak	Weak	Strong	CTC
PC5_2	n/a	n/a	n/a	n/a		n/a	n/a					Strong	Non	Non	CTC
PC5_3	n/a	33.64	n/a	n/a		n/a	n/a					Non	Non	Non	CTC
PC5_4	n/a	34.3	n/a	n/a		36.7	n/a					Weak	Strong	Weak	Possible CTC
PC2_5	n/a	32.54	n/a	n/a		n/a	n/a					Non	Strong	Weak	Leukocyte
PC2_6	n/a	31.03	n/a	n/a		n/a	n/a					Weak	Non	Strong	CTC
PC2_7	n/a	n/a	n/a	n/a		n/a	n/a					Weak	Weak	Strong	CTC
PC2_8	n/a	30.98	n/a	33.2		n/a	n/a					Strong	Strong	Non	CTC
PC2_9	n/a	n/a	n/a	n/a		n/a	n/a					Weak	Weak	Weak	Possible CTC
PC2_10	n/a	35.19	n/a	n/a		n/a	n/a					Non	Non	Weak	CTC
PC1_4	n/a	n/a	n/a	n/a		n/a	n/a					Weak	Non	Strong	CTC
PC1_5	n/a	n/a	n/a	n/a		n/a	n/a					Weak	Non	Strong	CTC
PC1_1	35.38	29.04	n/a	n/a	n/a	36.8	n/a	n/a	n/a	n/a	n/a	Non	Weak	Weak	Leukocyte
PC1_6	n/a	n/a	n/a	n/a		n/a	n/a					Weak	Non	Strong	CTC
PC1_7	n/a	33.48	n/a	n/a		n/a	n/a					Weak	Non	Strong	CTC
PC1_8	n/a	n/a	n/a	n/a		n/a	n/a					Strong	Weak	Weak	CTC
PC7_1	n/a	n/a	n/a	n/a		n/a	n/a					Strong	Non	Weak	CTC
PC7_2	n/a	34.04	n/a	n/a		n/a	n/a					Weak	Non	Strong	CTC
PC7_3	n/a	32.55	n/a	n/a		n/a	n/a					Non	Strong	Strong	Leukocyte
PC7_4	n/a	29.8	n/a	n/a		n/a	n/a					Weak	Non	Strong	CTC

PC3_4	n/a	37.3										Weak	Weak	Strong	CTC
PC3_1	32.81	29.8	n/a	n/a	30.01	n/a	n/a	n/a	n/a	n/a	n/a	Strong	Strong	Weak	Possible CTC
PC3_5	n/a	n/a										Strong	Non	Weak	CTC
PC3_6	n/a	n/a										Strong	Non	Non	CTC
PC3_7	n/a	n/a										Weak	Strong	Weak	Possible CTC
PC3_2	32.75	31.22	n/a	n/a	31.07	n/a	n/a	n/a	n/a	n/a	33.59	Weak	Strong	Weak	Possible CTC
PC1_9	n/a	n/a										Non	Weak	Weak	Leukocyte
PC1_10	n/a	31.05										Weak	Non	Weak	CTC
PC1_11	n/a	n/a										Non	Strong	Weak	Leukocyte
PC1_12	n/a	n/a										Weak	Non	Strong	CTC
PC1_13	n/a	n/a										Strong	Weak	Weak	CTC
PC2_1	31.27	31.74	n/a	33.9	n/a	n/a	34.81	n/a	n/a	n/a	34.04	Weak	Non	Strong	CTC
PC2_11	n/a	32.81										Strong	Non	Weak	CTC
PC2_12	n/a	31.71										Non	Non	Strong	CTC
PC2_13	n/a	29.07										Weak	Non	Strong	CTC
PC2_2	32.98	31.8	n/a	n/a	31.05	n/a	33.19	n/a	n/a	n/a	n/a	Weak	Strong	Strong	Possible CTC
PC2_3	32.01	27.67	n/a	n/a	30.02	32.3	34.34	n/a	n/a	n/a	35.55	Non	Strong	Strong	Leukocyte
PC5_5	n/a	n/a										Weak	Weak	Strong	CTC
PC5_6	n/a	33.02										Weak	Weak	Weak	CTC
PC5_7	n/a	n/a										Non	Strong	Weak	Leukocyte
PC6_1	n/a	28.97										Weak	Non	Weak	CTC
PC6_2	n/a	n/a										Non	Strong	Strong	Leukocyte
PC6_3	n/a	31.79										Weak	Weak	Weak	CTC
PC6_4	n/a	n/a										Strong	Non	Weak	CTC
PC6_5	n/a	n/a										Strong	Non	Weak	CTC
PC6_6	n/a	n/a										Non	Non	Strong	CTC
PC7_5	n/a	28.37										Non	Non	Weak	CTC
PC7_6	n/a	n/a										Weak	Strong	Weak	Possible CTC
PC7_7	n/a	n/a										Weak	Weak	Strong	CTC

PC7_8	n/a	n/a										Weak	Weak	Strong	CTC
PC7_9	n/a	32.25										Weak	Strong	Weak	Possible CTC
PC7_10	33.63	n/a	n/a	n/a	n/a	n/a	n/a	n/a	n/a	n/a	n/a	Weak	Weak	Weak	CTC
PC1_2	33.52	29.16	n/a	n/a	31.03	34.8	n/a	n/a	n/a	n/a	n/a	Strong	Weak	Weak	CTC
PC1_3	33.15	30.11	n/a	n/a	30.98	36.8	n/a	n/a	n/a	32.49	34.43	Strong	Weak	Weak	CTC
PC1_14	n/a	n/a										Weak	Non	Strong	CTC
PC1_15	33.87	n/a										Strong	Non	Weak	CTC
PC1_16	n/a	n/a										Strong	Non	Weak	CTC
PC1_17	n/a	n/a										Non	Weak	Weak	Leukocyte
PC1_18	n/a	32.43										Weak	Strong	Weak	Possible CTC
PC1_19	n/a	32.03										Weak	Weak	Weak	CTC
PC5_8	n/a	n/a										Weak	Weak	Non	CTC
PC5_9	n/a	29.73										Weak	Non	Non	CTC
PC5_10	n/a	30.91										Non	Strong	Weak	Leukocyte
PC5_11	n/a	37.84										Weak	Non	Strong	CTC
PC7_11	n/a	n/a										Strong	Non	Non	CTC
PC7_12	n/a	n/a										Weak	Weak	Weak	CTC
PC7_13	n/a	n/a										Weak	Weak	Weak	CTC
PC2_14	n/a	n/a										Weak	Weak	Weak	CTC
PC2_15	n/a	n/a										Non	Strong	Weak	Leukocyte
PC2_16	n/a	n/a										Weak	Weak	Strong	CTC
PC2_17	n/a	n/a										Weak	Weak	Weak	CTC
PC2_4	34.18	31.05	n/a	34.4	29.9	35.6	n/a	n/a	n/a	n/a	n/a	Non	Strong	Weak	Leukocyte
PC3_8	n/a	n/a										Non	Non	Weak	CTC
PC3_3	36.29	29.95	n/a	n/a	29.7	35.9	n/a	n/a	n/a	n/a	n/a	Strong	Non	Weak	CTC
PC3_9	n/a	33.97										Weak	Non	Strong	CTC
PC3_10	34.45	n/a										Strong	Weak	Weak	CTC
PC3_11	n/a	n/a										Non	Non	Non	CTC
PC3_12	n/a	n/a										Weak	Weak	Weak	CTC

PC4_2	n/a	32.91										Weak	Weak	Weak	CTC
PC4_3	n/a	n/a										Non	Strong	Weak	Leukocyte
PC4_4	n/a	n/a										Non	Non	Non	CTC
PC4_1	33.69	32.68	n/a	n/a	n/a	n/a	n/a	n/a	n/a	n/a	35.55	Non	Non	Weak	CTC